Tesi di Laurea Magistrale

FUNCTIONALIZATION OF TI6AL4V SURFACE WITH A PEPTOID FOR ANTIBACTERIAL PURPOSES

Relatori :
Silvia Maria Spriano
Sara Ferraris
Francesca Gamna

Candidata:
Giulia Carà

A mio papà

"Soffierà nel vento una lacrima
Che tornerà da te
Per dirti ciao, ciao!
Mio piccolo ricordo in cui
Nascosi anni di felicità, ciao
E guardami affrontare questa vita
Come fossi ancora qui"

Contents

Chapter 1

Introduction

The increasing resistance of bacteria to conventional antibiotics and the limited therapeutic efficacy of current alternative antimicrobial agents have propelled society to a post-antibiotic era. Dental implants have been the focus of extensive investigation in recent years with the fundamental aim of preventing implant failure and antimicrobial resistance. The principal etiologic factor that causes inflammation condition of peri-implant tissues is the oral biofilm in the trans-mucosal region, particularly around the collar and abutment of the implant, which significantly differs from the interface between the gingiva and natural teeth. Antimicrobial peptides (AMPs) have gained attention as possible alternative drugs thanks to their advantages, including the ability to hamper the development of resistance by pathogens and their high selectivity. However, AMPs have shown clinical issues (mainly their enzymatic degradation) that limit their possibility of being put on the market with success. Peptoids are a group of synthetic and bio-mimetic biomolecules, also known as poly-N-substituted glycines, whose success is in continuous growth. These compounds have been investigated as novel biologically active thanks to their important biochemical properties, including structural diversity compared to peptide, resistance to proteolytic degradation, reduced immunogenicity, enhanced cellular permeability, and ability to fold into higher-order nanostructures.

This thesis aims to investigate the behavior of a chemically treated (CT) titanium surface, functionalized with a peptoid, to promote adhesion and proliferation of gingival fibroblast while simultaneously reducing bacterial adhesion. A synthesized peptoid GN2-Npm9 was chemically adsorbed on the titanium alloy Ti6Al4V (ASTM B348 Grade 5) and its properties were investigated. Firstly, surface characterization was conducted using the XPS analysis, zeta potential titration curves, and confocal microscopy. The results confirmed the homogeneous dispersion and electrostatic adsorption of the peptoid on the CT surface, which has a negative surface charge at pH 7.4. Biological tests were performed on CT specimens and CT_GN2-Npm9 specimens: a test was conducted on cultured human mesenchymal stem cells to evaluate the cytocompatibility, while the antimicrobial properties were studied against oral microbiota from healthy and pathological patients. The biological evaluations confirmed that CT_GN2-Npm9 surfaces emerge as a promising combination of nano-topography and bioactive compounds. They exhibit a selective ability to hinder bacterial infection

while preserving the cells' capacity to colonize the device, making them particularly attractive for potential biomedical applications.

Chapter 2

An Introduction to Peptoids

2.1 A growing oral health crisis

2.1.1 The urgent need for alternative solutions

The discovery of penicillin in 1928 and the introduction of antimicrobial drugs in 1940s have had a significant impact on human health, thanks to the utilization of widespread antibiotics. However, the prevalence of bacterial resistance to conventional drugs has increased, resulting in a reduction of their effectiveness in treating certain bacterial $infections$[1]. In advanced countries, antimicrobial resistance (AMR) is the third most prevalent cause of mortality, primarily attributed to antibiotics-resistant diseases. Approximately 700 thousand deaths occur in a year, a number that may dramatically surges to 10 million by 2050[2]. Many research findings have illustrated the disastrous financial impact of AMR, including increases in healthcare costs attributed to higher hospital admissions and escalated drug $consumption$[3]. Therefore, the growing of pathogenic organisms' resistance to common antibiotics and the limited therapeutic efficacy of current antimicrobial agents have propelled society to a post-antibiotic-era where the demand of alternative drugs is essential to prevent and hinder the growth of $pathogens$[1].
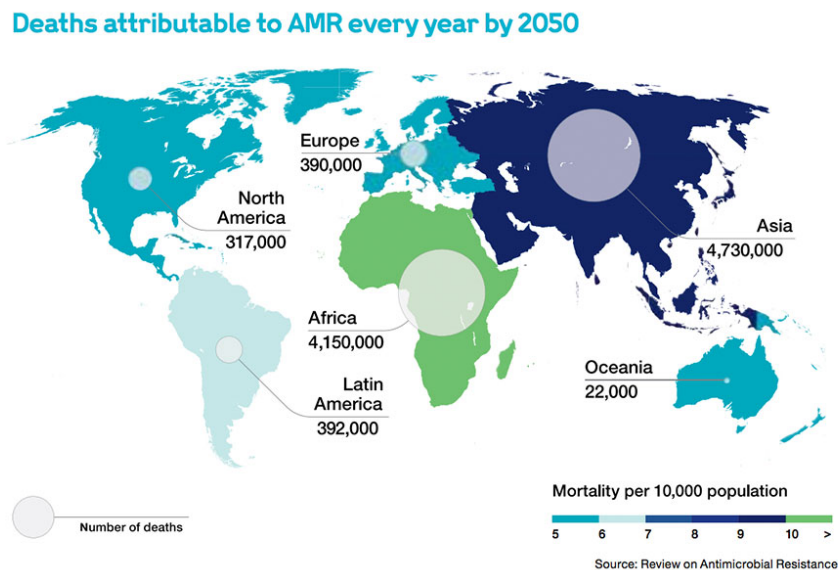
Figure 2.1: A prediction of the mortality by 2050, due to the increased AMR, according to a 2017 report from the United Nations Foundation and the Wellcome Charitable Trust. The map shows the inequal distribution: the deaths in Asia and Africa are expected to be about twice the deaths in North America, Europe, and $Australia$[2].

2.1.2 Oral implant complications

Bacterial resistance is typically a mechanism that involves drug inactivation, target site modification and biofilm growth. The latter one is particularly common in bacterial pathogens and leads to in-vivo treatment failure and mortality. The field of contemporary dentistry is highly interested in studying the biological complications that arise in relation to osseointegrated implants and biofilm formation. Peri-implant mucositis and peri-implantitis are the two distinct clinical trials that can be identified. Although both conditions share the presence of an inflammatory lesion associated with bacterial resistance, peri-implantitis have the loss of bone support, while in peri-implant mucositis only the soft tissue is involved. It has been studied that mucositis typically occurs before the development of $peri-implantitis$[4]. Peri-implantitis has a social impact, because it significantly affects patient's quality of life, causing elevated levels of anxiety and limitation in social interactions and $private relationships$[5]. A significant percentage of worldwide adult population experience periodontal diseases, about 20-50%, and it is identified as the main reason of tooth lack. This entails a clinical challenge among the nations because the inflammatory condition may provoke the development of other diseases, including obesity and autoimmune $disorders$[6].

Nowadays, several risk indicators that accelerate the advancement of bone degeneration have been identified, including inadequate oral hygiene, previous history of periodontitis, tobacco smoking, and diabetes, but the principal etiologic factor that cause inflammation conditions of peri-implant tissues is the oral $biofilm$[8]. Therefore,
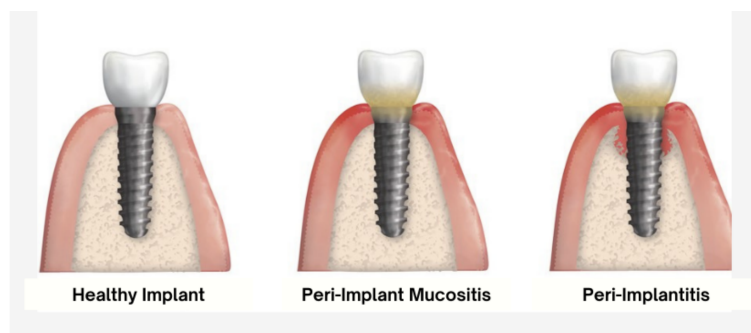
Figure 2.2: Clinical characteristic of health and ill $peri-implant$[7].

there is a pressing requirement to identify antibacterial agents with the capability to inhibit biofilm growth and effectively combat the increasing problem of antibiotic resistance.

2.2 Antimicrobial peptides (AMPs)

Antimicrobial resistance requires concerned research efforts to prevent the emergence of drug-resistance infections and guarantee the efficacy of alternative classes of antibiotics, preserving human and animal health. During the last decades, a group of emerging molecules named antimicrobial peptides (AMPs), also called host defense peptide, have been investigated as potential therapeutic agents for drug evolution and pharmacological applications, since their discovery in the 1980s. AMPs play a critical role in the innate immune system of a big number of organisms, including animals, humans, plants, and microorganisms, as summarized in Figure 2.3, and are involved in important biological processes, including wound repair, inflammation responses, homeostasis control and angiogenesis. They have been found to inhibit growth or kill a wide range of invading pathogenic microorganisms, such as filamentous fungi, enveloped viruses (including feline calicivirus, RNA and DNA viruses), Gram-positive and Gram-negative bacteria, and parasites species, showing versatility, high selectivity and low propensity to biofilm development and de novo $resistance$[9]. To date, 4571 sequences of AMPs (both natural and synthetic) have been isolated and stored in the database DRAMP (data repository of antimicrobial peptides)[10].

Peptide	Origin	Number of aminoacids in the molecule	Structure
Magainin 2	Frog	23	α-helical
Cecropin A	Insect	37	α-helical
Cathelicidin	Mammal (human)	37	α-helical
α-defensins	Mammal (human)	29-35	β-sheet
Nisin	Bacteria	34	Polycyclic
Protegrin 1	Mammal (pig)	18	β-sheet
Lactoferricin	Mammal (bovine)	25	Loop (containing one disulphide bond)

Figure 2.3: AMPs have been isolated from several living species in nature, ranging from prokaryotes to humans. Here some examples of AMPs as natural component with a focus on the different *structures*[9].

2.2.1 Structure and mode of action

AMPs are characterized by short peptides with a variable number of amino acids residues (typically between twelve and one hundred) classified into different families, according to amino acid composition and length. Most AMPs display a net positive charge (+2 to +9), heat stability (100 °C, 15 min) and no drug resistance. In addition, they typically have an amphipathic structure that allows their accommodation into bacterial cytoplasmatic membranes.[9,11].

It has been studied that the overall biological activity is influenced by a combination of size, charge, helical content, hydrophobicity, and amphipathic stereo geometry. Smaller AMPs have the advantages of swift diffusion and secretion, ensuring a faster defense response. Hydrophobic residues selectively target prokaryotic membranes and incite more folding of AMPs, which improves antibacterial activity. Positive charge is identified as decisive distinguishing feature for selective and strong electrostatic interaction with negatively charged lipids on bacterial surfaces, which leads to the disintegration of the bilayer. Negatively charged AMPs have shown an active action against a big number of bacteria as well. Accordingly, AMPs are divided in two categories: cationic, with a substantial number of lysine and/or arginine, and anionic, containing aspartic and glutamic acids.[12,13] AMPs have been found to exist in four main structural conformation: alpha-helices (the most common), beta-sheet, which is combined with one or more disulfide bonds, extended conformation, and loop. The variety of secondary structure is essential for their antimicrobial activity.

The differences in bacterial and eukaryotic membrane composition make the antimicrobial action of AMPs more selective towards bacterial cells than the eukaryotic ones, because of the high percentage of negative charges displayed by phospholipids, contrary to plants and mammals' membranes, which leads to the disruption of the integrity of bacteria membranes, without compromising the host cells. Furthermore,
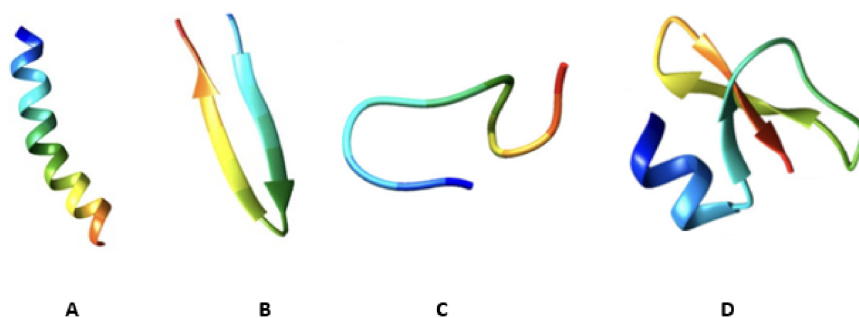
Figure 2.4: Structure of A Clavavin (alpha-helices) B Protegrin (beta-sheet) C Temporin B (linear extension) and D Human beta-defensin-1 (both alpha-helices and beta-sheet).[14]

cholesterol, absent in bacterial cells, and transmembrane potential in eukaryotic cell produce a zwitterionic surface, which also prevents the attack by AMPs (figure 2.5).[15,16] Despite a great number of characteristics related to AMPs have been identified, their mechanism of action at molecular level have still to be analyzed exhaustively. The most common involves the bound of AMP both to the interface of hydrophilic head groups and to hydrophobic fatty acyl chains in order to permeabilize the cytoplasmatic membrane. Permeabilization leads to the collapse of transmembrane electrochemical gradient and to the disruption of membrane integrity. Alternatively, they can form pores or accumulate on microbial membranes, causing cell lysis and death.[16]
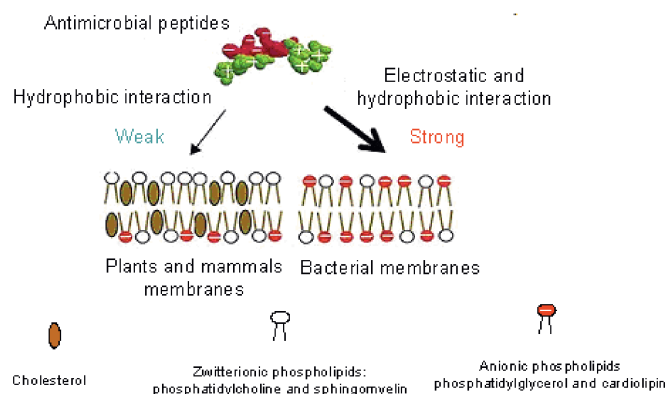
Figure 2.5: . Major differences in interaction between AMPs and mammals' membrane and between AMPs and AMPs and bacteria membrane.[16]

2.2.2 Clinical trials

AMPs have gained attention as possible alternative drugs thanks to their ability to make the development of resistance difficult for pathogens, wide range of antimicrobial activity, fast mechanism of action, and immunomodulatory properties. However, AMPs show clinical issues, that limit their possibility to be put on the market with success.

They often display toxicity, even if administered locally, and have revealed a lower potency in vitro than the expected one. In Figure 2.6 an overview about advantages and disadvantages of AMPs as alternative to potential antibiotics.[17,18]

Advantages of AMPs	Disadvantages of AMPs
Broad-spectrum activity	Potential systemic and local toxicity
High selectivity and potency	Susceptibility to proteolytic degradation
Efficacy, safety and tolerability	High cost of production
Rapid killing action	Instable chemical and physical activity based on pH sensitivity, salt and serum
Low tendency for induced resistance	Poor pharmacokinetics and pharmacodynamics (e.g limited tissue distribution)
Bactericidal activity	Vulnerable to hydrolysis and oxidation
Standard synthesis protocol	Sensitization and allergy after recurrent application
Short time to mark the target	Low membrane permeability
	Short half-life and fast elimination
	Tendency to aggregate
	Poor oral bioavailability

Figure 2.6: A summary of AMPs as prospective drugs.

2.3 Peptidomimetics

To provide a resolution, molecular modelling and rational drug design have identified strategies to optimize in vivo metabolic stability against proteolysis, reactivity, and bioavailability, while retaining potency and selectivity of the original AMP against biological targets. Peptidomimetics are synthetic compounds that mimic peptide structure and function, using a peptide or a protein as pharmacore. They are synthesized through chemical modification of peptide structure (size, length, hydrophobicity, charge) and the incorporation of non-conventional amino acid residues. Peptidomimetics offer numerous advantages over the previous peptides, such as an enhanced resistance to enzymatic degradation and the possibility to add hydrophobic residues, increasing transport through lipid bilayer of cells. Among the great number of studied strategies, approaches that incorporate single non-natural amino acid residues and approaches that completely change the backbone of the peptide have been identified. Peptoids belong to the latter one.[19]. In Figure 2.7 a schematization of common strategies of peptidomimetics.
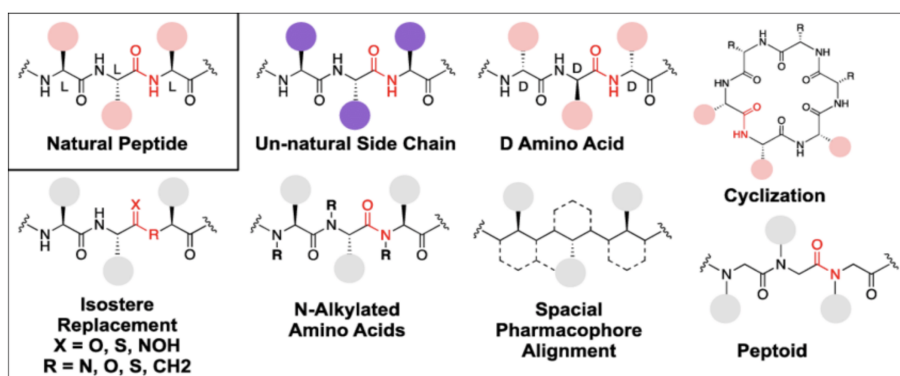
Figure 2.7: Common strategies to synthesize peptidomimetics and chemical difference with peptides.[20]

Peptoids are a class of non-natural sequence-specific heteropolymer peptidomimetics, whose success is in continuous growth. These compounds have been investigated as novel biologically active and nanostructured materials, thanks to their important biochemical properties, such as structural variety, resistance to proteolysis and hydrolysis, reduced immunogenicity, enhanced cellular permeability, and ability to fold into higher order nanostructures. However, peptoids still face challenges hindering the large-scale production, including the complexity of the synthesis and the high cost of production, partly due to the elevated waste generation.[21]

2.4 Peptoids: Origins and Solid Phase Synthesis

Peptoids are a group of synthetic and bio-mimetic polymers, also known as poly-N-substituted glycines, developed for the first time in California in the late 1980s by Zuckermann and coworkers. Since their development, they have gained significant attention in various field, including chemical biology and drug discovery. Nowadays, researchers continue to expand their potential applications and explore their distinctive properties.[22] Since the discovery of peptoids, the interest and development of peptoid synthesis strategies have increased. Peptoids are usually synthesized using solid phase synthesis, similar to that of peptides, which completely allow sequence and side chain control. This process involves stepwise addition of monomers on a solid support, a resin. One of the key advantages of using an excess of reagents is that the progress of the reaction can be driven, through the incorporation of diverse side chains to create a peptoid with tailored properties, such as hydrophobicity and charge. Any unused reagents and by-products can be conveniently removed trough washing. After completing the entire sequence, the peptoid is separated from the solid support through acidic cleavage conditions. This separation enables the purification of the peptoid.[22,23] Solid phase synthesis can be automated, because of its repetitive steps and high stability. Firstly, a monomer approach was implemented. Later, an enhanced approach known as sub-monomer method was developed.

2.4.1 Monomer approach

The synthesis of peptoid oligomers was initially approached involving the utilization of monomer method. In this approach, Fmoc-protected monomers are sequentially added into the growing peptoid chain on a solid resin support, that is insoluble. The Fmoc group the monomers serves as a temporary protecting group for the N-terminus, and it helps in the prevention of secondary reactions, contributing to the final purification of the product by reducing the presence of undesired products. Its removal does not hamper the bound between the peptoid and the resin.[24] The coupled of each monomer to the previous is facilitated by common coupling activators. After each coupling step, Fmoc protecting group is removed, similar to the process in peptide synthesis, and the next monomer is incorporated. The chain extension proceeds from the carboxy terminus (C) to the amino terminus (N), until the desired sequence is achieved.[22] In Figure 2.8 the monomer approach is schematized. The monomer approach demonstrated efficacy on a broad-spectrum of monomers. However, the process needs a laborious and time-consuming preparation of Fmoc protected peptoid building blocks. The time required for producing Fmoc protected N-substituted glycine monomers often far surpasses the time taken to synthesize an entire collection of peptoids on a resin. Therefore, it is more convenient when a few peptoid building blocks are desired, and less useful when a high diversity of residues must be incorporated.[22]
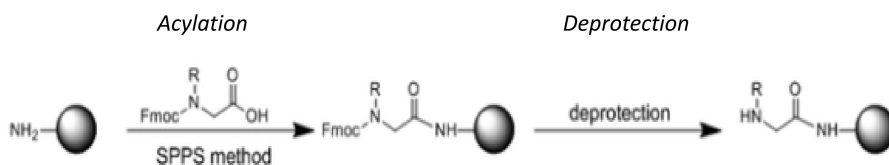
Figure 2.8: Scheme of monomer approach. Acylation step uses conventional activating agents. Deprotection step is conducted with 20% piperidine in DMF.[25]

2.4.2 Sub-monomer approach

Sub-monomer method is currently the most used approach among scientist researchers for synthesizing peptoids. This method has guaranteed several advantages, including a greater variety of side chains that can be incorporated, improved efficiency in the reactions and higher yields in the process.[22] In 1992, Zuckermann and colleagues discovered a significant advancement in peptoid synthesis compared to the limitations of the traditional monomer approach. They introduced a new method named sub-monomer approach, which provides more efficiency in synthesizing peptoid molecules. This technique involves two main steps: acylation and displacement. The first step entails a haloacetic acid, such as bromo or chloroacetic acid, that is used to attach an acyl group to the increasing chain. Then, a displacement step uses a primary amine to replace the halogen atom, thereby integrating the desired side chain onto the peptoid. This approach is summarized in Figure 2.9.[26]
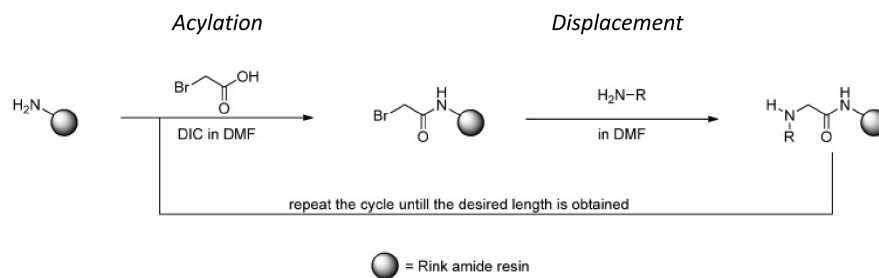
Figure 2.9: Submonomer approach. Acylation step is conducted with appropriate coupling activator and bromoacetic (or chloroacetic) acid. Successively, SN2 displacement with a primary amine.[27]

In the acylation step, bromoacetic acid is typically used in combination with the activating agent N,N'-diisopropylacarbodiimide (DIC). However, sometimes the side chain of the peptoids contains unprotected heteroatoms, such as imidazoles or pyridines. In these cases, chloroacetic acid is preferred to bromoacetic acid, because the latter one is a richer alkylating agent, which means it is more likely to cause undesired alkylation (chemical reaction that inserts an alkyl group) at the heteroatoms in the side chain. However, chloroacetic acid has a limitation: it reduces the speed of the following displacement step, which involves the addition of the amine to get the desired side chain. This slowdown can be overcome using iodide, that reacts with chloroacetic acid through a process called Finkelstein halide exchange, forming a reactive compound: iodoacetamide.[22,28] Generally, protecting groups are not necessary, unless the specific amine side chain functionality requires. Additionally, there is a wide range of affordable available amines that can be used. Researchers have also developed numerous submonomers that can be incorporated into peptoids. They often possess chemical features that enable selective conjugation and efficient connections between different peptoids.[29] In summary, using sub-monomer approach has several benefits, because it allows the introduction of a large variety of chemical components into peptoid libraries. This means that potentially more diverse side chains can be used compared to traditional peptide synthesis. However, it's important to notice that the methods for protecting the side chain need to be investigated, because they are not as developed as peptide one.

Challenges in sub-monomer approach

Sub-monomer synthesis allows accurate control over the sequence and can be automated using robotic synthesizer. However, this method is technically challenging, expensive, and time-consuming, because it is typically limited to milligram scales and short oligomers. For longer chain lengths, that require the incorporation of specific side chains or functional groups, the cumulative yield loss in individual reaction becomes significant, resulting in lower overall reaction yields. These characteristics can limit the diversity of peptoid structures, the accessibility of high molecular weight polypeptoids and the scalability of peptoid synthesis. Nevertheless, all necessary reagents for peptoid synthesis are commercially available, and internally synthesized amines can

also be incorporated. Peptoids display the advantage of a variety of side chains with significant properties in diverse applications, but some of these, such as hydrophobic, chiral, and charged, may require a unique synthetic protocol. Despite appropriate chiral amines are selected to induce chirality and decrease backbone flexibility, high steric hindrance of chiral amines often leads to lower yields, slower reactivity, lower efficiency, and difficulties in the purification, with consequent higher reaction time and temperatures. Moreover, side chain with functionalities (e.g amino or carboxyl groups) need protection strategies, while side chain protecting groups need deprotection step to prevent undesired reaction.[21]
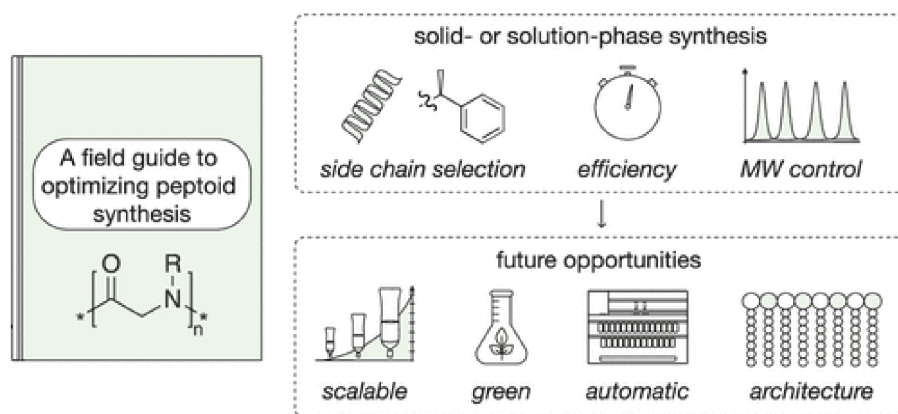
Figure 2.10: Challenges in peptoid synthesis.[21]

Although these methods currently limit monomer diversity, the resulting chains have well-defined lengths and minimal dispersity. As synthesis involves the translation of peptoids from laboratory to industrial scale, it will be crucial to develop versatile synthetic approaches that create a link between scalability and sequence specificity.[21]

2.5 Experimental secondary structures

Peptoids are characterized by a variety of secondary structures, similar to those studied in peptides. However, the higher flexibility of the backbone and the lack of hydrogen bonding lead peptoids to adopt configurations diverse from the traditional well-defined structures formed by peptides. Furthermore, the lack of chiral centers involves the control of peptoids secondary structures by non-covalent bonds (steric and electrostatic interactions), unlike the amino acids linked by covalent interactions in peptides. Stable peptoids configurations have been identified, such as helices Alpha-peptoids and Beta-peptoids.

2.5.1 Differences between peptide and peptoid structures

As illustrated in figure 2.11, peptoids share with peptides a similar structure. However, despite both peptide and peptoid consist of amido acids sequence, there are notable differences. The side chain group in each peptoid is functionally bound to the amide

nitrogen atom, instead of Alpha-carbon. Therefore, the repeating units of the peptoid are N-substitute glycine monomers. The loss of amide proton implicates the lack of a stereogenic center on the backbone of the peptoid, in contrast to peptide that has a chiral backbone.[22]
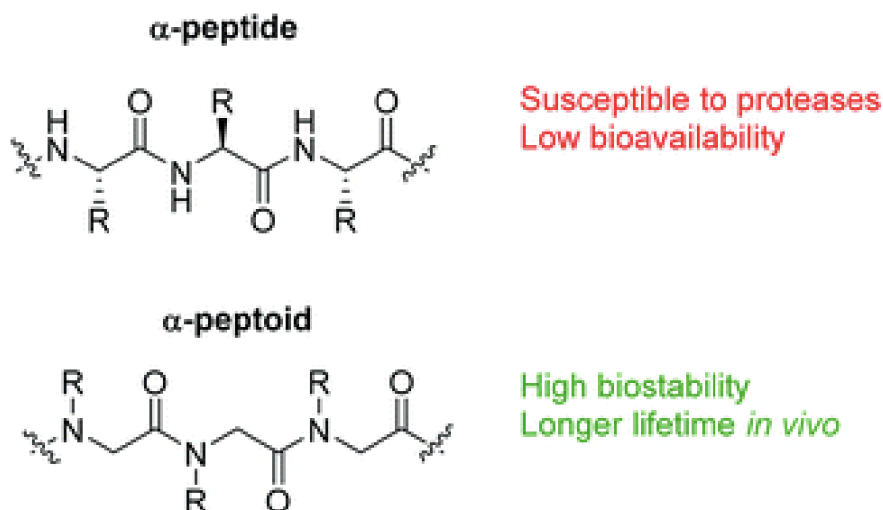
Figure 2.11: A comparison between peptide and peptoid structure. The loss of the amide proton has considerable effects on the distinctive chemical properties of peptoids.[30]

Structural advantages and limitations

The N-substitution enhances peptoids cell-permeability and improves their proteolytic stability compared to their peptide counterparts. Consequently, peptoids emerge as promising peptidomimetic candidates for drug development. However, although the loss of amide proton and chirality provides several advantages over peptides, they also implicate some limitations. In peptides, amide protons allow intra-chain hydrogen bonds, which are essential for the formation of secondary structural conformations, such as Alpha-helices and Beta-sheet, while in peptoids the lack of amide hydrogen on the backbone hinders inter- and intra- chain hydrogen bonds. Moreover, amide bonds in peptoid can isomerize between cis and trans conformation (Figure 2.12) more quickly and willing than secondary amides in peptide. These characteristics lead to an increased peptoid chain flexibility in comparison to peptides. Peptoid conformational flexibility is also due to the absence of both backbone chirality and hydrogen bond donors in the backbone, which hamper backbone aggregation. These properties result in a greater chain diversity and improved bioavailability, that is an important characteristic for drug discovery.[31,33]

However, the absence of amide protons and the consequent lack of inherent hydrogen bonds make peptoids structure less defined compared to peptide one. These features obstruct the design of well-developed secondary structures. This means that often peptoids have not the ability to form defined Alpha-helices and Beta-sheets, which
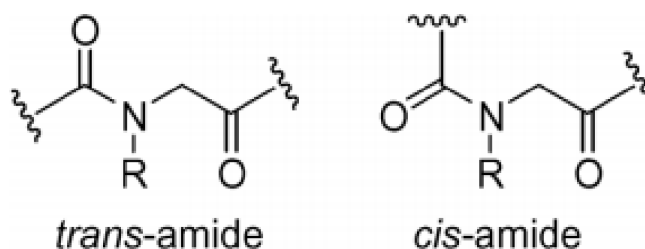
Figure 2.12: Peptoid backbone in trans and cis conformation.[33]

are important in most biological processes, limiting their functionality in particular applications. For instance, most peptoid ligands exhibit a moderate binding affinity to their biological target due to their inherent conformational flexibility, which leads to a significant reduction in entropy during the binding process between peptoids and biomacromolecules. In addition, peptoids generally lack the ability to fold into intricate tertiary structure, which limits their potential mimicking of complex folding patterns and the achievement of functional properties of proteins.[33,34]

2.5.2 Linear and cyclic peptoids

Linear and cyclic peptoids are relatively simple molecules usually synthesized with solid-phase strategy. Linear peptoids are made up with straight chain of N-subsituted glycine monomers and can adopt various secondary structure, including helical and random coil conformations. Cyclic peptoids have a closed ring structure designed by covalent bonds between carboxylic acids and terminal amines, as shown in Figure 2.13.[5]
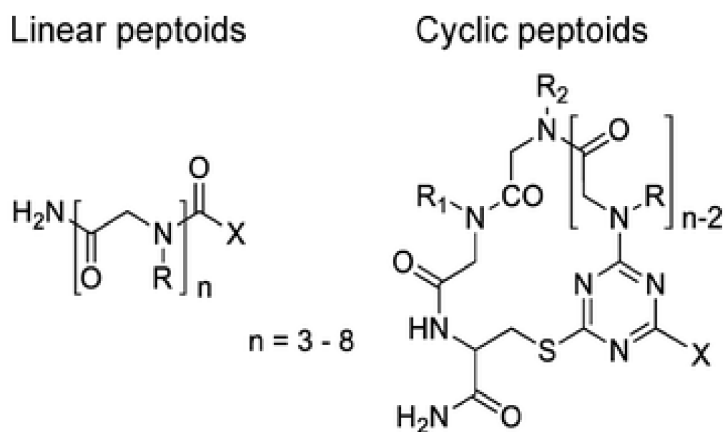
Figure 2.13: General structures of cyclic and linear peptoids.[35]

2.5.3 α-peptoid helices

Alpha-ppeptoid oligomers have been deeply studied because of their well-defined structures and chemical and thermal stability shown by helices, which reduce the denatura-

tion. Researchers have explored a lot of strategies to design peptoids that can mimic the well-defined structure and function of stable Alpha-peptides. Predictive design rules have been established: i) the oligomer must have at least 50% of Alpha-chiral monomers; ii) carboxyl terminus must contain an Alpha-chiral, aromatic monomer; iii) in order to have enhanced stability (thanks to a greater number of steric and electrostatic interactions) and more supported helix conformation, the oligomer must contain at least sixteen residues.[36,37]
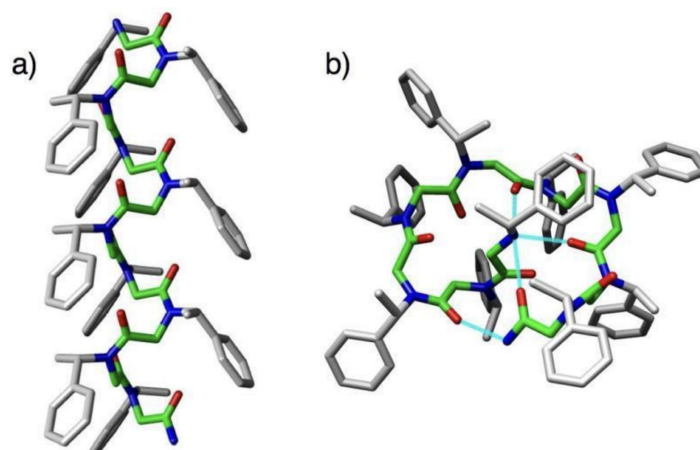
Figure 2.14: (a) peptoid helix containing 3 residues per turn and all cis-amide bonds. (b) peptoid threaded loop, which can easily be converted to peptoid helix through the disruption of intramolecular hydrogen bonds. [38]

In this context, the mentioned design rules can be studied on the peptoid of interest GN2-Npm9, an Alpha-helices lysine/tryptophan-rich peptoid.
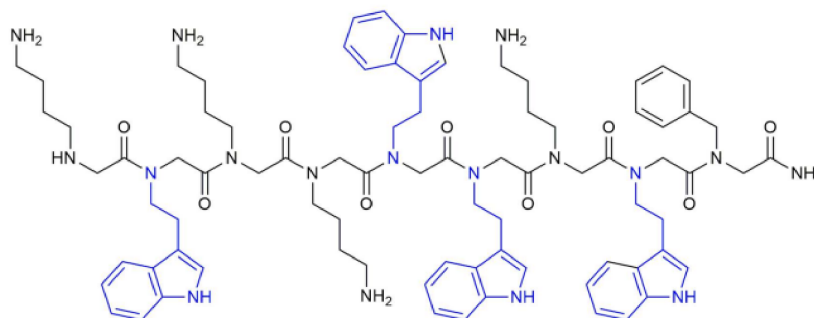
Figure 2.15: Peptoid GN2 – Npm9.[39]

Firstly, the peptoid has more than 50% of Alpha-chiral monomers; specifically, lysine and tryptophan-like monomers are Alpha-chiral, which constitute approximately 90% of its structural composition. Secondly, the carboxyl terminus incorporates N-(1-phenylmethyl)glycine, an aromatic and chiral N-substituted glycine. Thirdly, the peptoid is composed of 9 monomers. Despite the third rule is not followed, previous studies on GN2 peptoids demonstrated that shortened peptoids can exhibit improved antibacterial activity and lower retention time, concluding that the effect of chain length

on the antimicrobial activity and selectivity should be analyzed with considerations about hydrophobicity, amphiphilicity and the charge of the peptoid, as examined in the following chapter.[40]

2.5.4 β-peptoids

In the context of antibacterial research, they are interesting molecules with an easy preparation, due to the unnecessary chiral Beta-amino acids production. Beta-peptoids are usually synthesized via solid-phase methods and exhibit numerous functions. However, their practical use and large-scale industrial production are hindered by their complex and time-consuming synthesis with elevated cost.[41] For these reasons, Beta-peptoids are a class of potential peptidomimetics that has been much less studied than Alpha-peptoids.
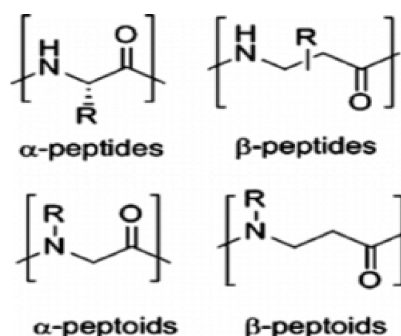
Figure 2.16: Peptidomimetics architecture from peptides to peptoids.[42]

2.6 Zeta potential measurement for biological analysis

2.6.1 Zeta potential

Zeta potential is an important electrokinetic property that describes the charging behavior at the solid-liquid phase. In this project, the electrochemical double-layer model (Chapter 2.4.2.1) has been used to define the zeta potential. Here, zeta potential is described as the electric potential at the shear plane of molecules dispersed in a solution, and the shear plane is described as the region at the interface between the stationary solid surface, where the charge is established, and the mobile surrounding liquid. It is important in the determination of biomedical systems, including an implant in contact with fluids in the body.[43] It is related to the pH of solution, but it also depends on other several factors, including temperature, ionic strength, and concentration of the solution.[44] Zeta potential is generally measured using laser Doppler velocimetry. This technique involves the application of an electric field to two gold electrodes (previously added to solution) and the subsequent measurement of the resulting particle velocity as a function of voltage. When a laser hits the particles in the cell, each particle advances

through the laser and the velocity is evaluated by analyzing the frequency of scattered light, as it is proportional to the speed. The magnitude of zeta potential is an essential parameter for understanding the stability of the particle. Specifically, a higher absolute potential value indicates an increased stability, as electrostatic repulsion increase. Conversely, lower magnitude reveals particle aggregation and instability. [45,46]

Zeta potential measurement

In general, the zeta potential is employed to investigate the behavior of colloidal systems, such as emulsions, and to assess their stability. However, zeta potential can also be employed as a significant parameter in analyses of macroscopic solid surfaces, using the same theorical concept, but with a different purpose. In this sense, zeta potential is an important in analyses of functionalized or treated titanium samples. Indeed, peptoids can have charged side chain or functional groups, which contribute to functionalization of titanium surfaces to optimize biological properties, such as the prevention of bacterial colonization. As such, zeta potential of functionalized surfaces can be obtained in function of pH to have information about the stability of modified layer and surface charge. In addition, it can be used to understand how the functionalization influence the electrostatic attraction or repulsion between titanium surface and the interacting peptoid, that affects bacterial attachment. Finally, zeta potential can also be used to control the release on the surface, improving localized delivery of antibacterial agent.[47] Zeta potential of solid surfaces can be assessed through the application of the electrical double layer model (EDL) by measuring an electrokinetic phenomenon due to the relative motion of solid-liquid interface. In this model, when a solid surface encounters an aqueous solution, it acquires a charge, leading to a distinct charge distribution in the liquid phase. Consequently, a double layer forms, comprising a stationary immobile layer and diffusing mobile layer of counterions (ions with opposite charge to the surface charge on the solid). The interface plane delineating these two layers is referred to as shear plane, as previously explained, and the electrical potential in this juncture is the zeta potential (Figure 2.17).[48]
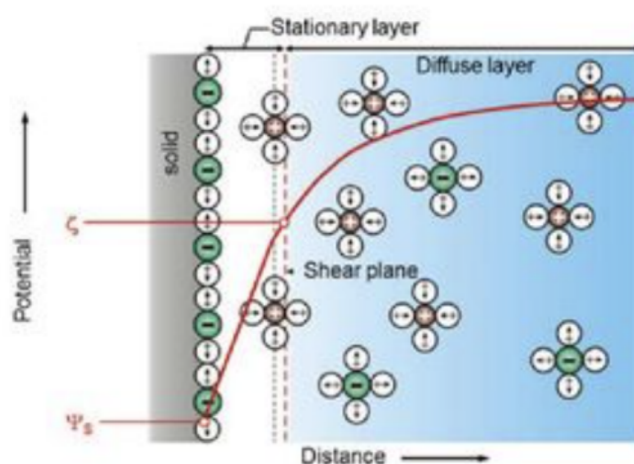
Figure 2.17: Model of the electrical double layer at solid-liquid interface.[48]

The surface charge induces a variation in potential that is related to the distance from the surface. This relationship is depicted in Figure 2.17, where the potential decreases as the distance increases. Electrokinetic phenomena are observed at the interface. Specifically, when an aqueous solution flows through a capillary system, it triggers an electrical response. Depending on the measurement conditions, this response can manifest as either a DC current or a continuous voltage.[43] As the aqueous solution enters in the capillary, it induces the generation of a charge on the solid surface, which is balanced by counterions present in the aqueous solution, resulting in the development of a shear force on the counterions causing them to move in the direction of the flow. Consequently, an electric force opposing the liquid flow emerges. This electric force generates an electrical potential difference, which is subsequently detected by electrodes. Various factors can influence the measurement. The shear rate at the solid-liquid interface which affects the charge separation; it depends on the capillary size and solution flow rate. The occurrence of charge separation is conditioned by the quantity and strength of ions within the aqueous solution. The capillary's geometry plays a role in determining the generated current or voltage. The generation of charge at the solid-liquid interface is a result of both acid-base reactions and the physical adsorption of water ions. Both of these mechanisms are influenced by the pH level of the aqueous solution, making it the most crucial factor affecting the zeta potential. Figure 2.18 illustrates how the zeta potential of solid surfaces with acidic, basic, and amphoteric properties changes at various pH values. It becomes evident that at a specific pH value, the zeta potential reaches 0 mV and changes its polarity. This point is referred to as the isoelectric point (IEP), which is defined as the pH level of the aqueous solution where there is a balance between positively and negatively charged surface groups. When the zeta potential is plotted as a function of pH using well-defined curves, surfaces display only one type of functional group. The curve exhibits a plateau at different positions depending on whether the surface demonstrates acidic, basic, or amphoteric behavior.
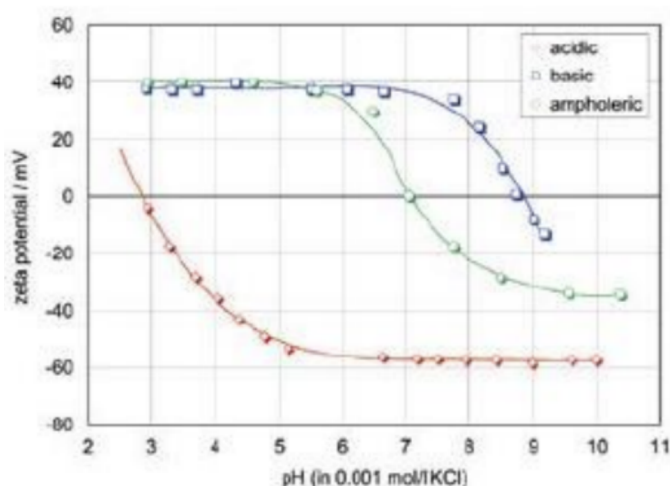
Figure 2.18: Dependence of the zeta potential for surfaces with acidic, basic, amphoteric properties.[48]

To calculate the zeta potential, the Helmholtz- Smoluchowski equation (1) is used, which provides a linear relationship between fluid flow rate and the zeta potential.

$$(1) \qquad \zeta = \frac{Istr}{\Delta p} * \frac{\eta}{\varepsilon * \varepsilon 0} * \frac{L}{A}$$

Where Istr is the flow current, Deltap is the pressure difference within the cell, Eta is the viscosity of the electrolyte solution, Epsilon*Epsilon0 is the dielectric coefficient of the electrolyte solution, L is the length of the rectangular channel formed by the two parallel samples, and A is the area defined by the distance between the two samples and their width.[48]

2.6.2   Isoelectric point

The isoelectric point (IEP) is the pH of a solution at which the protein carries no net electrical charge. When IEP is lower than the pH of the solution the net protein charge is predominantly negative, while IEP value above the pH of the solution occurs when the surface charge of the protein is mostly positive. Therefore, IEP is the value at which there is a balance of positive charges (protons) and negative charges. This is due to the decrease of repulsive electrostatic forces at the IEP and, consequently, the prevalence of attractive electrostatic forces, that leads to aggregation and/or precipitation.
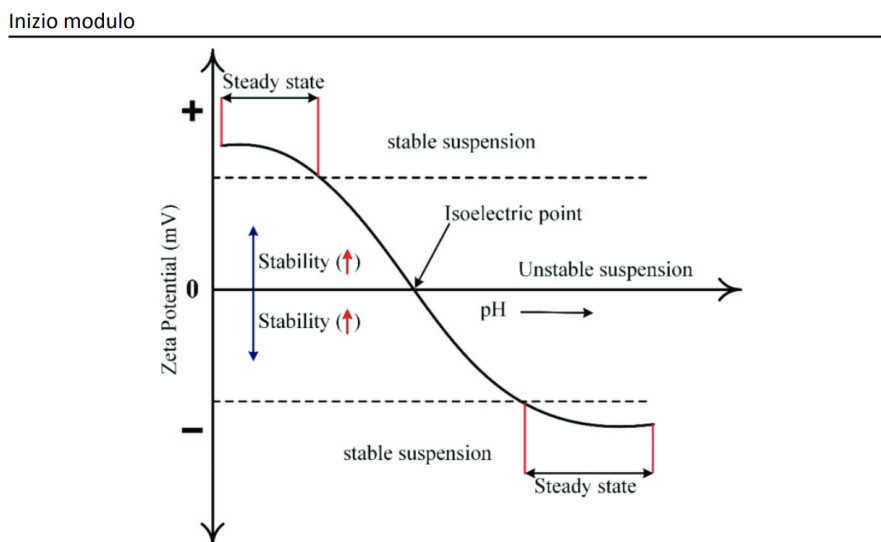
Figure 2.19: Diagram of zeta potential vs. pH, which show the isoelectric point and the areas of stability. [49]

It is influenced by the type and the number of groups ionizable in solution. Therefore, isoelectric point in a protein can be calculated by the average of acid dissociation constant (pKa) values of ionizable groups. For instance, lysine has two amino acid

groups that must be considered, that can gain or lose protons, depending on the pH of the environment. The difference is that the isoelectric point provides information about the global basic (IEP>7) or acid (IEP<7) character of protein, while pKa alone is not a significant value. [50] Isoelectric point can be determined through zeta potential measurement (Figure 2.19) and can be useful in evaluating the success of functionalized titanium on the surface and investigate changes in terms of surface charges. In addition, IEP provides information about the stability of antibacterial agent on titanium substrate, peptoid's adsorption, and pH value at which the electrostatic interaction between the biomolecule (the peptoid in our case) and the surface is the highest.[47]

2.7   Applications

Peptoid have gained significant interest in biomedical applications, including drug discovery and development, medicine, and nanotechnologies. They have shown to be an important resource in biomaterial research for several reasons, e.g degradable backbone, simple synthesis, biocompatibility, low toxicity, stability, and tolerance to thermal processing. Peptoids have shown considerable potential in neurotherapy, diagnostic and therapeutic, especially in neurological disorder and neurogenerative diseases51, as well as lung surfactants.[52] They can also be used as tools to investigate biological processes and chemical reactions. In this area, they can be applied as ligands for relevant targets in pharmaceutic context53, inhibitors of protein-protein interaction54, and biosensors55. Furthermore, peptoids have demonstrated promising clinical perspective to create antifouling coating on the surface of medical devices.[56] Thanks to their ability to simulate nature self-organization, they have also been explored as drug deliverer[57], molecular scaffolds[58], and nanotubes.[59]
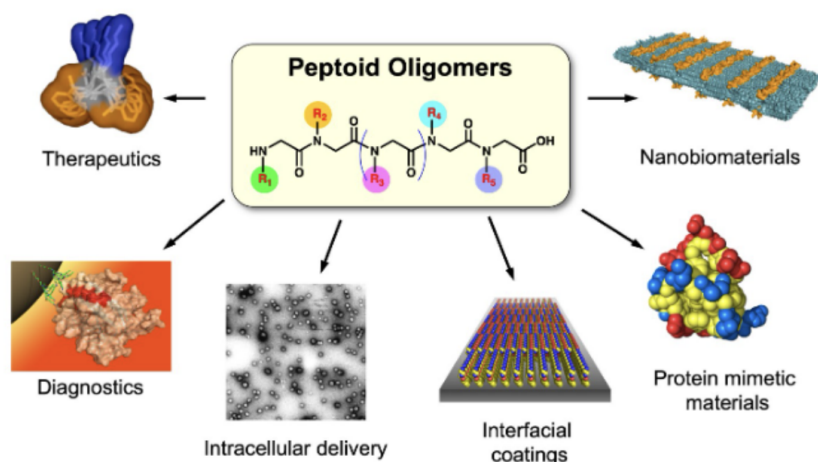
Figure 2.20: Main applications of peptoid in biomedicine and nanotechnologies. [60]

2.8 Future perspectives

The significant progress and the unique advantages in peptoids have increased the interest in the scientific community. However, there are still several critical issues that may hinder the translation of peptoids into practical applications. These have propelled researchers to face different challenges to increase the industrial production and development of peptoids. To date, the research is mainly focused on the prediction of structure-activity relationship, basing on peptoid sequences. It is necessary to understand how the specific modification of the sequence (e.g hydrophobicity or cationic content) may influence the properties and the biological activity. Conventional techniques commonly employed for studying peptides, such as X-ray crystallography or NMR, present challenges when applied to peptoids. This is essentially due to the lack of an amide proton, the amide bond isomerization and the little size possessed, making data interpretation arduous. The lack of high-quality structural characterization methods hinders the validation and the optimization of peptoid design and reduce the comprehension of peptoids conformation and dynamics.[62] Other issues about peptoids concern toxicity and susceptibility to hydrolytic degradation. Despite the high number of identified potential antimicrobial peptoids with negligible or absent toxicity, some studies have demonstrated that some peptoid compounds increase their toxicity on mammalian cells with the increase of their antimicrobial activity, resulting in a lower biocompatibility, compared with natural peptides.[63] The susceptibility to hydrolytic degradation may limit peptoid stability and bioavailability in diverse therapeutic applications.[52] Concurrently, there is growing research on solid-phase synthesis methods to address its limitations and produce polypeptoids with higher molecular weight. It is intended to delineate approaches to enhance solid-phase synthesis, offer technical insights into automated synthesizers, and provide a perspective on the progress in synthetic methodologies.[21]

References: Chapter 2

1. Frank Schwarz, Jan Derks, Alberto Monje, Hom-Lay Wang. "Peri-implantitis". Journal of periodontology (2018), Volume 89, Issue S1.

2. Angel Insua, Alberto Monje, Hom-Lay Wang, Richard J. Miron. "Basis of bone metabolism around dental implants during osseointegration and peri-implant bone loss". Journal of Biomedical Materials Research (2017), Volume105, Issue7, 2075-2089.

3. Muhammad Ashraf Nazir. "Prevalence of periodontal disease, its association with systemic diseases and prevention". Int J Health Sci (Qassim). (2017); 11(2): 72–80.

4. Andrea Ravidà, Matthew Galli, Rafael Siqueira, Muhammad H. A. Saleh, Pablo Galindo-Moreno, Hom-Lay Wang. "Diagnosis of peri-implant status after peri-implantitis surgical treatment: Proposal of a new classification". Journal of periodontology (2020). Volume91, Issue12, 1553-1561.

5. Philipp Sahrmann, Fabienne Gilli, Daniel B. Wiedemeier, Thomas Attin, Patrick R. Schmidlin, and Lamprini Karygianni. "The Microbiome of Peri-Implantitis: A Systematic Review and Meta-Analysis". Microorganisms (2020); 8(5): 661.

6. Lars-Ove Brandenburg, Julika Merres, Lea-Jessica Albrecht, Deike Varoga, and Thomas Pufe. "Antimicrobial Peptides: Multifunctional Drugs for Different Applications". Polymers (2012) 539-560.

7. Linlin Fan, Jian Sun, Meifeng Zhou, Jie Zhou, Xingzhen Lao, Heng Zheng, Hanmei Xu. "DRAMP: a comprehensive data repository of antimicrobial peptides". Scientific Report (2016).

8. Katsumi Matsuzaki. "Control of cell selectivity of antimicrobial peptides". Biochimica et Biophysica Acta (BBA) - Biomembranes (2009) 1687-1692.

9. Muthuirulan, Pushpanathan, Paramasamy Gunasekaran, and Jeyaprakash Rajendhran. "Antimicrobial Peptides: Versatile Biological Properties". Int J Pep (2013).

10. K A Brogden, M Ackermann, and K M Huttner. "Small, anionic, and charge-neutralizing propeptide fragments of zymogens are antimicrobial". Antimicrob Agents Chemother (1997) 1615–1617.

11. Miray Tonk-Rügen, Daniel Ruzek, Andreas Vilcinskas. "Compelling Evidence for the Activity of Antiviral Peptides against SARS-CoV-2". Viruses (2021) 13,912.

12. F. Guilhelmelli, N. Vilela, P. Albuquerque, L.d.S. Derengowski, I. Silva-Pereira. "Antibiotic development challenges: the various mechanisms of action of antimicrobial peptides and of bacterial resistance" Front. Microbiol. (2013) 4-353.

13. W. Kutner. "Mechanism of disruption of model bacterial cell membranes by antimicrobial peptides". ZB 02 - Group of molecular films research (2018).

14. Amy T. Y. Yeung, Shaan L. Gellatly & Robert E. W. Hancock. "Multifunctional cationic host defence peptides and their clinical applications". Cellular and Molecular Life Sciences (2011) Vol.68, 2161–2176.

15. Keld Fosgerau, Torsten Hoffmann. "Peptide therapeutics: current status and future directions". Drug Discovery Today (2015) 122-128.

16. Josef Vagner , Hongchang Qu, Victor J Hruby. "Peptidomimetics, a synthetic tool of drug discovery". Curr Opin Chem Biol. (2008). 12(3): 292–296.

17. Dylan E. Parsons, Soo Hyeon Lee, Young Joo Sun, Gabriel Velez, Alexander G. Bassuk, Mark Smith, Vinit B Mahajan. "Peptidomimetics Therapeutics for Retinal Disease". Biomolecules (2021) 11(3):339.

18. Abigail Mae Clapperton Jon Babi and Helen Tran. "A Field Guide to Optimizing Peptoid Synthesis". ACS Polym. (2022), 2, 6, 417–429.

19. Ronald N. Zuckermann. "Peptoid origins". Peptide Science (2010), Vol. 96, 545-555.

20. N. Gangloff, J. Ulbricht, T. Lorson, H. Schlaad and R. Luxenhofer, "Peptoids and polypeptoids at the frontier of supra- and macromolecular engineering," Chemical Reviews, vol. 116, no. 4, pp. 1753-1802, 2016.

21. Diego Arantes Teixeira Pires, Marcelo Porto Bemquerer, Claudia Jorge do Nascimento. "Some Mechanistic Aspects on Fmoc Solid Phase Peptide Synthesis". Int J Pept Res Ther (2014) 20:53–69.

22. Konstantin Andreev. "Membrane-drug interaction mechanisms of peptoid-based antimicrobial agents". Thesis for: Doctor of Philosophy (2017).

23. R.N. Zuckermann, J.M. Kerr, S.B.H. Kent, W.H. Moos. "Efficient method for the preparation of peptoids [oligo(N-substituted glycines)] by submonomer solid-phase synthesis" J. Am. Chem. Soc. (1992) 114, 10646.

24. Dominik K. Kölmel, Daniel Fürniss, Steven Susanto, Andrea Lauer, Clemens Grabher, Stefan Bräse, Ute Schepers. "Cell Penetrating Peptoids (CPPos): Synthesis of a Small Combinatorial Library by Using IRORI MiniKans"Pharmaceuticals (2012) 5(12):1265-1281.

25. J. Seo, B.C. Lee, R.N. Zuckermann. "Peptoids: Synthesis, Characterization, and Nanostructures". P. Ducheyne, K.E. Healy, D.W. Hutmacher, D.W. Grainger, C.J. Kirkpatrick (eds.) Comprehensive Biomaterials (2011), vol. 2, 53-76 Elsevier.

26. Tetsuo Uno, Eric Beausoleil, Richard A. Goldsmith, Barry H. Levine and Ronald N. Zuckermann. "New Submonomers for Poly N-Substituted Glycines (Peptoids)". Tetrahedron Letters 40 (1999) 1475-1478.

27. Kevin L. Bicker and Steven L Cobb. "Recent advances in the development of anti-infective peptoids". Chemical Communication (2020) 56, 11158-11168.

28. Abshar Hasan, Varun Saxena, Valeria Castelletto,Georgina Zimbitas, Jani Seitsonen, Janne Ruokolainen, Lalit M. Pandey,Jan Sefcik, Ian W. Hamley, and King Hang Aaron Lau. "Chain-End Modifications and Sequence Arrangements of Antimicrobial Peptoids for Mediating Activity and Nano-Assembly". Frontiers in Chemistry (2020) 8:416.

29. Bingyun Li and Thomas J. Webster. "Bacteria Antibiotic Resistance: New Challenges and Opportunities for Implant-Associated Orthopaedic Infections". J Orthop Res. (2018) 36(1): 22–32.

30. Sarah A. Fowler and Helen E. Blackwell." Structure-function relationships in peptoids: Recent advances toward deciphering the structural requirements for biological function". Org. Biomol. Chem. (2009) 7, 1508-1524.

31. Kalita D, Sahariah B, Pravo Mookerjee S, Kanta Sarma B. "Strategies to Control the Cis-Trans Isomerization of Peptoid Amide Bonds". Chem Asian J. (2022); 17(11)

32. Min-Kyung Shin, Yu-Jung Hyun, Ji Hoon Lee, and Hyun-Suk Lim. "Comparison of Cell Permeability of Cyclic Peptides and Linear Peptides". ACS Combinatorial Science. (2018), 237–242.

33. Miller S.M., Simon R.J., Ng S., Zuckermann R.N., Kerr J.M., Moos W.H. Comparison of the proteolytic susceptibilities of homologous L-amino acid, D-amino acid, and Nsubstituted glycine peptide and peptoid oligomers. Drug Develop. Res. (1995), 35:20– 32.

34. Cindy W. Wu, Tracy J. Sanborn, Kai Huang, Ronald N. Zuckermann, and Annelise E. Barron. "Peptoid Oligomers with α-Chiral, Aromatic Side Chains: Sequence Requirements for the Formation of Stable Peptoid Helices". Journal of the American Chemical Society. (2001), 123, 28, 6778–6784.

35. Sarah A. Fowler and Helen E. Blackwell* Structure-function relationships in peptoids: Recent advances toward deciphering the structural requirements for biological function. Org Biomol Chem. (2009); 7(8): 1508–1524.

36. A. Lone, A. Arnous, P. R. Hansen, B. Mojsoska, and H. Jenssen. "Synthesis of Peptoids Containing Multiple Nhtrp and Ntrp Residues: A Comparative Study of Resin, Cleavage Conditions and Submonomer Protection". Front. Chem. (2020), vol. 8, no. April, pp. 1–12.

37. Nyembe PL, Ntombela T, Makatini MM. Review: Structure-Activity Relationship of Antimicrobial Peptoids. Pharmaceutics. 2023 May 15;15(5):1506.

38. Ximian Xiao, Dr. Min Zhou, Zihao Cong, Jingcheng Zou, Prof. Runhui Liu. "Advance in the Polymerization Strategy for the Synthesis of β-Peptides and β-Peptoids". ChemBioChem (2023), Vol. 24, Issue 3.

39. Emiliana De Santis, Thomas Hjelmgaard, Cecile Caumes, Sophie Faure. "Effect of capping groups at the N- and C-termini on the conformational preference of α,β-peptoids"Organic & Biomolecular Chemistry (2011), 10(5):1108-22.

40. S. Spriano, V.S. Chandra, A. Cochis, F. Uberti, L. Rimondini, E. Bertone, A. Vitale, C. Scolaro, M. Ferrari, F. Cirisano, G.G. di Confiengo, S. Ferraris. "How do wettability, zeta potential and hydroxylation degree affect the biological response of biomaterials?" Mater. Sci. Eng. C 74 (2017) 542–555.

41. Guang Wei Lu, Ping Gao. Handbook of Non-Invasive Drug Delivery Systems". Non-Invasive and Minimally-Invasive Drug Delivery Systems for Pharmaceutical and Personal Care Products (2010), Chapter 3, Pages 59-94.

42. Vijayakumar Selvamani. "Characterization and Biology of Nanomaterials for Drug Delivery". Nanoscience and Nanotechnologies in Drug Delivery (2019), Chapter 15, 425-444.

43. Punamjyoti Das, Malay K. Das. "Nanocosmeceuticals". Innovation, Application, and Safety (2022), Chapter 4, 95-138.

44. Virginia Alessandra Gobbo, Mari Lallukka, Francesca Gamna, Mirko Prato, Alessandra Vitale, Sara Ferraris, Ziba Najmi, Andrea Cochis, Lia Rimondini, Jonathan Massera, Silvia Spriano. "Functionalization of a chemically treated Ti6Al4V-ELI alloy with nisin for antibacterial purposes". Applied Surface Science (2023).

45. Luxbacher T. "The ZETA Guide Principles of the Streaming Potential Technique." Anton Paar, Graz, 2014.

46. Surendran V. Sujith, Hansoo Kim, Joonho Lee. "A Review on Thermophysical Property Assessment of Metal Oxide-Based Nanofluids: Industrial Perspectives". Metals - Open Access Metallurgy Journal (2022) 12(1):165.

47. Serban C. Moldoveanu, Victor David. "Properties of Analytes and Matrices Determining HPLC Selection". Selection of the HPLC Method in Chemical Analysis (2017) 189-230.

48. Lauren M. Wolf, Shannon L. Servoss, and Melissa A. Moss. "Peptoids: Emerging Therapeutics for Neurodegeneration". Journal of Neurology & Neuromedicine (2017).

49. Cindy W Wu 1, Shannon L Seurynck, Ka Yee C Lee, Annelise E Barron. "] Helical peptoid mimics of lung surfactant protein C.". Chem Biol. (2003) 10(11):1057-63.

50. Di Cai, A-Young Lee, Cheng-Ming Chiang, and Thomas Kodadek. "Peptoid Ligands That Bind Selectively to Phosphoproteins". Bioorganic & Medicinal Chemistry Letters (2011) Volume 21, Issue 17, Pages 4960-4964.

51. Toshiaki Hara, Stewart R Durell, Michael C Myers, Daniel H Appella. "Probing the structural requirements of peptoids that inhibit HDM2-p53 interactions". J Am Chem Soc. (2006) 128(6):1995-2004.

52. Adrian S Culf. "Peptoids as tools and sensors". Biopolymers (2019), Volume 110, Issue 6.

53. Andrea R Statz, Robert J Meagher, Annelise E Barron, Phillip B Messersmith. "New peptidomimetic polymers for antifouling surfaces". J Am Chem Soc. (2005), 127(22):7972-3 23.

54. Christian Secker, Sarah M. Brosnan, Robert Luxenhofer, Helmut Schlaad. "Poly(α-Peptoid)s Revisited: Synthesis, Properties, and Use as Biomaterial". Macromoleculare Bioscience (2015), Volume 15, Issue 7, pages 881-891.

55. Boyeong Kang, Woojin Yang, Sebok Lee, Sudipto Mukherjee, Jonathan Forstater, Hanna Kim, Byoungsook Goh, Tae-Young Kim, Vincent A Voelz, Yoonsoo Pang, Jiwon Seo. "Precisely tuneable energy transfer system using peptoid helix-based molecular scaffold". Scientific Reports volume 7 (2017).

56. Viswanathan S. Saji. "Supramolecular organic nanotubes for drug delivery". Materialstoday Advances, Volume 14 (2022).

57. Michael D. Connolly, Sunting Xuana, Natalia Molchanova and Ronald N. Zuckermann "Submonomer synthesis of sequence defined peptoids with diverse sidechains."

58. James R. B. Eastwood, Ethan I. Weisberg, Dana Katz, Ronald N. Zuckermann, Kent Kirshenbaum. "Guidelines for designing peptoid structures: Insights from the Peptoid Data Bank". Peptide Science (2023), Volume 115, Issue 3.

59. H. L. Bolt, G. A. Eggimann, C. A. B. Jahoda, R. N. Zuckermann, G. J. Sharples, and S. L. Cobb. "Exploring the links between peptoid antibacterial activity and toxicity". Medchemcomm. (2017); 8(5): 886–896.

Chapter 3

Peptoids Antibiofilm Activity

3.1 Oral implant infections

3.1.1 Microbiota correlated with healthy implant tissue

The oral microbiota in health conditions involves harmless microorganisms known as commensal. Healthy peri-implant tissues are predominantly populated by a high number of coccoid aerobic Gram-positive species, including Streptococcus species, Granulicatella species, Abiotrophia species, Methanogens (Methanobrevibacter oralis, Methanobrevibacter massiliense) and Gemella species. Gram positive filamentous (Actinomyces), and Gram-negative cocci (Veillonella and Neisseria) are also observed. On the other hand, anaerobic species, Gram-negative species and periodontopathogenic bacteria are in low proportions.[1,3] A microbial balance within the oral microbiome has a key role in strengthening the immune system through a phenomenon known as "colonization resistance". This mechanism guarantees the bacteria action as a protective barrier against harmful external microorganisms.[4,5] In addition, oral bacteria have been shown to convert nitrate into nitrite, which is then transported through the bloodstream and converted into nitric oxide, a natural molecule that helps the regulation of blood pressure. Oral bacteria that reduce nitrate into nitrite have been found to have antimicrobial effects against acid-producing bacteria like Streptococcus, preventing caries.[6,7]

3.1.2 Microbiota correlated with implant infections

Humans and bacteria generally have a symbiotic relationship, wherein unicellular organisms depend on nutrients and biochemical signals provided by multicellular organisms. Scientific studies have demonstrated that maintaining a balance of resident microflora in human body is extremely important for the overall health, because these microorganisms in human mouth play a crucial role in regulating host metabolism and immune system. However, oral homeostasis can be disrupted by physiological and environmental factors, including immune dysregulation, the placement of implants or the use of antibiotic therapy. When the organization of bacteria is not balanced, the condition is known as dysbiosis, a condition in which bacteria possess the ability to

negatively influence host immune response, leading to a damage of periodontal tissues through the production of enzymes and metabolites. In this situation, a more aggressive immune-inflammatory response occurs and, consequently, the disruption of periodontal tissue is more rapid and intense (figure 3.1).[7,8]

Microbiota associated with peri-implantitis are more complex and diverse compared to the microbiota found in healthy peri-implant conditions. The analysis on biofilms in peri-implantitis revealed the prevalence of Aggregatibacter actinomycetemcomitans, Bacteroidetes spp., Actinomyces spp., Campylobacter rectus, Treponema denticola P. gingivalis, F.nucleatum, Tanerella forsythia, S. aureus and Prevotella intermedia, absents in healthy and periodontal implants. Researchers also observed a predominance of Eubacterium nodatum, Fusobacterium spp., Veillonella spp., Treponema spp., and Synergistetes cluster A around diseased implants. Therefore, the microbiome associated with unhealthy conditions is characterized by Gram-positive aerobe rods, bacillo and bacillo-cocci anaerobic Gram-negative bacteria, and fusiform pathogens P. nigrescens and E. nodatum.[1,2]

Patient health condition is also relevant in implant infections microbiota studies. For instance, smokers tend to exhibit a higher microbial diversity in both healthy and diseased states in comparison with non-smokers.[2]
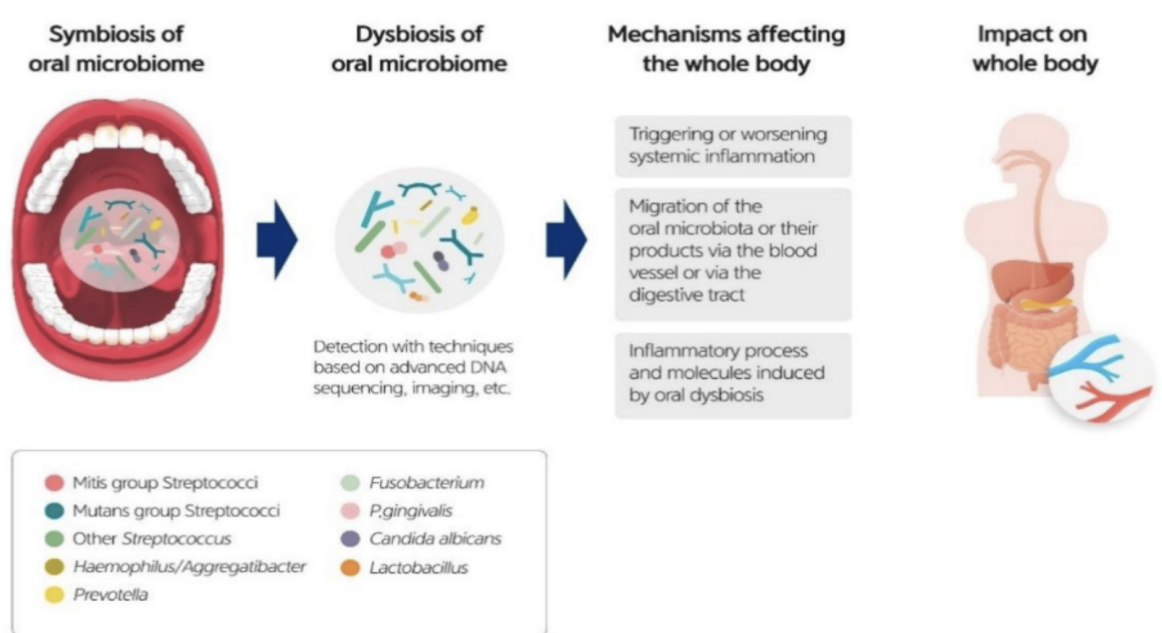

Figure 3.1: Impact of unbalanced microbiota on the whole human health in the oral cavity.[9]

3.2   Biofilm

Biofilms are described as complex aggregation of bacteria enclosing and growing in an exopolysaccharide matrix, through which they are attached to the tooth surface. The increasing problem of antibiotic resistance has led to the ineffectiveness of antibiotics and the generation of infections related to biofilm formation.[10] Biofilm found on the tooth surface is named dental plaque. Dental plaque is the main etiologic cause of dental diseases (about 65%), including periodontitis, caries and peri-implantitis. It is also the principal reason of implant failure.[11]

3.2.1   Common dental implants

In order to understand the material properties and functionality of an implant, it is essential to know its various component parts. Each implant may exhibit some variations, but the fundamental components remain consistent across the different systems. Dental implants essentially consist of three primary components: the screw, also known as the implant, which is insert into the alveolar bone through surgical procedure, the abutment, positioned on the top of the implant, serving as a connection between the screw and the external part of the device, the crown, bridge, or denture, that is the external part (figure 3.2). Oral implants can be fabricated using metals and their alloys, ceramics, and polymers.[12]
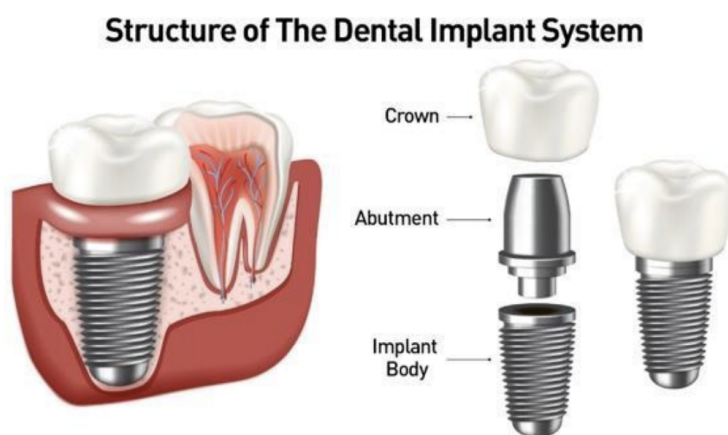
Figure 3.2: The different components of a dental medical device.13

3.2.2   Dental plaque formation on titanium surfaces

The formation of the oral biofilm, also known as dental plaque, on the surface of dental implants involves several sequential steps. The immediate biological response of the human body to the insertion of a titanium implant in the oral cavity involves a process of protein adsorption. The rapid contact of titanium surface to the protein-rich fluid, saliva or blood plasma, lead to the formation of a thin protein layer on titanium surface. This biological interaction is facilitated by the proteins that compose the thin layer formed on titanium, including fibronectin, serum albumin, apolipoprotein, and

fibrinogen, and the corrosion on titanium surface is prevented by the organic and inorganic species that predominantly compose the salivary pellicle, such as glycoproteins, lipids, calcium, phosphate, and amino acids. However, high bacterial density can limit this protective mechanism. The subsequent step involves the adhesion of bacteria on the surface. Oral bacteria can adhere to the surface through multiple interactions with host molecules and receptors of other bacteria, such as electrostatic forces, Van der Waals forces and hydrogen bonding.[14] The attachment of bacteria on the tooth surface through interactions involves the so-called pioneers (or early colonizer), acting as receptors for late colonizer bacteria. Pioneers bound to tooth surface are represented by Streptococcus, Actinomyces spp., Haemophilus spp., Capnocytophaga spp., Veillonella spp., and Neisseria spp.. They provide additional binding sites for subsequent bacteria, known as late colonizer, including Aggregatibacter actinomycetemcomitans, Porphyromonas gingivalis, and Fusobacterium nucleatum, which recognize receptors on the bacterial surface and promote biofilm growth and higher pathogenicity over time, causing the maturation of dental plaque.[14,15] This attachment of bacteria entails the formation of an organized microbial accumulation and the subsequent development of biofilm. The well-structured bacterial community produce a matrix, known as extracellular polymeric substance (EPS), in which bacteria are embedded. EPS enhances microbial adhesion, establishes an acidic microenvironment, and provides nutrients, hindering the mechanical removal of the biofilm and increasing the resistance to antimicrobial drugs on the metal surface.[14]
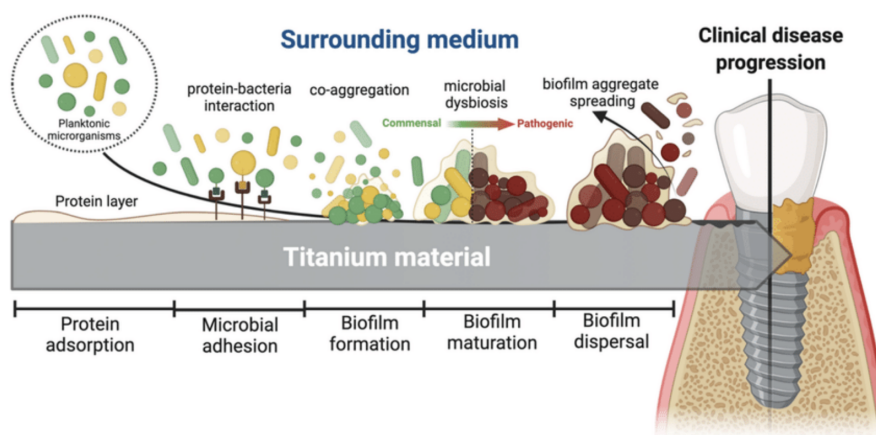
Figure 3.3: Steps involved in the formation of biofilm on dental implants and their impact on the progression of diseases related to titanium implant.[14]

3.2.3 Quorum sensing

Quorum sensing (QS) is a vital mechanism employed by oral bacteria within biofilm to communicate each other and coordinate their activity via chemical signaling. QS involves the release of signaling molecules known as autoinducers (AI), into the surrounding environment, which grows with bacteria density. Once the extracellular concentration of AI reaches a particular threshold, biofilm bacteria detect the presence

of these signaling compounds and consequently modulate gene expression, resulting in coordinate responses among bacteria, which act as a collective entity, permitting more effective response to environmental changes. These responses can include the regulation of biofilm development, such as the secretion of EPS, as well as biofilm maturation and dispersal, and the production of virulence factors.[16] The accumulation of biofilm bacteria within the self-induced EPS, generally made of polysaccharides, allows an increasing bacteria resistance against antimicrobial agents and host immune defenses and the alteration of gene expression contribute to the resistance of biofilm to common drugs, that are not able anymore to target specific active pathways in biofilm.[16,17] An explored study of QS has demonstrated that the majority of pathogenic microorganisms involved in periodontitis is associated with the Gram-negative anaerobe P. gingivalis, which presence in significant proportion drive to dysbiosis throughout the entire microbiota. Generally, the researchers are mainly focus on the red-complex species, including P. gingivalis, T. denticola and T. forsythia, because of their crucial role in periodontal pathogenesis. F. nucleatum has also been recognized as the responsible for the accumulation of commensal bacteria and pathogenic periodontal microorganisms in EPS.[16]

3.3 Antimicrobial peptoids mode of action

The development of antibiofilm compounds is a critical tool in managing human infections. The presence of EPS reduces the effectiveness of conventional drugs, as they can't penetrate through the biofilm and reach bacteria inside. Furthermore, biofilms are typically less metabolically active than planktonic bacteria, reducing the susceptibility to antibiotics used for metabolic processes. Antimicrobial peptoids have been proposed as potential anti-biofilm therapeutic agents, which can substitute the inefficient common drugs.[17,18]

3.3.1 Bacterial classification and membrane composition

Bacteria can be classified as Gram-positive or Gram-negative based on the characteristics of their cell wall, as depicted in Figure 3.3.
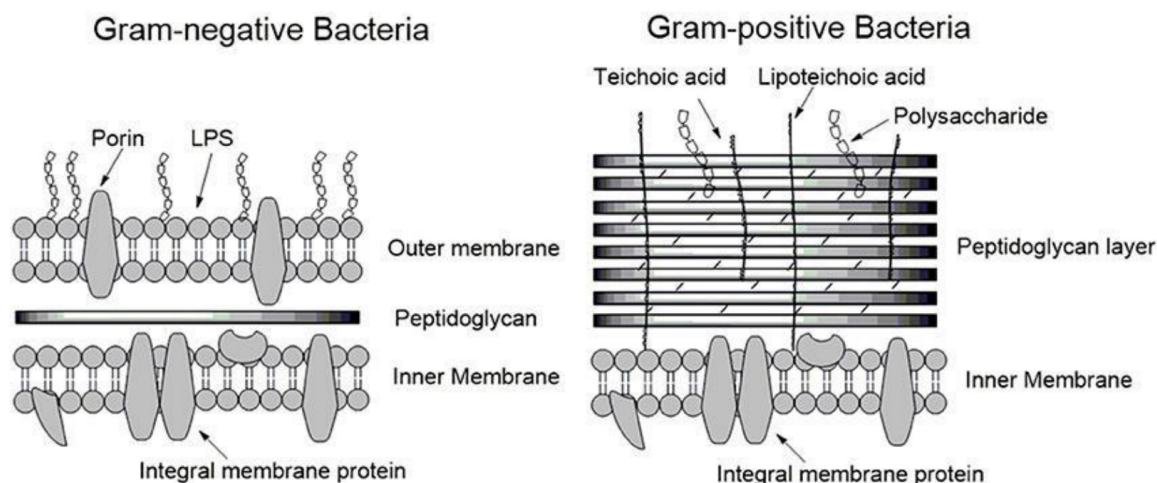
Figure 3.4: Schematic diagram that shows the differences of Gram-positive and Gram-negative cytoplasmatic membranes.[19]

Gram-negative bacteria are composed of a double bilayer structure, with a thin (2-3 nm) peptidoglycan layer included between the two bilayers. In addition, they have an outer membrane with lipopolysaccharides. Consequently, increasing the hydrophobicity is believed to enhance peptoids' insertion into the core of the membrane, leading to improved permeabilization. On the other hand, Gram-positive bacteria are made up of a single lipid bilayer with a thick (20-80 nm) outer layer of peptidoglycan. They generally exhibit greater susceptibility to membrane-active compounds, due to the absence of an outer lipid membrane.[19,20] These differences in membrane composition among pathogenic bacteria are important to understand peptoids response.

It is believed that the antimicrobial peptoid mechanisms of action that lead to membranes destabilization show a lot of similarities to those of antimicrobial peptides. This is reinforced by findings indicating that these two classes of molecules exhibit a synergic action.[26] Based on structural similarities, it is also thought that the mechanism of action of peptoids strongly relies on charge and hydrophobicity, like AMPs. In AMPs, a balance between charge and hydrophobicity facilitates electrostatic interactions with bacterial cell wall, leading to membrane lysis. With this in mind, the mechanism of action for these antimicrobial agents is closely associated with either the creation of pores, that disrupt bacterial membranes, or the penetration of bacterial membranes and subsequent targeting of cytoplasmatic compartments.[21]

3.3.2 Linear and cyclic peptoids

Linear and cyclic structures exhibit a non-significant damage on erythrocytes' membranes and a strong and selective antimicrobial activity against a wide range of microorganisms, including bacteria and fungi. Peptoids with a cyclical structure are more active than their linear counterpart, because of their higher conformational rigidity, stability, and well-defined secondary structure, which allow the ability to form tighter bounds with microbial targets, without considerable entropy penalty. There-

fore, cyclic peptoids are particularly used as targets of intracellular proteins. However, cyclic peptoids have shown lower cellular uptake, regardless of their size and side chains, indicating that linear peptoids may have an enhanced cellular permeability. Therefore, linear peptoids have a considerable ability to interact with biological target and mimic some peptide motifs. These results suggest that peptoids structural characteristics can condition and modulate their biological activity.[22,23]

3.3.3 α-peptoid helices

An investigation on the effect of hydrophobicity and amphipathicity on linear α-peptoids noticed that an increased hydrophobicity in helical peptoids leads to a greater antibacterial activity (comparison between 1 and 2, Figure 3.5). It was also studied the effects of the length, demonstrating a lower potency in shorter peptoids (peptoid 3 with 6 residues shows a higher MIC value against E. coli compared to peptoid 4 with 15 residues), but a greater hemolysis in longer peptoids. In addition, it was noticed that positively charged side chains increase peptoids antibacterial potency (in peptoid 5 the negative charge result in an almost inactive compound).[24]

Linear sequences	Net charge	MIC (µM)	Selectivity ratio
1.(NLysNssbNspe)$_4$	+4	31	>3.9
2.(NLysNsmbNspe)$_4$	+4	7.4	>16
3.(*N*Lys-*N*spe-*N*spe)$_2$	+2	27	+13
4.(*N*Lys-*N*spe-*N*spe)$_5$	+5	5.5	0.55
5.(NGluNspeNspe)$_4$	-4	>219	n/a

Figure 3.5: A summary of mentioned peptoids and their associated antibacterial data. The selectivity ratio is SR = (10 % hemolytic dose)/ (MIC E. coli). Minimal inhibitory concentration (MIC) is the lowest concentration of an antimicrobial agent to be inhibit the proliferation of a particular bacteria.

The findings regarding (NLysNspeNspe)-motifs appear to be aligned with previous studies on the α-peptoids GN-2, which will be examined in depth in the following chapters.[25,27]

3.3.4 β-peptoids

The antibacterial activity of βpeptoid was studied by Shuey and coworkers, which investigated a screening of twenty-one βpeptoid compounds with different hydrophobic and cationic content. They noticed that the positive charges allowed an easier disruption of membranes integrity and, consequently, bacterial death. The lowest activity

of 128 micro-g/mL against E. coli had been displayed in six peptidomimetics, about one order of magnitude lower than natural antimicrobials one, revealing a significant antibacterial activity.[28]

3.3.5 Investigation of GN-2 peptoid as antibacterial agents

GN-2 peptoids are a collection of peptoids modeled upon the synthetic GN-2 peptides, which were identified through a QSAR-based in silico approach as part of a cohort of peptides. Preliminary investigations have shown promise as effective antimicrobial agents, indicating that both the peptoid variants and the original peptide GN-2 displayed antimicrobial properties, as they induced significant membrane damage. However, it is important to note that while GN-2 peptides and GN-2 peptoids share some similarities, they are not exact analogues, suggesting potential differences in their mechanisms of action or spectrum of activity.[29]
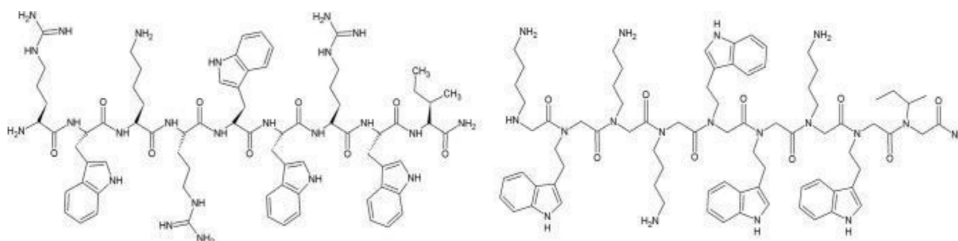

Figure 3.6: Chemical configuration of GN-2 peptide on the left, and chemical structure of GN-2 peptoid on the right.[30]

GN2-Npm9 has emerged as a promising alternative in antimicrobial research due to its high level of potency against biofilms, which is achieved even at low concentrations. Many studies have investigated the mode of action of diverse GN2 peptoids against biofilm bacteria.[29,31,32] Particular interest was showed for peptoids GN-2, GN-2-Nlys1-4-Ntrp5-8, and GN2-Npm9. The investigation of GN2 and GN2-Npm9 has revealed important insight into their penetration mode of action in Gram-negative E. Coli. The concentration of peptoid was found to influence its penetration through the outer membrane, with higher concentrations promoting greater penetration. Once across the outer membrane, GN2-Npm9 showed a lower penetration compared with GN2, probably due to the presence of the aromatic Npm residue, which enhanced the hydrophobic interactions with the outer membrane lipids. However, these interactions were facilitated by electrostatic forces between positively charged antimicrobial surface and lipid bilayer.

Investigated GN2 peptoids demonstrated a potential to undergo oligomerization trough aromatic side-chain interactions, enabling deeper penetration into the hydrophobic extracellular polymeric substance matrix, that protects bacterial biofilms. The remarkable efficacy of these antimicrobials against biofilms is given by the significantly higher tolerance of antibiotic concentration, compared to the tolerance of planktonic cells. In Figure 3.8, a comparison between GN2 peptides and peptoids structures show
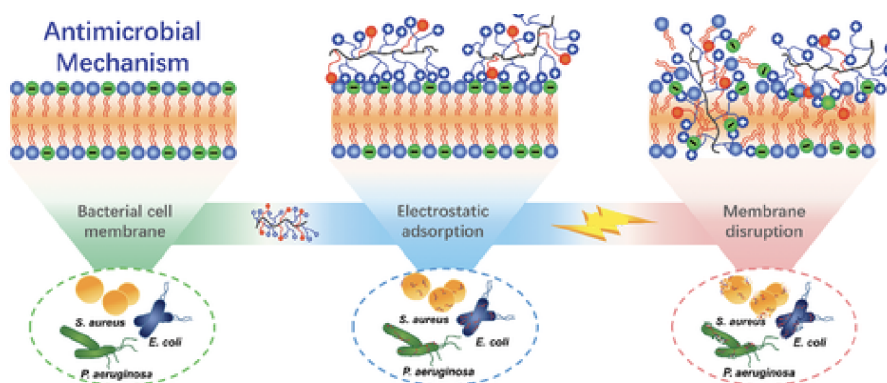
Figure 3.7: Schematic representation of AMPs and peptoids mode of action.[31]

the significant improvement in biofilm eradication of peptoids. This confirms the high potential role of peptoids as alternative drugs to prevent infections.
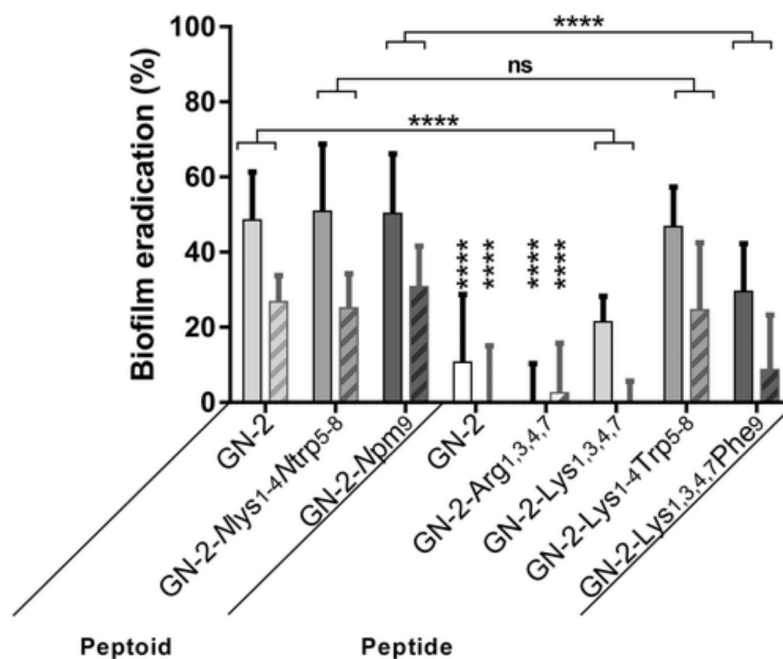
Figure 3.8: Biofilm eradication in peptides and peptoids. [29]

3.4   Structure-activity relationship in GN2 peptoids

With the goal of enhancing the effectiveness of AMPs, the properties charge, hydrophobicity and amphipathicity have been considered as the most significant structural elements which influence the overall peptoid antimicrobial activity. The combination of these three elements lends diverse physio-chemical properties that affect how peptoids interact with bacterial and mammalian membranes. Therefore, it is important to find a balance between these properties to guarantee efficient activity and selectivity, while

minimizing toxicity towards mammalian cells.[27,30] Chongsiriwatana's group demonstrated that helical peptoids possess broad-spectrum antimicrobial activity. They observed that peptoids with an appropriate net charge and moderate hydrophobicity exhibited significant antimicrobial activity, while peptoids with high hydrophobicity and amphipathicity were more likely to cause hemolysis, the disruption of red blood cells.[26] The effect of these properties was deeply studied in GN2 peptoids by Jenssen and colleagues. In Figure 3.9 and table 3.10 the obtained results are shown.[10]

1	GN-2	H-Nlys-Ntrp-Nlys-Nlys-Ntrp-Ntrp-Nlys-Ntrp-Nile-NH2	10.54	>128	168
2	GN-2-Ntrp$_{1,2,8,9}$Nile$_7$Nlys$_{3-6}$	H-Ntrp-Ntrp-Nlys-Nlys-Nlys-Nlys-Nile-Ntrp-Ntrp-NH2	10.93	>128	173
3	GN-2-Nlys$_{1-4}$Ntrp$_{5-8}$	H-Nlys-Nlys-Nlys-Nlys-Ntrp-Ntrp-Ntrp-Ntrp-Nile-NH2	11.48	128	110
4	GN2-Npm$_9$	H-Nlys-Ntrp-Nlys-Nlys-Ntrp-Ntrp-Nlys-Ntrp-Npm-NH2	10.79	128	104
5	GN-2-Nae$_{1,3,4,7}$	H-Nae-Ntrp-Nae-Nae-Ntrp-Ntrp-Nae-Ntrp-Nile-NH2	10.81	>128	
6	GN-2-Ndpe$_6$	H-Nlys-Ntrp-Nlys-Nlys-Ntrp-Ndpe-Nlys-Ntrp-Nile-NH$_2$	11.46	16	80
7	GN-6-Ndpe$_{4-7}$	H-Nlys-Nlys-Nlys-Ndpe-Ndpe-Ndpe-Ndpe-Npm-Nlys-NH$_2$	15.43	16	
8	GN-6	H-Nlys-Nlys-Nlys-Ntrp-Ntrp-Ntrp-Ntrp-Npm-Nlys-NH$_2$	10.10	<128	203

Figure 3.9: Analytical retention time (Rt) in vitro, hemolytic concentrations and cytotoxicity of GN2 peptoids against Gram-positive S. aureus bacteria and Gram-negative E. coli and P. aeruginosa. Retention time is, in pharmacokinetics, the duration of a drug remains in the body after administration.[30]

	MIC (µg/µl)			Selectivity ratio
	S.aureus	E. coli	P. aeruginosa	
1	32	32	4	>2-32
2	8	64	4	>2-32
3	8	8	4	4-32
4	8	16	2	8-64
5	16-32	64	8	>4-16
6	4	16	2	0.5-8
7	16	64	64	0.25-1
8	8-16	64	64	<2-16

Figure 3.10: MIC and selectivity ratio of GN-2 peptoids against selected Gram-negative and Gram-positive bacteria.[30]

3.4.1 Effect of charge

Studies have suggested that the charge has an effect on activity and selectivity.[28,33] Chongsiriwatana and coworkers observed that peptoids with a lower charge have less effectiveness against bacteria and similar levels of cytotoxicity. They replaced NLys (N-lysine) side chain groups with zwitterionic NGlu (glutamic acid), noticing the negative impact on antibacterial properties. Their lower antibacterial activity was explained by the lack of strong electrostatic interactions between the peptoid and the negatively charged bacterial membranes. However, it is also important to notice that totally replacing Nlys with uncharged NGlu showed a completely inactive sequence against considered bacteria.[26] In another study on lysine-peptoids, a strong correlation between the hemolytic activity and the number of NLys residues in the sequence was successfully demonstrated. They found that the hemolytic activity was significantly lower, retaining the antibacterial activity, when the number of NLys is higher. However, relying solely on the net charge may not be the most accurate method for the prediction of peptoid hemolytic activity. Instead, the consideration of charge distribution over the entire peptoid can be more beneficial. Recent research findings on lysine-peptoid hybrids have indicated that the charge distribution significantly influences the overall hemolytic activity and antimicrobial activity of the peptoids. Placing all cationic residues at a single end resulted in an increase of hydrophobicity, consequently leading to a higher hemolytic activity, while a pairwise distribution of cationic residues maintained negligible hemolytic effect despite a slightly higher hydrophobicity. Moreover, a distribution with separated charge had the potential to prevent self-association without the alteration of the helix structure, which is important fot its bioactivity. In addition, it was observed that separate distribution of positive charges decreased the hemolytic

activity of peptoids with similar hydrophobicity, but only if a balance between peptide hydrophobicity and charge distribution occured.[27] The overall findings indicate effective strategies for achieving a balance between the hydrophobicity of peptides and their charge distribution, facilitating their efficient penetration and disruption of bacterial membranes while retaining the integrity of mammalian (host) membranes.

3.4.2 Effect of hydrophobicity

Studies conducted on AMPs have shown a relationship between the hydrophobicity of the sequence and the antimicrobial activity. This correlation is attributed to the strong hydrophobic interaction with the target membrane, especially when it is composed of zwitterionic lipids, which is a characteristic of mammalian cells.[30] Barron and coworkers also studied the effect of hydrophobicity. They discovered that higher hydrophobicity is correlated to an increase in antimicrobial activity. However, an increase in the level of hydrophobicity was found to be associated with increased cytotoxicity, leading to lower selectivity ratios.[20] These findings were also demonstrated in the investigation of GN2, GN4 and GN6 peptoids by Jenssen's group. In order to investigate these connections, in Figure 3.9 and 3.10 GN peptoids are reported. Hydrophobicity was increased by substituting Ntrp monomer in peptoid 1 with Ndpe (peptoid 6), resulting in a notably increased antibacterial activity against all tested bacteria, despite it also resulted in higher retention time. However, this also led to a higher toxicity in both human red blood cells and Hela cells, resulting in the lowest selectivity ratios when compared to the other investigated GN-2 peptoids. Moreover, peptoid 3 exhibited higher antimicrobial potency against E. Coli than peptoid 2, suggesting that the position of the individual hydrophobic monomers along the peptoid chain may play a role in the observed behavior.

Jenssen's group observed that an excessive level of hydrophobicity resulted in a dramatic reduction in antimicrobial activity and, consequently, a selectivity ratio, see peptoid 16, whose SR values are 0.25 and 1. Furthermore, they thought that the diminished antimicrobial activity associated with high hydrophobic profiles, was attributed to the strong self-association of the peptoid caused by its excessive hydrophobicity, which hinders its ability to penetrate through the bacterial cell walls. Therefore, maintaining a balance between hydrophobicity and cytotoxicity is crucial for further clinical development, as noticed in chapter 3.4.1.[30] Peptoid 3 and 4 exhibit an excellent hydrophobicity, leading to the highest selectivity ratios, see Figure 3.10. It suggested that the presence of Nlys in the hydrophobic region in peptoid results in a significant reduction of the toxic effect.[30]

3.4.3 Effect of amphiphilicity

The effect of amphiphilicity on peptoid activity was examined through structural analogs designed to investigate if the potency could be affected by altering the sequence of monomers along the peptoid chain, leading to changes in amphiphilicity and charge distribution. In one case, a rearranged version of peptoid 8, resulting in peptoid 4, disrupted the charge cluster located at the N-terminal end, resulting in increased

hydrophobicity. However, this did not significantly show increase in its activity against S. aureus; instead, it exhibited four times higher potency against Gram-negative bacteria E. coli and P. aeruginosa. Despite peptoid 4 appeared to have higher level of toxicity to HeLa cells, the disrupted amphiphilic nature suggested that imperfect separation between charged and hydrophobic monomers can enhance its ability to disrupt bacterial membranes.[10] These results confirmed the previously considerations about lysine-peptoid hybrids analyzed 3.4.1.[27] Another sequence rearrangement involved peptoid 1, where charged residues were placed differently along the peptoid chain. This produced peptoids 2 and 3, with distinct retention times. Peptoid 3, showing increased hydrophobicity at the C terminus, showed enhanced activity against Gram-positive S. aureus, and significantly higher effectiveness against an E. coli. However, no difference in antibacterial activity was observed against P. aeruginosa strains. Regarding toxicity, all three peptoids displayed low hemolytic activity and slightly different toxicity profiles against HeLa cells.[30] Finally, sequence rearrangement in peptoids 1 and 8 resulted in two peptoids, 3 and 4, with optimal hydrophobicity, yielding the highest selectivity ratios among the investigated peptoids.[30]

3.4.4   Overall antimicrobial activity

GN2 peptoids revealed consistently high to moderate antimicrobial activity compared to structurally similar AMPs, retaining the broad-spectrum antibacterial activities. The selectivity ratio provides information about peptoids cell selectivity. Remarkably, different peptoids within the library distinct selectivity in killing specific bacterial strains, indicating the likelihood of diverse mechanism of antibacterial activity. High selectivity ratios exhibited by peptoid 3 and 4 lead to the conclusion that these two peptoids show the highest selectivity. This means that they can selectively target and kill bacterial over mammalian cells. In addition, peptoid 3 and 4 have demonstrated a higher protease stability than previous peptide.[30]

3.5   Peptoids activity against F. nucleatum

Fusobacterium nucleatum was studied for its critical role in the formation of oral plaque biofilms. This bacterium facilitates the adherence of pathogenic Gram-negative bacteria to the commensal microorganisms, which can lead to oral infections, discussed previously. As alternative approach to antibiotic, AMPs with demonstrated efficacy against F. nucleatum were considered to design new potential peptoids

Peptoid 1	(NaeNpheNphe)4-NH2
Peptoid 2	(NahNspeNspe)3-NH2

Figure 3.11: Peptoids considered to reduce the presence of F. nucleatum in oral biofilm.[33]

Fibroblasts are important components in oral wound healing, involving ECM synthesis, tissue remodeling, and immune response modulation. Therefore, a considerable

vitality of fibroblast must be guaranteed. In a study, peptoid 1 and peptoid 2 was identified as effective inhibitors of the formation of F. nucleatum biofilms. The reduction of fibroblasts vitality was also evaluated, and the result were very successful, showing a no significant decrease in the vitality. This study has increased researchers' interest in considering peptoids as promising compounds to combat diseases related to oral biofilms.[33]

References: Chapter 3

1. Jørn A. Aas, Bruce J. Paster, Lauren N. Stokes, Ingar Olsen, and Floyd E. Dewhirst. "Defining the Normal Bacterial Flora of the Oral Cavity". J Clin Microbiol. (2005); 43(11): 5721–5732.

2. Virginie Gazil, Octave Nadile Bandiaky, Emmanuelle Renard, Katia Idiri, Xavier Struillou and Assem Soueidan. "Current Data on Oral Peri-Implant and Periodontal Microbiota and Its Pathological Changes: A Systematic Review". Microorganisms (2022), 10, 2466.

3. Javier Ata-Ali, María Eugenia Candel-Marti, Antonio Juan Flichy-Fernández, David Peñarrocha-Oltra, José Francisco Balaguer-Martinez, María Peñarrocha Diago. "Peri-implantitis: Associated microbiota and treatment". Med Oral Patol Oral Cir Bucal. (2011) 1;16 (7):937-43.

4. Ilseung Cho and Martin J. Blaser. "The Human Microbiome: at the interface of health and disease". Nat Rev Genet. (2012); 13(4): 260–270.

5. P D Marsh, R S Percival. "The oral microflora – friend or foe? Can we decide?". International Dental Journal (2006) 56, 233-239.

6. Mirco Govoni , Emmelie A Jansson, Eddie Weitzberg, Jon O Lundberg. "The increase in plasma nitrite after a dietary nitrate load is markedly attenuated by an antibacterial mouthwash". Nitric Oxide (2008);19(4):333-7.

7. Jérôme Frédéric Lasserre,* Michel Christian Brecx, and Selena Toma. "Oral Microbes, Biofilms and Their Role in Periodontal and Peri-Implant Diseases". Materials (Basel). (2018); 11(10): 1802.

8. Lina J. Suárez, Hernan Garzón, Silie Arboleda, and Adriana Rodríguez. "Oral Dysbiosis and Autoimmunity: From Local Periodontal Responses to an Imbalanced Systemic Immunity. A Review". Front Immunol. (2020); 11: 591255.

9. Yeon-Hee Lee, Sang Wan Chung, Q-Schick Auh, Seung-Jae Hong, Yeon-Ah Lee, Junho Jung, Gi-Ja Lee, Hae Jeong Park, Seung-Il Shin and Ji-Youn Hong. "Progress in Oral Microbiome Related to Oral and Systemic Diseases: An Update". Diagnostics (2021), 11(7), 1283.

10. Zohra Khatoon, Christopher D. McTiernan, Erik J. Suuronen, Thien-Fah Mah, Emilio I. Alarcon. "Bacterial biofilm formation on implantable devices and approaches to its treatment and prevention". Heliyon (2018); Volume 4, Issue 12, e01067

11. Sangeeta Dhir. "Biofilm and dental implant: The microbial link". J Indian Soc Periodontol. (2013); 17(1): 5–11.

12. Reham B Osman, Michael V Swain . "A Critical Review of Dental Implant Materials with an Emphasis on Titanium versus Zirconia". Materials (Basel) (2015) ;8(3):932-958.

13. FDA. U.S Food and Drug Administration. "Dental Implants: What You Should Know"

14. Raphael C. Costa, Victoria L. Abdo, Patrícia H. C. Mendes, Isabella Mota-Veloso, Martinna Bertolini, Mathew T. Mathew, Valentim A. R. Barão, João Gabriel S. Souza. "Microbial Corrosion in Titanium-Based Dental Implants: How Tiny Bacteria Can Create a Big Problem?". Journal of Bio- and Tribo-Corrosion volume 7, Article number: 136 (2021)

15. Philip D. Marsh. "Microbiology of Dental Plaque Biofilms and Their Role in Oral Health and Caries". Dental Clinics of North America (2010); Volume 54, Issue 3, 441-454

16. Patricia P. Wright and Srinivas Sulugodu Ramachandra. "Quorum Sensing and Quorum Quenching with a Focus on Cariogenic and Periodontopathic Oral Biofilms". Microorganisms 2022, 10(9), 1783

17. P S Stewart, J W Costerton. "Antibiotic resistance of bacteria in biofilms". Lancet. 2001 Jul 14;358(9276):135-8.

18. Rafael Gomes Von Borowski, Simone Cristina Baggio Gnoatto, Alexandre José Macedo and Reynald Gillet. "Promising Antibiofilm Activity of Peptidomimetics". Frontiers in Microbiology (2018)

19. J. Li, J. J. Koh, S. Liu, R. Lakshminarayanan, C. S. Verma, R. W. Beuerman, "Membrane active antimicrobial peptides: Translating mechanistic insights to design", Frontiers in Neuroscience 2017, 11, 1–18.

20. A. M. Czyzewski, H. Jenssen, C. D. Fjell, M. Waldbrook, N. P. Chongsiriwatana, E. Yuen, R. E. W. Hancock, A. E. Barron, "In Vivo, In Vitro, and In Silico Characterization of Peptoids as Antimicrobial Agents.", PloS one 2016, 11.

21. Kim A Brogden. "Antimicrobial peptides: pore formers or metabolic inhibitors in bacteria?". Nat Rev Microbiol (2005) 3:238–250.

22. Min-Kyung Shin, Yu-Jung Hyun, Ji Hoon Lee, and Hyun-Suk Lim. "Comparison of Cell Permeability of Cyclic Peptoids and Linear Peptoids". ACS Combinatorial Science. (2018), 237–242

23. Mia Lace Huang, Dr. Sung Bin Y. Shin, Meredith A. Benson, Prof. Victor J. Torres, Prof. Kent Kirshenbaum. "A Comparison of Linear and Cyclic Peptoid Oligomers as Potent Antimicrobial Agents". ChemMedChem (2012);7(1):114-22

24. Nathaniel P. Chongsiriwatana, James A. Patch, Ann M. Czyzewski, Michelle T. Dohm, Andrey Ivankin, David Gidalevitz, Ronald N. Zuckermann, and Annelise E. Barron. "Peptoids that mimic the structure, function, and mechanism of helical antimicrobial peptides". Proc Natl Acad Sci USA (2008), 105(8): 2794–2799.

25. Bang, J. K.; Nan, Y. H.; Lee, E. K.; Shin, S. Y. Bull. Korean Chem. Soc. 2010, 31, 2509.

26. Biljana Mojsoska, Ronald N. Zuckermann, and Håvard Jenssen. "Structure-Activity Relationship Study of Novel Peptoids That Mimic the Structure of Antimicrobial Peptides". Antimicrob Agents Chemother (2015); 59(7): 4112–4120.

27. Trine S Ryge, Paul R Hansen. "Novel lysine-peptoid hybrids with antibacterial properties". J Pept Sci. (2005) Nov;11(11):727-34.

28. Steven W. Shuey, William J. Delaney, Mukesh C. Shah, Mark A. Scialdone. "Antimicrobial β-peptoids by a block synthesis approach". Bioorganic & Medicinal Chemistry Letters (2006), Volume 16, Issue 5, 1245-1248.

29. Paola Saporito, Biljana Mojsoska, Anders Løbner Olesen, Håvard Jenssen. "Antibacterial mechanisms of GN-2 derived peptides and peptoids against Escherichia coli". BioPolymers (2019); Volume110, Issue6

30. Biljana Mojsoska, Ronald N. Zuckermann, and Håvard Jenssen. "Structure-Activity Relationship Study of Novel Peptoids That Mimic the Structure of Antimicrobial Peptides". Antimicrob Agents Chemother (2015); 59(7): 4112–4120.

31. Bo Zhang, Meng Zhang, Min Lin, Xinzhe Dong, Xutao Ma, Yuanhong Xu, Jing Sun. "Antibacterial Copolypeptoids with Potent Activity against Drug Resistant Bacteria and Biofilms, Excellent Stability, and Recycling Property". Nano.Micro Small (2022) Volume18, Issue11.

32. Biljana Mojsoska, Gustavo Carretero, Sylvester Larsen, Ramona Valentina Mateiu and Håvard Jenssen. "Peptoids successfully inhibit the growth of gram negative E. coli causing substantial membrane damage". Scientific Reports volume 7, Article number: 42332 (2017)

33. Jamie Toole, Hannah L. Bolt, John J. Marley, Sheila Patrick, Steven L. Cobb, and Fionnuala T. Lundy. "Peptoids with Antibiofilm Activity against the Gram Negative Obligate Anaerobe, Fusobacterium nucleatum". Molecules 2021, 26(16), 4741

Chapter 4

Surface Functionalization of Titanium and its Alloys

Dental implants offer a variety of options in terms of materials, shapes, and surface treatments. Titanium and its alloys have been widely utilized because of their outstanding mechanical and physiological properties, including high resistance to corrosion, low elastic modulus, biocompatibility, minimal reactivity, and significant fatigue strength, attributing the necessary criteria for biomedical application.[1] Among these, the most significant one is their biocompatibility, which refers to their ability to safely interact with host tissue when it is placed in human body, without causing harmful reactions.[2] Titanium is classified as the most biocompatible metal.[3] The resistance to corrosion also plays a crucial role, since it prevents the release of metal ions, which cause allergic and toxic reactions in the host.[4] However, despite the big number of advantages of titanium and its alloys, the failure of these implants poses important economic and healthcare challenges, due to growing occurrence of simultaneous microbial infections and poor osseointegration.[1] Typically, among dental application, Ti6Al4V alloy is commonly employed, thanks to its higher compressive strength, fatigue and corrosion resistance, and lower density.[5]

4.1 Osseointegration of dental implants

The long-term success of dental implants relies on the osseointegration, which is defined as the direct contact between bone and the endosseous implant without the growth of the fibrous tissue at the interface. This biological process guarantees the complete integration of the implant with the bone, and typically takes 3 to 4 months in the mandibular arches and 4 to 6 months in the maxillary arches.[6,7] An implant is considered successfully integrated when there is no movement between the implant and the adjacent bone. Several factors can influence the interface between implant and bone and the progress of the osteointegration, such as the applied load, the characteristics of the surface, the properties of the implanted material, the method of the surgery, the quality and quantity of poor bone.[7] The healing process in the implant closely resembles the natural healing of bones.[8] Initially, a layer of water molecules covers the surface, followed by proteins adsorption. This, combined with the release of cytokines

from damaged cells and blood coagulation, represents the reaction of the host to the
foreign body.[9] Osseointegration occurs when mesenchymal stem cells differentiate into
osteoblasts and osteocytes, stimulating new bone formation. This process is initiated
by an inflammatory response, where neutrophils and monocytes are attracted to the
implant site. If this response is not triggered, fibroblast proliferation and the formation
of fibrous capsule can hinder a proper contact with the bone tissue.[9] After implanta-
tion, a blood clotting forms in close proximity to the implant surface, and, within 24
hours, neovascularization initiates. Whitin 2 to 4 days after implant placement, the
peri-implant gap is characterized by a growing influx of monocytes and macrophages,
which play a crucial role in the removal of the debris during the healing process. In-
deed, they can fuse together to form foreign body giant cells. These cells can also
activate platelets (a rich source of growth factors) on the inside of blood clotting. By
the fourth day, mesenchymal cells are recruited from the bone marrow that surrounds
the new vessel to gradually replace the blood clotting. The activated platelets allow
the differentiation of mesenchymal cells into osteoblasts. This enables the so called
"contact osteogenesis" by 4 weeks, in which immature bone formed by collagen fibers
without a regular arrangement is observed on the implant surface. Upon reaching 8
to 12 weeks, bone is remodeled into mature lamellar bone, which establishes a direct
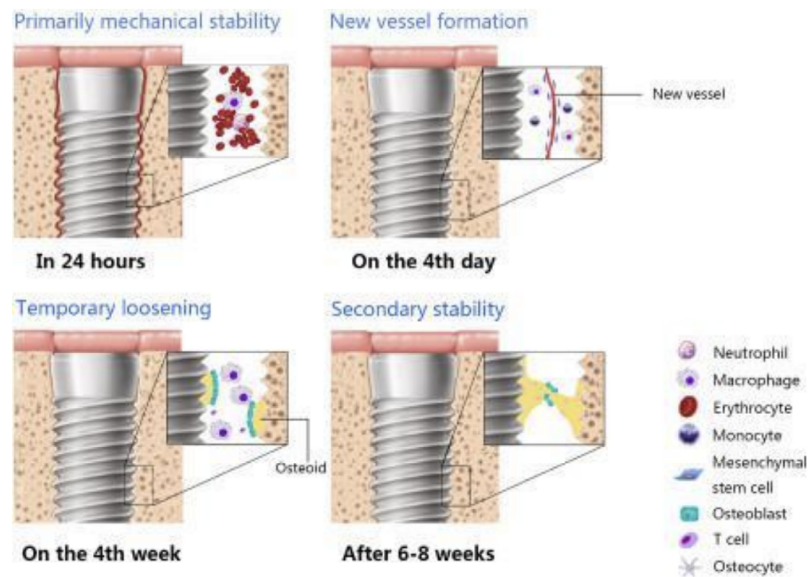contact with the surface.[9,10]

Figure 4.1: Progress of osteointegration in dental implants over time.[10]

4.2 Challenges in the field of dental implantology

Over the years, numerous implant systems with different design have been developed to restore missing teeth. Despite the high success, there are still failures that lead to the removal of the implant. A study conducted on about eighty thousand implants revealed a higher failure rate in the upper jaw (3.14%), while lower jaw failure rates were 1.96%.[11] Several factors contribute to implant failures, including biological features, surface treatments of the implant, site of the implant fixture, an inadequate bone quality and quantity to support the implant and systemic diseases.[12]

4.2.1 Lack of osseointegration in dental diseases

Peri-implantitis is defined as an inflammatory process that has an effect on the marginal tissues, causing gradual loss of bone support. An insufficient support can't maintain osseointegration, leading to implant failure. The absence of proper osseointegration can generally be identified by the presence of radiological radiolucency and no implant stability.[13]
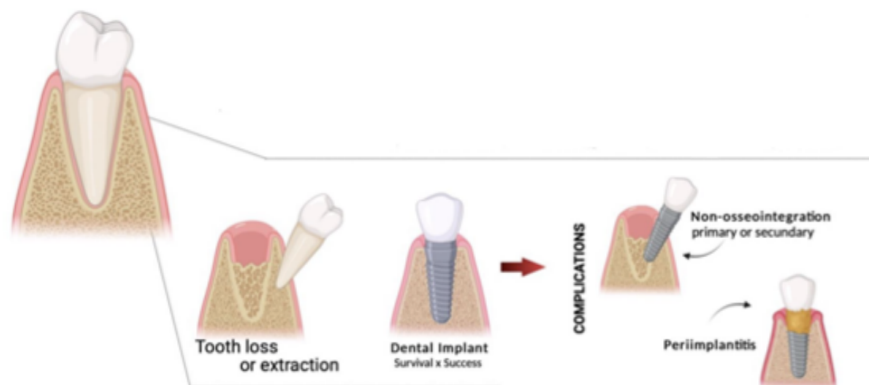

Figure 4.2: Complications of dental implants which lead to implant failure and removal.[14]

4.2.2 Titanium issues

Despite the excellent biocompatibility, titanium and its alloys have shown biological inertness, that means that no strong chemical bond forms between the implant and the bone.[16,17] They have a protective titanium oxide layer, usually only 2 to 5 nm thick, that forms on the surface of titanium when it comes into contact with air or other environments with the presence of oxygen. This layer is responsible for the resistance of titanium and its alloys to corrosion, but it is not fully bioactive, meaning that it lacks osseointegration, which can lead to failure over time.[19,20] For these reasons, researchers have investigated methods to improve titanium bioactivity and osteoconductivity through the modification of surface properties. In this way, an increased osseous tissue at the implant interface in terms of quality and quantity is achieved,

which is particularly important in areas where the cortical thickness of the jam is not sufficient for primary stability, like the edentulous posterior maxillae.[16,17]

4.3 Surface topographic modifications

Topography, roughness, and chemical composition of the surface are critical factors for tissues and cells response. Roughness provides a better bone connection with the implant surface, wettability and energy affect the interaction with the physiological environment, protein adsorption and osteoblast cells adhesion are essential for a successful contact.[16,17] The effect of surface wettability on bacterial adhesion varies depending on the bacterial species. For instance, S. Epidermidis tends to adhere more to hydrophobic surfaces, while S. Sanguinis does not show any preference for adhesion.[18] Concerning the energy, when a surface has high surface energy, it tends to adsorb biomolecules. As a result, the presence of these biomolecules can influence how cells and tissues interact with the material.[19] Generally, high hydrophilicity and roughness on the surface have shown better osseointegration.[16,17] Concerning topography and roughness, it has been shown that titanium implant with sufficient surface roughness and pores with diameter of at least 100μm allow bone growth into the implant, and enhanced stability, intensifying the contact between bone and implant.[19] It was also demonstrated that nano-textured surfaces and surfaces with low roughness don't attract bacteria as much as surface with roughness value above 0.2μm.[21] Smooth surfaces attract fibroblasts and epithelial cells, leading to strong adhesion, but rough surfaces promote osteoblastic proliferation and collagen synthesis, encouraging a more direct contact with the bone. This induces an optimized bone integration.[22] To date, various surface modification techniques have been explored to improve implant performances, enhancing bioactivity, reducing corrosion, and promoting osseointegration.[19]

4.3.1 Acid-etching

Acid-etching is a widely used process for roughening the surface of titanium implants, which involves strong acids such as HCl, H2SO4, HNO3, and HF. By acid-etching it's feasible to create a uniform and micro-porous roughness on the surface, enhancing its activity. In addition, it allows the growth of micro pits on the surface, with a diameter that ranges from 0.5 to 2μm, as displayed in Figure 4.3. By adjusting the etching parameters, such as the acid composition, exposure time, and temperature, it's possible to alter the texture of the surface, the thickness of the oxide layer, and the wettability of the surface. It has been demonstrated that the modified surfaces improved the proliferation of osteogenic cells, promoting their attachment to the surface. As a result, the presence of pores on the implant surfaces enhances osseointegration and mechanical stability by the growth of bone into the porous structure. This creates a strong contact between the tissue and the implant, promoting better support.[23] A technique combining acid etching and thermochemical oxidation has been developed for dental application, aiming to achieve a multi-scale topography and increased hydroxylation on titanium surfaces. This process firstly involves etching with hydrofluoric acid (HF) and then a thermal oxidation with hydrogen peroxide (H2O2). Hydroxyl groups play a crucial

role, as they promote apatite precipitation. The result is a surface consisting of a nano-texture with an overlay of micro-porous layer. These modifications on the surfaces have allowed bioactive properties, improved wettability, resistance to friction during the implantation process, and protein adsorption.[24,25]

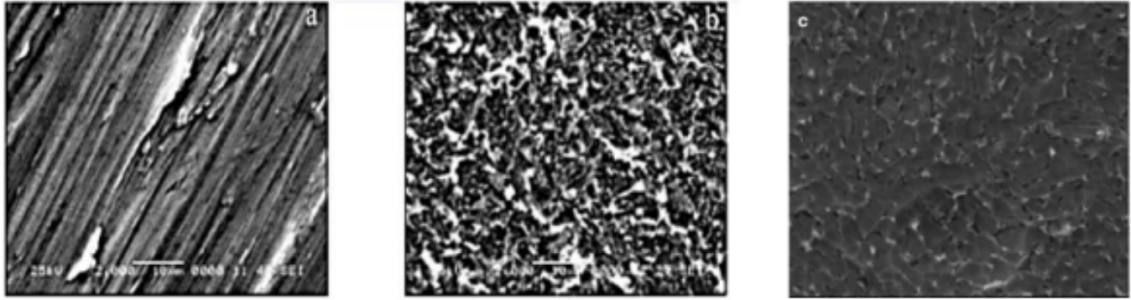

Figure 4.3: : SEM images of titanium discs. (a) Polished disc. (b) Etched disk HCl. (c) combined etching with HF and thermochemical oxidation.[25,26]

4.3.2   Anodic oxidation

Anodic oxidation, also known as anodization, is an electrochemical process that modifies the characteristics of TiO_2 layer on titanium implants, with a thickness that ranges from hundreds of nanometers to hundreds of micrometers. The process involves the immersion of the substrate of titanium in an electrolyte containing strong acids, such as HNO_3, and HF, H_2SO_4, H_3PO_4 and serves as the anode in an electrochemical cell. The cathode is also submerged in an electrolyte, separated from the anode.[27] The resulting titanium has a porous surface, with size of 10-100 nm per pore. When a high voltage is applied, the anodized surface is characterized by a lower uniformity, with an increased number of pores.[28] In this technique, the surface properties of titanium oxide can be controlled and modified trough different factors. Increasing the applied voltage leads to higher surface porosity, thickness, roughness, wettability, and crystallinity, due to the bigger number of electrochemical reactions. A prolonged anodization time generally leads to higher spark frequency, leading to the formation of a highly crystalline anodic layer and increased surface area. However, anodization time can't exceed over a limit, otherwise it may cause unstable sparks. Higher bath temperature improves the photoelectrochemical property of titanium oxide, but it may inhibit the formation of a porous oxide layer. Some studies have also shown that higher bath temperature can reduce the thickness of the anodic layer. A higher electrolyte concentration leads to higher surface porosity, thickness, roughness, and crystallinity of titanium oxide.[27]
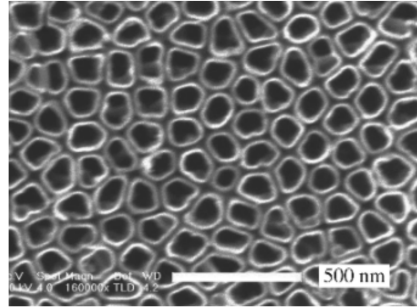
Figure 4.4: SEM image of anodized nanostructure formed with HF.[29]

Anodic oxidation has gained interest in biomedical applications for its high number
of advantages, including its simplicity and low cost. Furthermore, through anodic
oxidation the coating adhesion, and corrosion resistance are significantly improved,
ensuring the durability and long-term performance of biomedical device. One of the
key benefits is the creation of a porous structure that facilitates bone cells colonization,
enhancing biocompatibility.[27]

4.3.3 Grit-blasting

Grit-blasting is another technique that aims to regulate the surface roughness of biomed-
ical implants. It generates a rough layer without the production of pores, and this is
achieved by using particles of hard ceramic by selecting their specific sizes. In this
process, it is important that the used material is biocompatible, resorbable and os-
teoconductive. For this reason, commonly used materials include alumina, calcium
phosphate compounds, and titanium oxide.[30] The common size of used material par-
ticles is 25 μm for dental implants, which creates a surface with moderate roughness
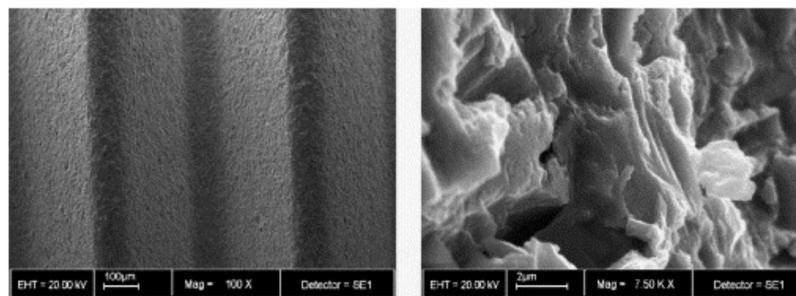level, typically 1-2 μm.[31]

Figure 4.5: SEM images of a TiO2 surface with grit blasted method.

For this method, researchers have particularly investigated surface treated with tita-
nia (TiO2) and alumina (Al2O3) particles.[31] They have shown superior osseointegration
rates at the interface. Alumina is the most used material for blasting titanium surface,
which offers the advantage of an easy adjustment of surface roughness by varying the
size of the grain. The resulting surface textures become randomized. This allows an

increment of the surface area, but it may also lead to random bone cells orientations and, consequently, to the formation of scarring tissue.[32] Residual alumina particle on the surface can persist despite various cleaning methods, including ultrasonic, acid passivation and sterilization, causing inflammatory reactions. In order to address this issue, alternative material can be used, such as titania, zirconia and hydroxyapatite.[31]

4.3.4 Plasma Spraying

Plasma spraying technology involves the deposition of titanium powders into a high temperature plasma torch, where titanium particles are released onto the surface of the implant, forming a film. Studies have shown that for the coating to be uniform, the thickness needs to be in the range of 40-50μm, with a resulting coating roughness of approximately 7μm, which increases the overall implant area.[33]
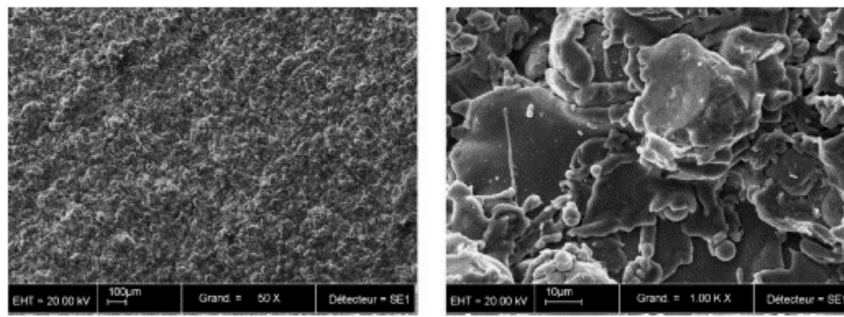

Figure 4.6: SEM images of titanium surface treated with plasma spraying technique.[31]

The resulting surfaces after the thermal spraying technique has higher rates of bone formation and a relevant percentage of porosity, of about 15%.[34] Metallic wear particle from implant have been found in other parts of the body, including liver and spleen. These occurrences can be attributed to the release of metal ions, due to processes like wear, dissolution, and fretting, and, as a result, may have effect on the genesis of local and systemic diseases, such as cancer.[35]

4.4 Antibacterial functionalization techniques

Once improved osseointegration, an important overview to increase antimicrobial properties on titanium surface need to be investigated. Peri-implantitis poses a significant risk for implant related infections. The most effective approach to combat peri-implantitis is preventing biofilm formation, as peri-implantitis is caused by its presence. Therefore, biofilm resistance to conventional antibiotics has led scientists and researchers to develop implant surfaces with antibacterial properties. Antimicrobial dental implants can either damage adhering bacteria or prevent their initial attachment. Despite titanium and its alloys have shown to respect the criteria for a successful implant material, it lacks antiseptic quality. Thus, it is essential to modify their surfaces to improve antimicrobial potential.[36] Different methods have been described to convert the surface of biomedical devices into bacterial surface.
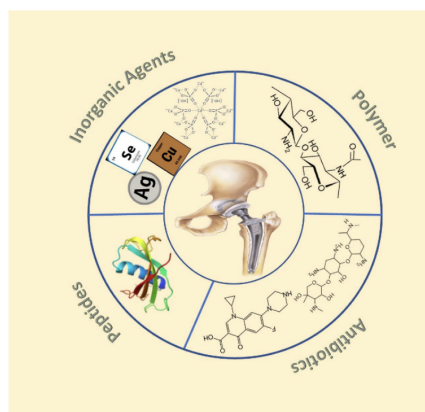
Figure 4.7: Common antimicrobial coatings on titanium surface implants.[37]

Surface grafting of titanium implants involves the bonding of bioactive materials to improve their performance and biocompatibility. In this chapter, some examples of grating on titanium implants are exposed.

4.4.1 Polymer coating

Polyethylene glycol (PEG) is a widely utilized polymer for imparting antifouling properties to titanium surfaces. While PEG demonstrates remarkable bacteriostatic properties thanks to its hydrophilic and flexible chains, its highly potent antibacterial qualities can hinder the osseointegration process, as it obstructs the attachment of osteoblasts. To address this issue, scientists have shown that the introduction of cell adhesive sequences to maintain biocompatibility, such as short peptides composed of arginine, glycine, and aspartic acid. This creation process can be expensive, and there is the possibility of polymer breakdown over time, which could affect the surface's durability and effectiveness of the coating. Furthermore, some polymers are not viable for use in polymeric coating for dental implant with titanium surfaces.[38] Another challenge involves the poor stability of PEG in biological environments. To overcome this issue, zwitterionic copolymers have been explored as a suitable alternative. Studies have shown that phosphonate zwitterionic copolymers prevent protein adsorption and bacterial adhesion on titanium surfaces, leading to a considerable enhancement of their anti-biofouling characteristics. Moreover, the application of synthetic biopolymers designed by combining elements of natural elastin and biopolymers on titanium surfaces has shown promising result in terms of lower serum-protein adsorption.[38]

4.4.2 Inorganic antimicrobial agents

Metal ions, nanoparticles and non-metals can be added to titanium surface to optimize antibacterial activity. Silver is extensively used in implant coatings because of its ability to efficiently kill a wide range of bacteria, its biocompatibility, and its long-lasting stability. Researchers has shown that silver nanoparticles are able to control the quorum sensing, regulating gene expression of S. epidermidis and S. aureus.[38] Sil-

ver exerts its effect in two main ways. It can form Ag+ ions, and then enter in the
cytoplasm of bacteria, hindering cellular metabolism and, consequently, leading to cell
death. Otherwise, Ag can interact with bacteria cell walls and plasma membranes
through direct contact, resulting in bacterial cell death due to their loss of cytoplasm
and vital substances.[39] Copper, zinc, and strontium are also used for their antibacterial
properties, bone-regenerating activity, and ability to enhance the biocompatibility of
the implant. Studies have shown that ceramics with strontium incorporated exhibit
increased bactericidal properties and contribute to the regeneration of bone tissue. In
addition, there are reports indicating that coatings containing zinc enhance the corro-
sion resistance of titanium and improve the differentiation of osteoblasts.[38] Zinc is a
vital element in our body, and it offers safety, minimal side effects and a prolonged an-
timicrobial effect. The mechanisms used as antimicrobial agent are very similar to silver
activity.[39] Hydroxyapatite is employed for its biocompatibility and structural similarity
to natural teeth. A variety of bioactive metals and metal oxide are used as additive
to improve the antibacterial and biomechanical characteristic of hydroxyapatite, such
as ZnO, which exhibits activity against E. coli and S. epidermidis. Coating supple-
mented with iodine also demonstrated efficacy in avoiding the presence of infections
after clinical operations.[37]

4.4.3 Antibiotics incorporation

Researchers have also explored the incorporation of antibiotics into titanium implant
coatings. Calcium is usually used as the base to form these coatings. They have demon-
strated efficient bacteriostatic activity and controlled release of antibiotics, including
cefthiophene, amoxicillin carbenicillin, vancomycin, cephalotin, and gentamicin.[16,39,40]
As bone healing involves intricate growth factor regulation, the used delivery system
is crucial for the success of the osteointegration to stimulate the regeneration of the
bone.[41] The locally release of antibiotic have demonstrated to be a potential method
to target specific sites and guarantee high activity over an extended period, without
exerting systemic toxicity. The efficacy of this system and the release rate significantly
depend on the approach used to incorporate the drugs into the coatings.[40] Typically,
growth factors are anchored onto calcium phosphate ceramics through protein ad-
sorption on titanium surface and under specific condition they will be released in a
controlled mode and prolonged time.[41]

4.4.3.1 The importance of calcium-phosphate coatings

Antibiotics can be administered either systemically or locally, with local administra-
tion offering several advantages, including cost-effectiveness, reduced toxicity risk, and
higher antibiotic concentrations at the specific treatment site. Loading devices with
antibiotics enables achieving the same local therapeutic effect while maintaining lower
systemic concentrations, thereby addressing issues associated with systemic adminis-
tration, including the emergence of antibiotic-resistant strains. Local drug delivery has
found applications in various fields such as orthopedics and dentistry. Sundblom and
coworkers investigated the loading and the delivery of gentamicin on calcium-phosphate
(CaP) and on titanium, concluding that among the clinically used materials, only CaP

demonstrated the ability to load gentamicin, offering a promising avenue for targeted antibiotic delivery in clinical settings.[42] Calcium-phosphate coatings emerge as an attractive option for antibiotic delivery due to their ability to promote implant integration with surrounding bone tissue and their effectiveness in loading gentamicin, resulting in a rapid release in vitro. This release aligns with the need for preventing peri-operative infections immediately following surgery. Importantly, it was showed that the thin CaP implant coating allows for efficient gentamicin loading within a minute, making it compatible with routine surgical procedures. Notably, gentamicin did not inhibit implant osseointegration, emphasizing the safety of this approach.[43]

4.4.4 Antimicrobial peptides

Surface treatments based on the presence of antimicrobial peptides are being recognized as promising substitutes for common antibiotic-based coatings on titanium implants, as they offer efficient action against microbes and demonstrated efficacy in combating infections even at low concentrations.[7] Various researchers have investigated these coating, discovering that the covalent bound of AMPs to titanium surface implants provides several advantages. It improves the long-term stability, retaining antimicrobial activity and no toxicity effect to bone cells like osteoblasts. Moreover, AMP-coated surfaces prevent the formation of biofilm. Continued research in this field, leading to the creation of coatings with robust solid surface with effect against a wide range of dental bacteria, such as S. epidermidis.[38,39]
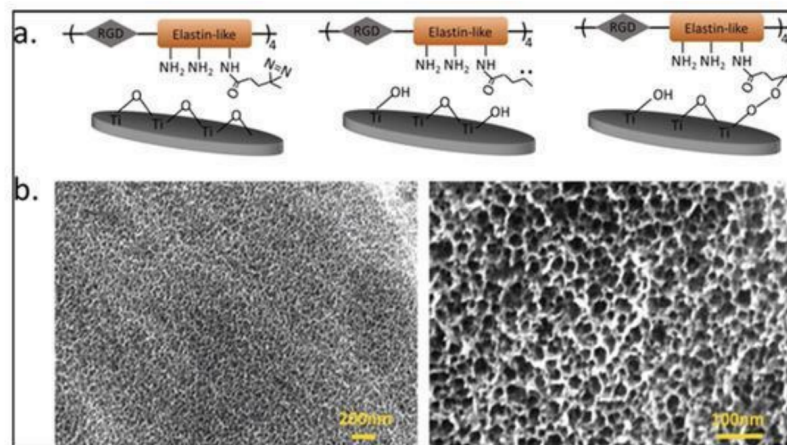

Figure 4.8: Titanium surface functionalization employing elastin-like polypeptide. (a) conceptual representation; (b) SEM images to observe the changes in the structures.[37]
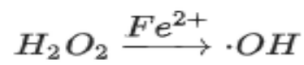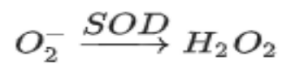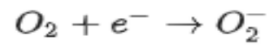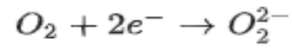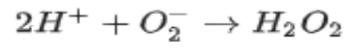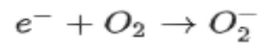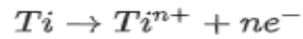
4.4.5 Bioactive glasses

Bioactive glass coatings have shown the promotion of stability through the formation of a strong contact with the bone that surrounds the implant, contributing to enhance soft tissue integration around the implant. These coatings can also act as a shield for the substrate from corrosion. Moreover, they serve as a scaffold for bone regeneration,

guaranteeing a sufficient bone volume at the implant site. Furthermore, their presence
can prevent the release of potentially harmful metal ions that may be in the substrate
material, contributing to make them a more biologically compatible implant. They can
be constructed as drug delivery systems, which release antimicrobial agents, such as
antibiotics or growth factors or ions, to alter the biological response, in order to ensure
a faster tissue healing by their release.[44]

4.4.6   Silver nanoparticles

Historically, silver has demonstrated efficacy in treating infections by inhibiting bac-
terial growth at low concentrations. The antimicrobial efficacy of silver nanoparticles
(AgNP) is related to the potent oxidative properties of AgNP surfaces and the liber-
ation of silver ions in biological surroundings. However, these combined actions have
a negative impact on cell structures and functions, ultimately leading to cytotoxicity,
genotoxicity, immune responses, and, in some cases, cell death.[45] The mechanism of
cytotoxicity is the production of free radicals, which lead to a state of oxidative stress.
At cellular level, the internalization of substances can occur in two ways: by interacting
with membrane proteins, triggering signaling pathways, or through passive processes
like diffusion and endocytosis. When it comes to the uptake of nano-silver particles,
it leads to the generation of reactive oxygen species (ROS) due to its interaction with
mitochondria, subsequently leading to mitochondrial dysfunction. When AgNPs are
internalized, they have the potential to damage nucleic acids by elevating the produc-
tion of reactive oxygen species (ROS), or by reducing ATP production. High levels
of ROS can result in cellular DNA damage, oxidative stress, and apoptosis.[46,47] It is
therefore necessary to maintain a controlled release of silver particles above the an-
tibacterial threshold and below the cytotoxicity threshold. This is made difficult by
the set-up of the conductivity of the treated Titanium surface with silver nanoparticles
in antibacterial activity.[48] When titanium surface encounters the silver nanoparticles,
galvanic pairs established, due to the different potentials of materials. In this process,
titanium oxidizes and donates electrons, which lead to the generation of ROS outside
the cell. Simultaneously, titanium can undergo electron transfer within the cell due to
the influence of silver nanoparticles, triggering the generation of ROS inside the cell.
In this scenario, the following reactions take place:

$$Ti \rightarrow Ti^{n+} + ne^-$$

$$e^- + O_2 \rightarrow O_2^-$$

$$2H^+ + O_2^- \rightarrow H_2O_2$$

$$O_2 + 2e^- \rightarrow O_2^{2-}$$

$$O_2 + e^- \rightarrow O_2^-$$

$$O_2^- \xrightarrow{SOD} H_2O_2$$

$$H_2O_2 \xrightarrow{Fe^{2+}} \cdot OH$$

In Figure 4.9 the induction of oxidative stress in both the surrounding solution and inside the bacterial cells is shown.
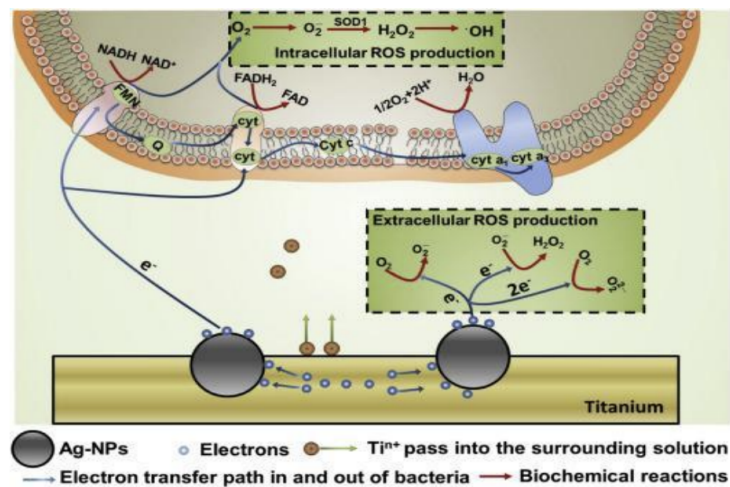

Figure 4.9: Generation of oxidative stress in the solution and inside bacteria.

References: Chapter 4

1. Allizond, V., Comini, S., Cuffini, A.M., Banche, G. "Current Knowledge on Biomaterials for Orthopedic Applications Modified to Reduce Bacterial Adhesive Ability". Antibiotics 2022, 11, 529.

2. C.N. Elias, J.H.C. Lima, R. Valiev, and M.A Meyers. "Biomedical Applications of Titanium and its Alloys". Biological Material Science (2008)

3. R.Z. Valiev, R.K. Islamgaliev, and I.V. Alexandrov. "Bulk Nanostructured Materials from Severe Plastic Deformation". Progress in Material Science (2000), Vol 45 (2), p. 103.

4. Krzysztof Pa lka and Rafa l Pokrowiecki. "Porous titanium implants: A review". Adv. Eng. Mater. (2018), 20(5):1700648

5. Reham B Osman, Michael V Swain . "A Critical Review of Dental Implant Materials with an Emphasis on Titanium versus Zirconia". Materials (Basel) (2015) ;8(3):932-958.

6. D'Ambrosio, Francesco, Alessandra Amato, Andrea Chiacchio, Laura Sisalli, and Francesco Giordano. 2023. "Do Systemic Diseases and Medications Influence Dental Implant Osseointegration and Dental Implant Health? An Umbrella Review" Dentistry Journal 11, no. 6: 146.

7. María B. Guglielmotti, Daniel G. Olmedo, Rómulo L. Cabrini. "Research on implants and osseointegration". Periodontology 2000 (2019); Volume79, Issue1, Pages 178-189.

8. Jayesh RS, Dhinakarsamy V. "Osseointegration". J Pharm Bioallied Sci. (2015);7(Suppl 1): S226-9.

9. Barberi J, Spriano S. "Titanium and Protein Adsorption: An Overview of Mechanisms and Effects of Surface Features". Materials (Basel). 2021 Mar 24;14(7):1590.

10. Yulan Wang, Richard J Miron, Yufeng Zhang. "Health, Maintenance, and Recovery of Soft Tissues around Implants: Soft Tissues around Implants". Clinical Implant Dentistry and Related Research (2015).

11. Fouda AAH. "The impact of the alveolar bone sites on early implant failure: a systematic review with meta-analysis". J Korean Assoc Oral Maxillofac Surg. (2020); 46(3):162-173.

12. Kochar SP, Reche A, Paul P. "The Etiology and Management of Dental Implant Failure: A Review. Cureus". (2022); 14(10): e30455.

13. Salah Sakka, Paul Coulthard. "Implant failure: Etiology and complications". Med Oral Patol Oral Cir Bucal. (2011);16 (1): e42-4

14. Sartoretto, S.C.; Shibli, J.A.; Javid, K.; Cotrim, K.; Canabarro, A.; Louro, R.S.; Lowenstein, A.; Mourão, C.F.; Moraschini, V. Comparing the Long-Term Success Rates of Tooth Preservation and Dental Implants: A Critical Review. J. Funct. Biomater. 2023, 14, 142.

15. Pandey C, Rokaya D, Bhattarai BP. "Contemporary Concepts in Osseointegration of Dental Implants: A Review". Biomed Res Int. (2022); 2022:6170452.

16. Lalit M. Pandey. "Design of biocompatible and self-antibacterial titanium surfaces for biomedical applications" Current Opinion in Biomedical Engineering (2023), Vol. 25, 100423

17. C.N. Elias and L. Meirelles. "Improving osseointegration of dental implants". Expert review of medical devices (2010); 7, 241-256.

18. Torsten Wassmann, Stefan Kreis, Michael Behr, and Ralf Buergers. "The influence of surface texture and wettability on initial bacterial adhesion on titanium and zirconium oxide dental implants". Int. J. Implant Dent. (2017), 3(1):32.

19. Shamaa Anjum, Arvina Rajasekar. "Surface Modification of Dental Implants - A Review". J Evolution Med Dent Sci 2021;10(17):1246-1250.

20. Chang Yao and Thomas J. Webster. "Anodization: A Promising Nano-modification Technique for Titanium for Orthopedic Applications". Nanotechnology For The Regeneration Of Hard And Soft Tissues (2007), chapter 3

21. S Ferraris and S Spriano. "Antibacterial titanium surfaces for medical implants". Mater. Sci. Eng. C Mater. Biol. Appl. (2016), 61:965–978.

22. A. Wennerberg and T. Albrektsson. "Suggested guidelines for the topographic evaluation of implant surfaces". The International journal of oral & maxillofacial implants (2000); 15, 331-344.

23. Zareidoost A., Yousefpour M., Ghaseme B., Amanzadeh A. "The relationship of surface roughness and cell response of chemical surface modification of titanium." Journal of materials science. Materials in medicine (2012). Vol. 23(6), 1479-148.

24. S Ferraris, A Bobbio, M Miola, and S Spriano. Micro- and nano-textured, hydrophilic and bioactive titanium dental implants. Surf. Coat. Technol. (2015), 276:374–383.

25. S Ferraris, S Spriano, G Pan, A Venturello, C L Bianchi, R Chiesa, M G Faga, G Maina, and E Vern'e. Surface modification of Ti-6Al-4V alloy for biomineralization and specific biological response: Part i, inorganic modification. J. Mater. Sci. Mater. Med. (2011), 22(3):533–545.

26. G. Juodzbalys, M. Sapragoniene, A. Wennerberg. New Acid Etched Titanium Dental Implant Surface,Stomatoloija, Baltic Dental and Maxillofacial Journal (2003), 5:101- 105.

27. J. Alipal, T.C. Lee, P. Koshy, H.Z. Abdullah, M.I. Idris. "Evolution of anodised titanium for implant applications". Heliyon (2021), Volume 7, Issue 7.

28. Liu X., Chu P. K., Ding C. "Surface modification of titanium, titanium alloys and related materials for biomedical applications." Material Science and Engineering (2004). Vol. 47, p. 49-121.

29. Zhaoxiang Peng and Jiahua Ni. "Surface properties and bioactivity of TiO2 nanotube array prepared by two-step anodic oxidation for biomedical applications". The royal society (2019).

30. Kumar P.S., KS S., Grandhi V., Gupta V. "The Effects of Titanium Implant Surface Topography on Osseointegration: Literature Review." JMIR Biomedical Engineer. (2019) Vol. 4(1):e13237.

31. Le Guéhennec L., Soueidan A., Layrolle P., Amouriq Y. "Surface treatments of titanium dental implants for rapid osseointegration." Dental Materials Journal (2007). Vol. 23(7), p.844-854.

32. Chen J., Bly R.A., Saad M.M., AlKhodary M.A., El-Backly R.M., Cohen D.J., Kattamis N., Fatta M.M., Moore W.A., Arnold C.B., Marei M.K., Soboyejo W.O. "In-vivo study of adhesion and bone growth around implanted laser groove/RGD-functionalized Ti-6Al-4V pins in rabbit femurus." Materials Science and Engineering (2011). Vol 31, p.826-832.

33. D. Buser, R. Schenk, S. Steinemann, J. Fiorellini, C. Fox, H. Stich. "Influence of surface characteristics on bone integration of titanium implants". A histomorphometric study in miniature pigs. J Biomed Mater Res (1991); 25:889–902.

34. Fousova M., Vojtech D., Jablonska E., Fojt J., Lipov J. "Novel Approach in the Use of Plasma Spray: Preparation of Bulk Titanium for Bone Augmentations" Materials (2010). Vol. 10, p. 987-1001.

35. R.M. Urban, J.J. Jacobs, M.J. Tomlinson, J. Gavrilovic, J. Black, M. Peoch. "Dissemination of wear particles to the liver, spleen and abdominal lymph nodes of patients with hip or knee replacement". J Bone Jt Surg Am (2000); 82:457–77.

36. Jasmin Grischke, Jörg Eberhard and Meike Stiesch. "Antimicrobial dental implant functionalization strategies —A systematic review". Dental Materials Journal (2016); 35(4): 545–558.

37. Akshaya, S.; Rowlo, P.K.; Dukle, A.; Nathanael, A.J. "Antibacterial Coatings for Titanium Implants: Recent Trends and Future Perspectives". Antibiotics (2022); 11, 1719.

38. Lu X, Wu Z, Xu K, Wang X, Wang S, Qiu H, Li X and Chen J. "Multifunctional Coatings of Titanium Implants Toward Promoting Osseointegration and Preventing Infection: Recent Developments". Front. Bioeng. Biotechnol. (2021); 9:783816.

39. Zheng TX, Li W, Gu YY, Zhao D, Qi MC. "Classification and research progress of implant surface antimicrobial techniques". J Dent Sci. (2022); 17(1):1-7.

40. Sui, J.; Liu, S.; Chen, M.; Zhang, H. "Surface Bio-Functionalization of Anti-Bacterial Titanium Implants: A Review". Coatings (2022), 12, 1125.

41. Bjelić D, Finšgar M. The Role of Growth Factors in Bioactive Coatings. Pharmaceutics. (2021) ;13(7):1083.

42. Sundblom, J., Gallinetti, S., Birgersson, U. et al. Gentamicin loading of calcium phosphate implants: implications for cranioplasty. Acta Neurochir 161, 1255–1259 (2019).

43. Thompson K, Petkov S, Zeiter S, Sprecher CM, Richards RG, Moriarty TF, Eijer H. Intraoperative loading of calcium phosphate-coated implants with gentamicin prevents experimental Staphylococcus aureus infection in vivo. PLoS One. 2019 Feb 1;14(2): e0210402.

44. Fiume, E.; Barberi, J.; Verné, E.; Baino, F. "Bioactive Glasses: From Parent 45S5 Composition to Scaffold-Assisted Tissue-Healing Therapies". J. Funct. Biomater. (2018), 9, 24.

45. Tianlu Zhang, Liming Wang, and Chunying Chen "Cytotoxic Potential of Silver Nanoparticles" Yonsei MED J. 2014 Mar 1; 55(2): 283-291

46. Danielle McShan, Paresh C. Ray, Hongtao Yu "Molecular toxicity mechanism of nanosilver" Journal of food and drug analysis 22 (2014) 116-127

47. Matthew Charles Stensberg, Qingshan Wei et al. "Toxicological studies on silver nanoparticles: challenges and opportunities in assessment, monitoring and imaging" Nanomedicine (Lond). 2011 July ; 6(5): 879–898.

48. Wang, G. et al. Antibacterial effects of titanium embedded with silver nanoparticles based on electron-transfer-induced reactive oxygen species. Biomaterials 124, 25–34 (2017).

Chapter 5

Materials and methods

5.1   Peptoid GN2 – Npm9

In the present project, we employed the design of a short (9-mer) GN2 peptoid, GN2-Npm9, in order to explore its potential application in functionalizing a chemically treated titanium alloy Ti6Al4V surface for antibacterial purpose. The peptoid was selected from a collection of novel N-substituted glycines designed by Biljana et al.[1] The peptoid had been previously synthesized and evaluated for its antibacterial properties and cytocompatibility[1-4]. It is mainly composed of lysine and tryptophan-like amino acids (Figure 5.1). The peptoid GN2-Npm9 was synthesized using the solid-phase Fmoc chemistry, involving amidation at the carboxyl terminus and purification through reverse-phase HPLC with C18 column (Higgins Analytical Inc. 10 μm 250x10 mm) and a gradient of water and acetonitrile. The accurate weight and purity levels of 95% were verified using electrospray ionization mass spectrometry (Dionex Ultimate 3000 RP-UHPLC; C18 Kinetex 100 x 2.1 mm, 100 Å). It was possible to synthesize a total amount of 34.5 mg of peptoid.
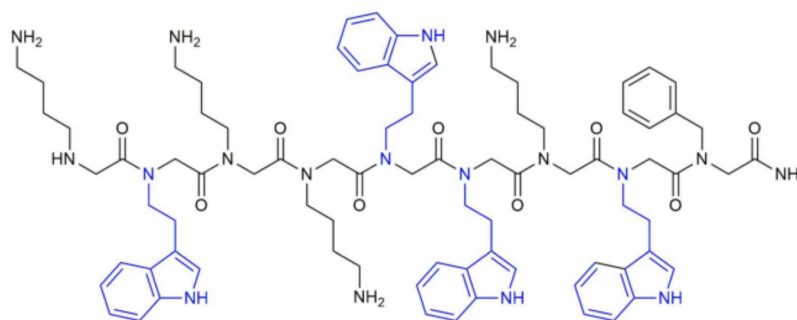

Figure 5.1: peptoid GN2 – Npm9.[4]

Lysine and tryptophan-like residues represent relevant amino acids in the development of peptoid with antibacterial properties. Lysine is important in the electrostatic interaction with negatively charged bacterial cell membranes because of its positive charge under physiological pH, due to the protonation of primary amino groups.[5] Moreover, lysine residues have the potential to inhibit bacterial growth and disrupt bacterial

membranes through DNA binding activity.[6] Tryptophan-like residue is a hydrophobic amino acid capable of inserting inside bacterial membranes, disrupting their integrity. In addition, peptoids containing tryptophan-like residue can selectively induce the creation of pores in bacterial membranes, leading to the efflux of strictly necessary cellular contents (ions and nutrients), to the disruption of bacterial cell membranes and, consequently, to bacterial death.[7]

5.1.1 Amines and calculations

Biljana et al. had previously analyzed a detailed protocol for tryptamine-rich peptoids, including GN2-Npm9, in which they evaluated diverse synthesis protocols in order to obtain the best result.[4] Considering this information, we firstly wrote a protocol and a calculation table detailing the required quantities of amino acids and other necessary compounds. In Figure 5.2 a library of essential data is summarized.
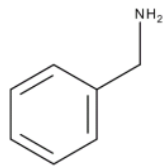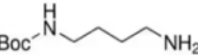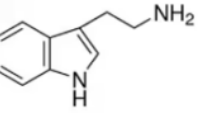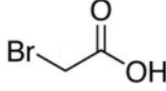
Abbreviation, side chain name, and CAS number	Molecular weight (g/mol)	Density (g/ml)	Formula and structure formula image	Concentration (mol/ml)
Npm Benzylamine 100-46-9	107.16	0.980	$C_6H_5CH_2NH_2$	0.5
Nlys N-Boc-1,4-butanediamine 68076-36-8	188.27	0.984	$(CH_3)_3COCONH(CH_2)_4NH_2$	0.5
Ntrp Tryptamine 61-54-1	160.22	0.978	$C_{10}H_{12}N_2$	0.5
Bromoacetic acid 79-08-3	138.95	1.93	$C_2H_3BrO_2$	0.6

Figure 5.2: Library of amines and chemicals used during the peptoid synthesis.

5.1.2 Synthesis

Peptoid GN2-Npm9 was synthesized employing the common submonomer solid-phase synthesis method, following a protocol defined by Biljana et al. in 2020 (Figure 5.3). The synthesis was carried out manually using 100 mg of resin for the first synthesis (200 mg for the subsequent ones) within a 5 ml single-use polypropylene syringe equipped with a PTFE filter.
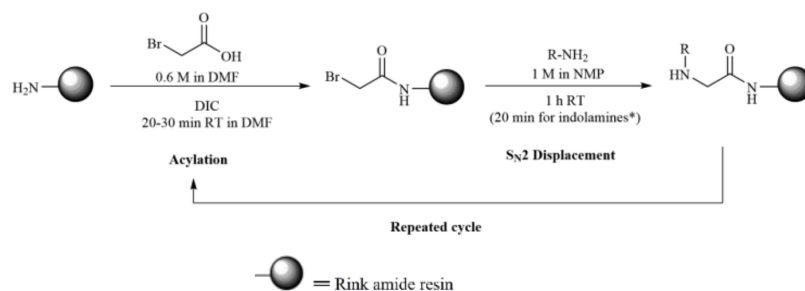

Figure 5.3: Solid-phase sub monomer peptoid synthesis of GN2-Npm9. The amine Ntrp requires displacement of 20 minutes, while Nlys and Npm require 1 hour of displacement for manual synthesis.[4]

The purchased resin was TentaGel S RAM because of its higher purity in the final product compared to Rink MBHA. It was previously demonstrated that TentaGel resin shows a better performance than Rink MBHA thanks to its lower loading capacity (respectively 0.22 and 0.65 mmol/g) and superior swelling in DMF (5 ml/g and 4 ml/g, respectively).[4] Initially, the resin was swelled in DMF for 40 minutes at room temperature and later washed 4 times. This was succeeded by Fmoc deprotection with 20% solution of 4-methylpiperidine in DMF for two sessions of 20 minutes each. Subsequently, the resin was rinsed using DMF for 8 times with a volume of 2 ml. Bromoacetylation processes were executed utilizing 1 ml of 0.6 M bromoacetic acid in DMF with 86 nanol of N,N'-diisopropylcarbodiimide (DIC). For each procedure, the solution was added into the syringe and incubated for a period of 20 minutes (extended to 30 minutes for the initial acylation step) at 35° and 200 rpm. The displacements were attained using 1 ml of a 0.5 M solution of the selected amine in NMP, and incubated for an hour, except for tryptamine which required 20 minutes. Before the cleavage, the syringe was left on a liquid reservoir for 30 minutes to dry.

5.1.3 Cleavage and side-chain deprotection

The cleavage from the resin was achieved using a mixture of trifluoroacetic acid (TFA), triisopropylsilane (TIPS) and water (TFA:TIPS:H2O, 95:2.5:2.5). TIPS was used in order to reduce the process of acylation and the formation of carbocations when the cleaved peptoid is produced. This is particularly crucial under acidic condition, where the indole side chain in tryptamine amine potentially react with electrophilic substances.[4] The cleavage cocktail was insert from the top of the syringe and subjected to shaking at room temperature for 30 minutes. Subsequently, the syringe was placed on a stationary holder, and the resulting cleavage cocktail solution, containing

the peptoid product, was collected. After completing the cleavage step, nitrogen gas was employed to evaporate the TFA until a crude oil residue was obtained (figure 5.4). This oil was then redissolved in a solution composed of acetonitrile and milli-Q water in a 1:1 ratio.
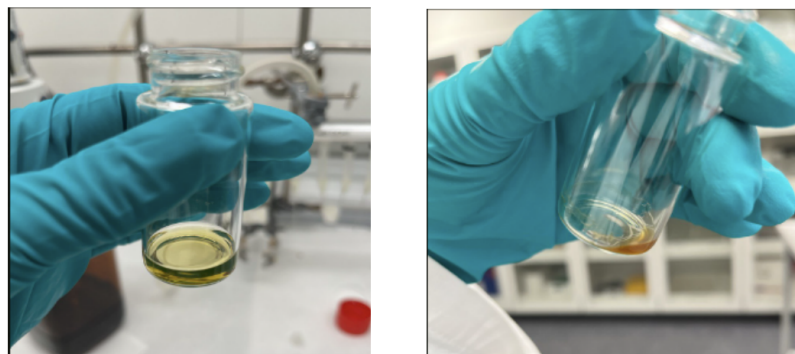

Figure 5.4: Cleavage cocktail solution before and after the evaporation of TFA via nitrogen gas.

The crude oil was then subjected to multiple freezing and lyophilization cycles until a fine white powder was obtained (figure 5.5). Subsequently, the crude product was accurately weighted and then stored as a dry powder at a temperature of -20°C.
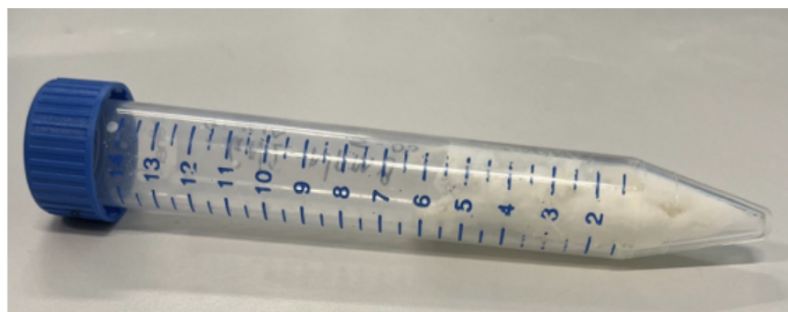

Figure 5.5: Fine white powder obtained after three cycles of freezing and lyophilization.

5.1.4 Characterization

In the pursuit of characterizing and identifying the obtained peptoid, high pressure liquid chromatography mass spectrometry (HPLC-MS) was employed. It involves the separation of peptoid through liquid chromatography followed by a precise mass measurement via mass spectrometry. This combination offers the possibility to quantify the components in the retrieved sample and determinate its molecular weight and purity with high selectivity and sensitivity.[8] The HPLC instrument forces the solvent through a closed column (C18 column) with fine particles inside. When a mixture of different substances flows through the column, the individual components interact with

the beads in distinct ways, depending on their properties. Consequently, the components with a lower interaction exit first, while those that interact more significantly will be released last.[9] Following the HPLC process, mass spectrometry (MS) analyzes the molecular mass of the peptoid. This method separates ions based on the ratio between mass and charge by capturing and detecting them. It is involved to identify the presence of the peptoid, assess the purity of the compound and evaluate potential errors.[10]
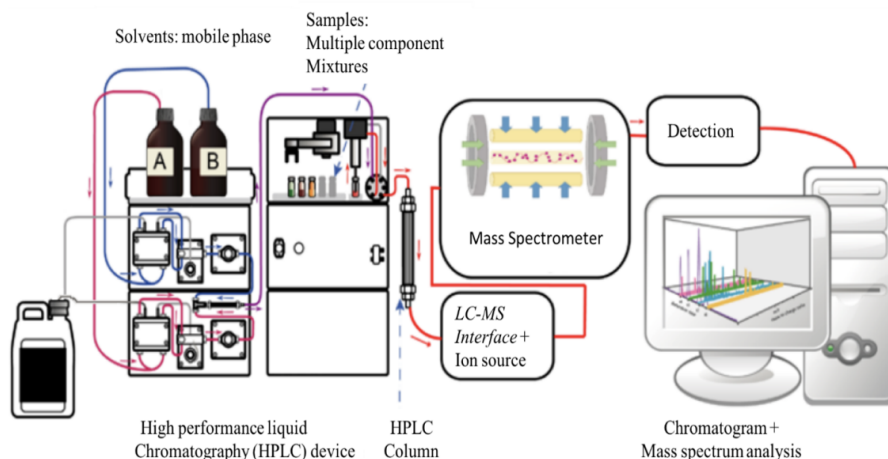

Figure 5.6: Components in HPLC-MS machine.11

The crude product of the peptoid was analyzed with mass spectrometry in order to verify the success of the synthesis. Before the analysis, a preliminary examination was executed. In this pre-analysis a solution of solely water and acetonitrile in ratio 90:10 was forced through the machine as a reference to test the presence of impurities within the column. Subsequently, a previously weighted crude peptoid was dissolved with a solution 90% water and 10% acetonitrile at a concentration of 200 nanog/ml. The consecutive identifications were conducted at a concentration of 500 nanog/ml. The mixture of the solution and the specimen of interest was forced into the HPLC-MS machine in order to identify the peptoid and the evaluate its purity. To enhance the understanding of the chromatogram's peaks, we plotted the base peak data that ranged from 250 to 2000.

5.1.5 Purification

The peptoid was purified using HPLC, which owns exceptional efficiency in separating complex mixtures with high resolution and precision. HPLC is an analytical technique employed as a tool to identify, quantify, and separate the constituents of the solution containing the target peptoid. The process involves two phases: a mobile phase, also known as column, which is the liquid that breaks down the peptoid, and a stationary phase, that interacts with the peptoid based on its physicochemical properties. When the solution of cleaved peptoid and acetonitrile/water is forced through the machine, the mobile phase traverses through the column, forced by the high pressure of a pump.

In the column, the peptoid is retained and subsequently eluted, resulting in a separation of the components in the sample. Then they are delivered to the detector at a constant flow regulated by the solvent delivery pump, identifying and quantifying distinct fractions of purified compound.[12]
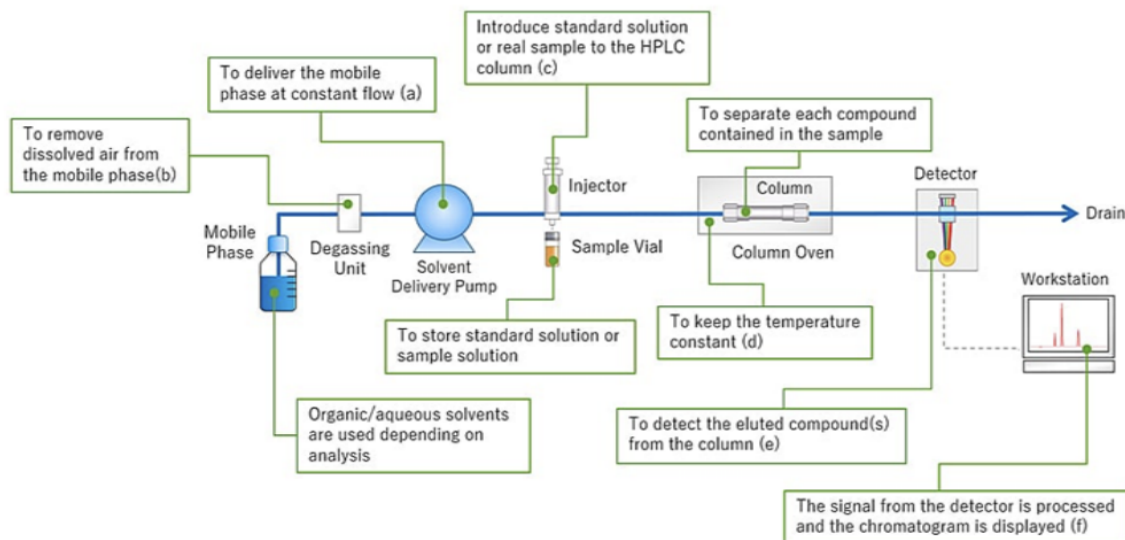

Figure 5.7: Components in HPLC machine and their role.[12]

In our project, the mobile phase, also used as pressurized liquids, was composed by solvent A, a mixture of water and 0.1% acetonitrile, and solvent B, solely acetonitrile. The pressure given by the solvents allows the utilization of smaller particles with a grater surface area, which makes the interactions of the molecules of the peptoid flowing through the column faster than column chromatography, resulting in a more detailed separation of components. The diverse affinity between the absorbent particles in the column and the mobile phase causes different elution rates and leads to the separation of the components as they flow out the column. The stronger the affinity the faster the component moves through the column along with the mobile phase. Once the machine was turned on, the air was removed from the four lines (connected to the pumps) using a syringe. A blank was sent into the system in order to clean and calibrate the machine. Once the blank run, the purification started and HPLC separated the targeted peptoid from other components in the solution. Throughout the experiment, we monitored the chromatogram using a UV detector set at three different detection wavelengths: 280 nm, 235 nm, and 214 nm.
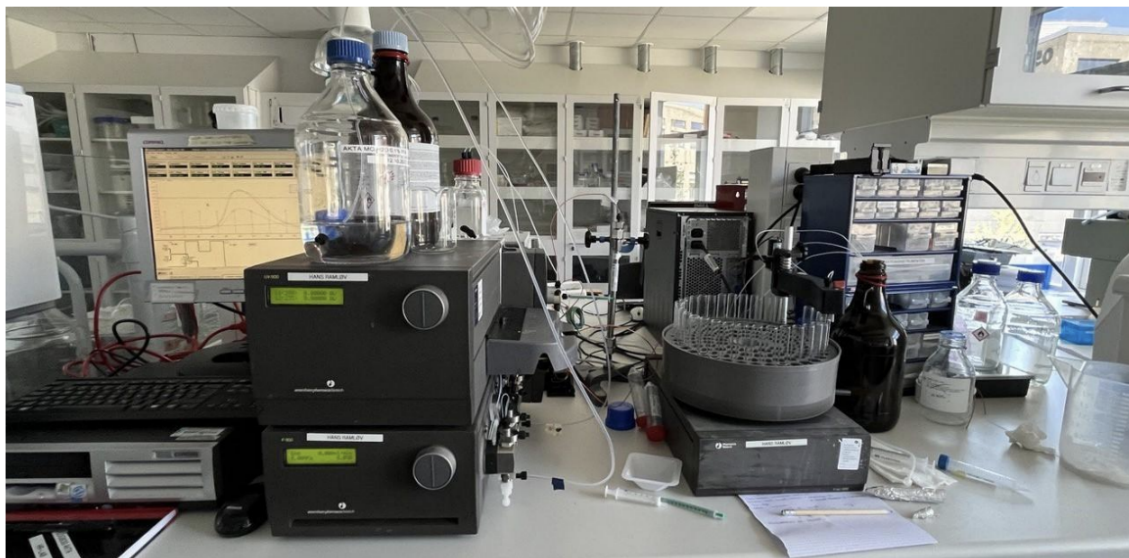
Figure 5.8: Setup at Roskilde University for peptoid purification. In the image the bottle with water and 0.1% acetonitrile and the bottle with acetonitrile, which constitute the mobile phase, can be seen on the left. They are connected to the four pumps below, that were previously checked to ensure the absence of bubbles to avoid electrical noise phenomena. On the right, it can be seen the waste container and the glassware for collecting the fractions expelled from the machine. On the computer screen, fractions that must be collected are displayed.

After the cleavage, 1 mg of crude peptoid was mixed with 1 ml of solution of acetonitrile and water, respectively 200 nanol and 800 nanol, and insert into the machine using a syringe. A standard method for the purification of the peptoid was identified, and it was implemented for the following batches. The purification of peptoid using HPLC involves the optimization of various parameters to achieve the best separation and purification. Adjusting the gradient is the most critical step in this process.

5.2 Preparation of the samples

In this project, titanium alloy Ti6Al4V (ASTM B348 Grade 5) was employed. In Figure 5.9 the specific chemical composition of the alloy is reported in comparison to pure titanium.

	N	C	H	Fe	O	Al	V	Ti
cp Ti	0.02	0.08	0.007	0.18	0.15	-	-	Balanced
Ti6Al4V	0.02	0.01	0.003	0.22	0.17	6.2	3.8	Balanced

Figure 5.9: Chemical composition of pure titanium and titanium alloy Ti6Al4V.[13]

Ti6Al4V is an α-beta alloy, in which aluminum is the α phase stabilizer and vanadium is the beta phase stabilizer. The alloy is characterized by remarkable specific strength, high protection against corrosion, and impressive properties at high temperature. In Figure 5.10 it can be noticed that Ti6Al4V has a higher yield strength and tensile strength than pure titanium, but lower elongation.

Types of Titanium for Implants	Yield Strength (MPa)	Ultimate Tensile Strength (MPa)	Elongation (%)
cp Ti grade 1	170	240	24
cp Ti grade 2	275	345	20
cp Ti grade 3	380	450	18
cp Ti grade 4	483	550	15
Ti6Al4V grade 5	795	860	10

Figure 5.10: Comparison of the properties of pure titanium and the titanium alloy Ti6Al4V14

The samples were previously obtained through a process involving the precise cutting of titanium cylindric bars into disks. These had a thickness of about 2 mm and a diameter of 10 mm. The specimens were washed with the polishing machine model Struers LaboPol-2 (Figure 5.11) using sequential grades of SiC abrasive papers under water irrigation and operating at a rotation speed of 250 rpm. The presence of the water was important to prevent any thermal or mechanical damage. Initially, each sample was polished employing P120 grit abrasive paper on both sides in order to eliminate the visible oxidative layer. Subsequently one side was marked with an electric pen. On the unmarked face, a set of 20 samples was ground using a sequence of abrasive papers with grits P320, P600, P800, P1200, P2500 and P4000, which allows optimal flatness and refined surface, while the unmarked side of 38 samples were ground with abrasive papers P320 and P400.

In order to remove residues and impurities resulting from the cutting and polishing processes, the polished samples were immersed one time in acetone for 5 minutes and, subsequently, two times in ultrapure water (milli-Q water) for 10 minutes each using ultrasonic bath (Sonica 2400 ETH S3 machine, Figure 5.12). The samples were then dried under a flow hood at room temperature.

5.3 Surface treatments

Surface treatments were conducted in pursuit of increasing micro-roughness, improving bone integration (osseointegration) also in case of poor bone quality, exposing a high density of hydroxyl groups to the surface, and enhancing biocompatibility. Moreover, they aimed to endow the alloy with bioactivity and antibacterial proprieties. 12 samples

Figure 5.11: Struers LaboPol-2 machine.

Figure 5.12: Sonica 2400 ETH S3

were not chemically treated but were investigated for comparative analysis. These treatments were carried out through a patented thermo-chemical process.[15] The process involved a first acid etching in hydrofluoric acid, which aimed to remove the native oxide layer (TiO2) characterized by a thickness of approximately 10 nm, followed by a controlled oxidation in hydrogen peroxide, which had the aim of creating a new thicker and rougher oxide layer on the surfaces. The samples were immersed in a solution of hydrofluoric acid, washed, and treated in hydrogen peroxide according to the process described in the European patent EP2214732B1. The obtained titanium oxide layer is characterized by a different crystalline structure (H2Ti3O7) and a thickness of around 300 nm. The resulting surface exhibited a nanostructure with violet, red or green color (depending on the thickness of the layer), that stimulated a favorable response from osteoblasts and possessed an abundance of hydroxyl groups on the surface, making it conducive to functionalization. The treated samples that were polished with a grain size up to 4000 and that were not superficially treated will now be called mirror polished (MP), while the treated samples that were polished to a grain size up to 400 will be referred to as chemically treated (CT).

5.4   Surface functionalization

In order to further activate the reactive hydroxyl groups on the surface, decrease the content of water and impurities, and facilitate the functionalization, the treated samples were exposed to UV irradiation for 1 hour. A solution containing PBS and GN2-Npm9 at a concentration of 1 mg/ml was prepared in the interim using a steerer. The peptoid was steered in PBS for 5 minutes at 300 rpm and subsequently filtered through a sterilized syringe (0.2nano filter) to avoid bacterial contamination. After the samples were removed from the UV exposure, they were carefully placed onto a Petri dish (Figure 5.13). Subsequently, a 100-nanol droplet of the solution was meticulously dispensed on each sample, ensuring the formation of a uniform layer that covered the entire surface.
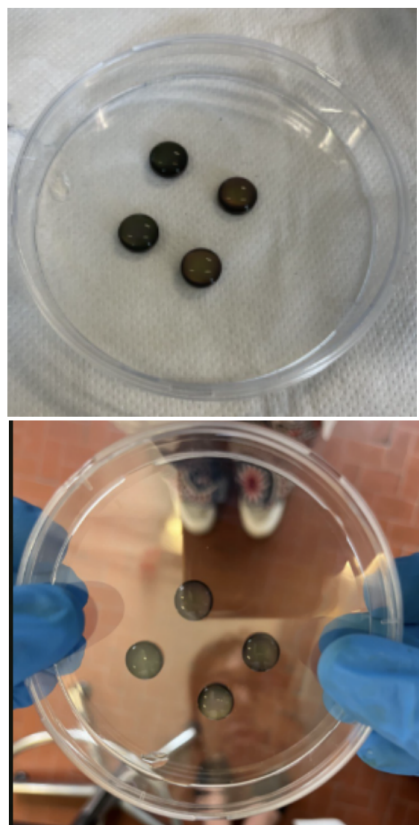

Figure 5.13: 100-μl drop onto CT_Ti6Al4V samples.

Subsequently, a moistened blotting paper was disposed along the interior perimeter of the Petri dish in order to maintain the moisture level. The Petri dish was placed within an incubator at 37°C for 2 hours. The samples were then rinsed in ultrapure water to eliminate any residual peptoid that didn't adhere to the surface and dried under a hood. Functionalized samples are now referred to as CT_GN2-Npm9. In Figure 5.14 the treatment steps for the different samples and their respective designation are reported.

Samples Name	Number of samples	Treatment
MP_ Ti6Al4V	12	*No Treatment, mirror polished*
CT_Ti6Al4V	18	*Acid etching and controlled oxidation*
CT_GN$_2$-Npm$_9$_Ti6Al4V	20	*Acid etching, controlled oxidation, and functionalization*

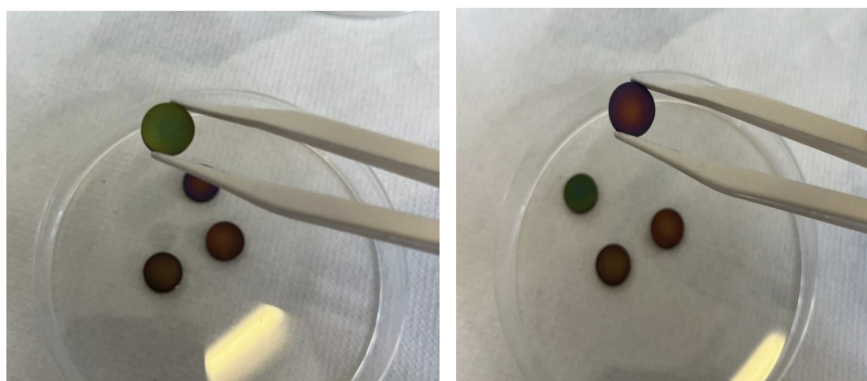Figure 5.14: Treatment for the different samples.

Figure 5.15: Samples after the functionalization with GN2-Npm9.

5.5 Surface characterization

5.5.1 X-ray photoelectron spectroscopy - XPS

X-Ray Photoelectron Spectroscopy (XPS) is a quantitative method employed for determining the chemical composition of a surface. It provides valuable insights into its elemental composition and how these elements are chemically bonded to other elements. The analysis is based on the photoelectric effect, illustrated in Figure 5.16.
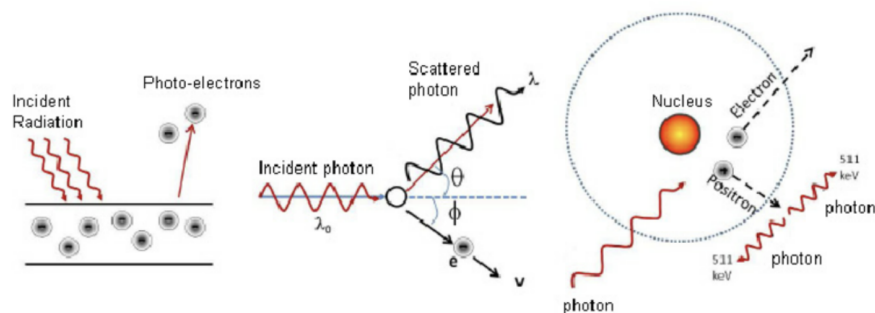
Figure 5.16: A scheme of the photoelectric effect. When an electromagnetic radiation irradiates a material, it emits electrons characterized by KE values. By measuring KE, an analysis on the chemical composition of the sample is carried out.[16]

When an atom or a molecule is invested by an electromagnetic radiation with energy E= hv and absorbs an X-ray photon, it ejects electrons from the inner energy levels. Electrons within the atom or molecule of the material are situated in specific energy levels, known as orbitals, each associated with a distinct binding energy (BE), which can be measured by analyzing the kinetic energy (KE) of the photoelectrons. Moreover, the measurement of KE allows the discernment of the elements that constitute the material's surface, elucidate their chemical configurations, and determine the specific binding energy of the involved electrons. In addition, this binding energy is influenced by the chemical surrounding of the original atom, the type of element which emits the electrons and the orbital from which it is ejected. Therefore, by examining the spectrum of photoemitted electrons, the constituent element of the sample can be determined. In this project, XPS was performed in order to investigate the chemical composition, expressed in atomic percentage of the elements, of the uppermost layer of the sample and to identify exposed functional groups and surface chemical bonds. A standard XPS spectrum, commonly referred to as a "Survey spectrum," depicts the number of detected electrons as a function of their binding energy. Each chemical element presents a distinctive set of peaks at specific energy values within this spectrum. The quantity of electrons exhibiting a particular kinetic energy corresponds to the amount of that element present on the sample's surface. To make meaningful comparisons of XPS intensities, it's most effective to express them as atomic percentage concentrations. This approach considers that not all emitted electrons are detected by the instrument, and it represents intensities as a percentage by relating the intensity of interest to the total electron intensity involved in the measurement. Furthermore, high-resolution analysis was performed, allowing for the differentiation of elements that might overlap in the Survey spectrum. This approach is valuable not only for identifying individual elements but also for discerning the oxidation state and the chemical environment surrounding a specific element. XPS spectra were acquired using a monochromatic Al x-ray source operated at a spot size of 100 nanom. High resolution spectra were obtained to identify and quantify chemical elements, in the regions of Ti, Al, V, O, C and N. The position of the elemental peaks on the binding energy scale provides insights into the chemical state. The spectra were set by using the C1s peak of hydrocarbon as internal standard at 284.80 eV.

5.5.2 Confocal microscopy

In this thesis, confocal microscopy was employed to evaluate the fluorescence of the targeted peptoid, which is attributed to the aromatic tryptophane-like residues. Intrinsic fluorescence of tryptophan-like residue is a valuable tool for studying structure, conformation and dynamic of peptoid.17 It enables the investigation of conformational changes, measurement of enzyme activities, ligand binding investigations, and insight into structural transition of protein.17,18,19 In general, among the three amino acids showing a ring structure with fluorescent property (tryptophan, tyrosine and phenylalanine), tryptophan-like residue is generally the preferred choice for detection because of its higher contribution to the intrinsic fluorescence emitted by the majority of protein.[20]

In our project, we employed a confocal microscope (Zeiss LSM900) to conduct advanced surface imaging and evaluate the fluorescence of functionalized samples. The microscope is equipped with fluorescence filters to detect the presence of fluorescent peptoid on the functionalized sample. The process for acquiring images involved more steps. We firstly placed the specimen onto the sample holder table. We then focused on a control sample not to excessively stimulate functionalized specimen, which might diminish its fluorescence. Subsequently, we activated the fluorescence mode, optimized the focus, and selected the acquisition area. Digital camera system was used for the acquisition of the images.

Figure 5.17: Confocal microscope Zeiss LSM900.[21]

We analyzed three samples, capturing one image for each: CT_Ti6Al4V, CT_GN2-Npm9_Ti6Al4V, and CT_GN2-Npm9_Ti6Al4V after a test release of 1 week. This approach allowed us to visually highlight differences among the samples resulting from the presence of tryptophan-like residues.

5.6 Zeta potential measurements of the peptoid in the solution

The measurement of zeta potential of the peptoid in the solution was conducted using the model of the Electric Double Layer (EDL), previously described in paragraph

2.6.1. When a charged particle is dispersed in a solution containing ions, these ions arrange around its surface because of the electrostatic interaction. On the surface of the particle, a first layer of adsorbed ions with opposite charge to that of the particle surface forms, and the electrostatic effect diminishes as the distance from the particle increases. The composition of the diffuse layer is dynamic and varies over time due to changes in pH, ionic strength, and concentration. When an electric field is imposed on the particle suspension, the particles migrate towards the electrode possessing an opposite charge. Between the first layer of adsorbed ions and the diffuse layer there is the shear plane, that represents the interface between the moving particles and the particles immobilized to this plane. The zeta potential is measured on the shear plane.[22] In dynamic light scattering (DLS) measurements, the motion of particles is carried out by the application of an electric field while it is simultaneously exposed to a laser beam. When the particle is in motion, the frequency of the light shifts (Doppler effect) proportionally to the velocity of the particle. In this project, the instrument consisted of a laser source that was split into two ways: one is used as a reference and the second is used to examine the sample containing the dispersion. Therefore, the frequency shift is determined, and the velocity of the particle and the zeta potential can be calculated (see Figure 5.18).
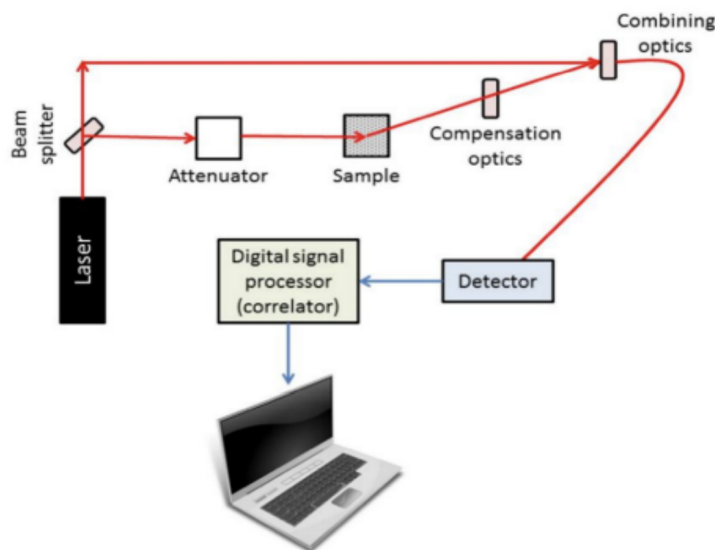

Figure 5.18: Scheme of the instrument employed for zeta potential measurement.[23]

In this project, the instrument Litesizer 500 was employed for the determination of the zeta potential of peptoid in solution. Two cuvettes were used to perform the measurement, both equipped with two electrodes to apply the electric field to the solution inside.

Figure 5.19: Instrument Litesizer 500 with the cuvettes inside.[23]

Firstly, a solution of peptoid and water was prepared with concentration 0.5 mg/ml; the zeta potential was measured as a function of pH in an electrolyte solution containing 0.001 M KCl. To create the zeta potential curve of the peptoid in solution as a function of pH, seven measurements were conducted at pH values of 3, 5, 6.7, 8, 9, 9.5, 10. The initial pH started at around 6.5, and it was changed using by adding either 0.05 M HCl or 0.05 M NaOH.

5.7 Release test

In order to evaluate in vitro bioactivity and stability of the peptoid adsorbed on the CT surface, a release test over the time was conducted in aqueous environment. 3 CT_GN2-Npm9_Ti6Al4V specimens were considered for the analysis and immersed in 2 ml of water. In each tube, the sample was soaked with the treated head upward, and the eventual release of the peptoid was investigated by the immersion of the material of interest for a period of 3 hours, 24 hours, 48 hours, 5 days, and 9 days. During the different period of time, the tubes were incubated at a controlled temperature of 37°C.

5.7.1 UV-Vis spectroscopy

Ultra-violet (UV) spectroscopy is an analytical technique used to examine solid or liquid samples by exposing them to UV-Vis light. This technique assesses the sample's properties by measuring how much light it absorbs or its transmittance, and this data is recorded in relation to the wavelength of the irradiating light, expressed in nanometers.[24] Therefore, by employing spectroscopy, the release of the peptoid in water solution was characterized by examining distinct peaks resulting from the inclination of the atoms, functional groups, and complexes within the compound to interact with UV radiation at specific wavelengths. In our project, the spectrometric analysis was conducted using a UV-Vis spectrophotometer (UV2600 Shimadzu, Figure 5.20). The instrument consists of a UV light source, a UV detector, and a PC for signal processing and display. In UV spectroscopy, liquid samples are analyzed by placing them in a cuvette, while water is put in another cuvette. The sample is positioned between

the source and the detector. The source emits UV-Vis spectrum radiation, some of which is absorbed, transmitted, reflected, or scattered by the sample. This happens due to the energy accumulation after irradiation, which is then detected. The UV-Vis spectrum characterizing the sample is the output of the measurement.[25] The solutions obtained after the release period of interest were analyzed, and their absorbance was measured within the wavelength spanning from 200 to 600 nm. The absorption peak corresponding to the solutions was plotted with the use of Versa Studio software.

Figure 5.20: UV2600 Shimadzu.[26]

5.8 Halo assay

We conducted a qualitative halo test against the non-pathogenic Gram-positive bacterium S. Epidermidis to qualitatively assess how the peptoid affects bacterial growth. A standard concentration bacterial suspension was prepared and subsequently placed on a blood agar plate to grow for 24 hours. For the preparation of selective agar plate (Muller Hinton agar), we mixed nutrient broth with a little quantity of bacterial colonies collected from the blood agar plate using a cotton swab. This process aimed to achieve a McFarland index of 0.50, starting from a value of 0.0 for the physiological solution, using a densitometer for the measurement of turbidity of the suspensions. The value of 0.5 corresponds to 108 CFU/ml. Once we reached the desired McFarland value of 0.5, we applied the contaminated solution uniformly onto the Muller Hinton agar plate, including the edges. We then placed 3 CT_Ti6Al4V samples on the upper side of the plate as a control, and 3 CT_GN2-Npm9_Ti6Al4V samples in the lower side of the plate, with the treated face in contact with the plate. Finally, the plate was incubated for 24 hours at 35°C.
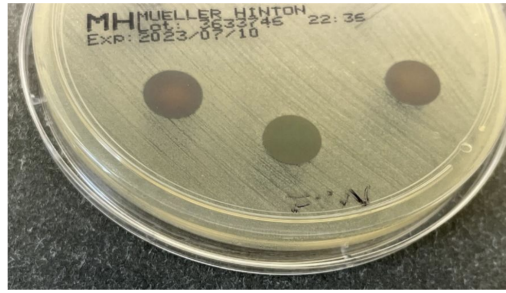
Figure 5.21: Muller Hinton plate with functionalized specimens tested with S. Epidermidis.

Figure 5.22: Muller Hinton plate with specimens of control tested with S. Epidermidis.

5.9 In vitro bioactivity test

Two CT_GN2-Npm9_Ti6Al4V samples and two CT_Ti6Al4V samples were used to examine in vitro bioactivity. The specimens were immersed in simulated body fluid (SBF) and incubated at 37 °C for 1 week and 2 weeks. SBF is a prepared solution that replicates the ionic concentration found in human plasma, and it was prepared following the protocol outlined by Kokubo.[27] In this method, 9 reagents were employed per 1000 ml of SBF solution (Figure 5.23). After 1 week of incubation at 37 °C, the solution was refreshed to simulate the natural exchange of physiological fluids in the body and the pH of the solution was checked. After the two weeks of exposition, the samples were washed and with ultrapure water and analyzed using FE-SEM to assess whether hydroxyapatite might have formed on their surfaces.

The hydroxyapatite is the main mineral component of the bone. Therefore, the development of a layer of apatite on the surface is crucial for the success of an implant designed to bond with bone-tissue post-implantation. When the biomaterial is immersed in SBF, calcium and phosphorus in the solution initiate the formation of apatite nuclei, which subsequently expand and form on the surface of the material. By immersing the specimen in BSF, we can investigate the potential formation of this apatite layer in vitro and predict its bioactivity when implanted in a living organism.[27]

REAGENTS PER 1000 mL of SBF	Amount (g)
NaCl	8.035 g
NaHCO3	0.355 g
KCl	0.255 g
K2HPO4.3H2O	0.231 g
MgCl2.6H2O	0.311 g
1M-HCl	39 mL
CaCl2	0.292 g
Na2SO4	0.072 g
TRIS	6.118 g
1M-HCl	0-5 mL

Figure 5.23: Reagents used in the method

5.10   Biological evaluation

Pseudomonas aeruginosa, a widespread Gram-negative bacterium, plays a considerable role in causing nosocomial infections and posing a grave threat to immunocompromised individuals, including post-surgery patients. In 2017, the World Health Organization designated P. aeruginosa as a priority pathogen for antibiotic research and development due to its life-threatening nature. The bacterium's intrinsic antibiotic resistance and adaptability often render common antimicrobial agents ineffective, resulting in higher mortality rates. Moreover, its ability to form protective biofilms obstructs the treatment of infections inhibiting phagocytosis and enabling colonization and persistence. This biofilm is frequently observed in chronic infections, such as those in the lungs, wounds, and sinuses, affecting millions of patients in the United States alone and incurring significant healthcare costs. In addition, P. aeruginosa ability to colonize various surfaces, including medical devices and food industry equipment, notably increases the urgency of addressing this pathogen.[28] Therefore, early diagnosis is crucial to combat P. aeruginosa infections to prevent biofilm formation, with alternative therapeutic strategies beyond traditional antibiotics. In this context, in this project the role of peptoid GN2-Npm9 as a potential solution had been investigated.

5.10.1   Bacteria cultivation

The dental plaque from patients affected by periodontitis was collected at the Dental Clinic of the Maggiore Hospital in Novara, with a non-invasive procedure and after obtaining the patient's informed consent according to the Declaration of Helsinki. Briefly, the specimen was collected by curettage from the supragingival aspect of the premolars or molars with Gracey curettes. After collecting the plaque, it is aseptically positioned inside a sterile containment tube and sent to the biomedical materials laboratory of the University of Eastern Piedmont. Here it was quickly dispersed inside a tube containing 30ml of sterile "cooked meat medium" (CMM, Merck, Darmstadt, Germany)

and everything was positioned at 37 degrees in a hood suitable for the growth of anaerobic bacteria, i.e. growing in the absence of oxygen (Fig. 1). The anaerobic hood uses nitrogen, a hydrogen-based mixture and palladium-based filters to remove oxygen and create an environment suitable for the growth of anaerobic species. To preserve the starting population, the bacteria are used immediately after the increase in the exponential growth phase. Before the experiment, the number of bacteria is diluted in medium until a concentration of 105/ml bacteria is obtained, in accordance with the optical density (OD 600 nm) read on the spectrophotometer equal to 0.001.

Figure 5.24: Hood suitable for the growth of anaerobic microorganisms.

5.10.2 Biofilm assay

The effect of the supernatants and PBS that contain the bacteria detached from the biofilm of different Ti-based surfaces (TI6AL4V, CT-GN-NpMg, CT) on multidrug-resistant clinical isolate P. aeruginosa MMA83[29] biofilm formation was monitored in 24-well microtiter plates with sterile glass slides (Sarstedt, Germany) using fluorescence microscopy (ZEISS Axioscope 5, Germany, 2000 × magnification). P. aeruginosa MMA83 (previously adjusted to 105 CFU/ml) was incubated for 24h with supernatants and the liquid after detaching the bacteria from the surface from different samples (TI6AL4V, POLY, CT-GN-NpMg, CT) (1/10 V) at 37°C to monitor the prevention of biofilm formation. After incubation, the planktonic cells were carefully rinsed three times with sterile phosphate-buffered saline 1xPBS (137 mM NaCl, 10 mM phosphate, 2.7 mM KCl; pH 7.4). Biofilms were stained at room temperature for 30 min with 2.5 μM propidium iodide and 2.5 μM SYTO9 (Thermo Fisher Scientific) resuspended in 1xPBS. The MMA83 culture was incubated under the same conditions as an untreated control.

5.10.3 Real time quantitative PCR (RT-qPCR)

RT-qPCR was used to analyze the effect of the supernatants of different Ti-based surfaces (TI6AL4V, CT-GN-NpMg, CT) on the relative mRNA levels of the genes QS (lasR. lasI, rhlR, rhlI,pqsA, pqsH mvfR,) and the genes involved in P. aeruginosa MMA83 virulence (lasB, phzM, rhlC,) compared to control (POLY). MMA83 cultures (adjusted to 1.5x107CFU/ml) were incubated overnight with supernatants collected

from different samples (final concentration 1/10 V) at 37°C for 12 hours under aeration (180 rpm). RNA isolation of the treated and untreated MMA83 culture was performed using the RNeasy Mini Kit (Qiagen, Germany) according to the manufacturers' instructions. Isolated RNA was purified from residual DNA using a DNA-free DNA removal kit (Thermo Fisher Scientific). The concentration and purity of isolated RNA were checked using the BioSpec-nano instrument (Shimadzu, Kyoto, Japan). Reverse transcription was performed using a Rever-tAid RT Reverse Transcription Kit (ThermoFisher) according to the manufacturer's protocol. The mixture for real-time quantification contained 2 × qPCR Universal Mix (Nippon Genetics, Dueren, Germany), FastGene IC Green, appropriate primers (Table 1), cDNA, and bidestilled water. The primers of the selected genes used in this analysis are listed in Table 1. RT-qPCR analysis was performed in a 7500 Real-Time PCR System (Applied Biosystems, Waltham, MA, USA) under the following reaction conditions: initial denaturation at 95 ℃ for 2 min and 40 cycles of denaturation 95 ℃/5 s, annealing and elongation 60 ℃ /32 s. The rpsL was used as an endogenous control to normalize obtained data following the 2-$\delta\delta$Ct method.[30] The changes in relative mRNA level of analyzing genes were determined compared to untreated control. Analysis was performed in triplicate and repeated three times.

Gene	Primer name	Sequence (5′-3′)	Length (bp)	Source
lasI	lasI_Fw	GCGTGCTCAAGTGTTCAAGG	125	31
	lasI_Rev	GGGCTTCAGGAGTATCTTCCTGG		
lasR	lasR_Fw	CTGTGGATGCTCAAGGACTAC	133	31
	lasR_Rev	AACTGGTCTTGCCGATGG		
rhiI	rhiI_Fw	CCATCCGCAAACCCGCTACATC	151	31
	rhiI_Rev	CTCCCAGACCGACGGATCGCTCGGC		
rhiR	rhiR_Fw	GGGCGTGTTCGCCGTCCTGG	143	31
	rhiR_Rev	GGTATCGCTCCAGCCAGGCCTTG		
pqsA	pqs_Fw	GACCGGCTGTATTCGATTC	74	31
	pqs_Rev	GCTGAACCAGGGAAAGAAC		
mvfR	mvfR_Fw	GTCGGGACGGCTACAAGGTCG	121	Present study
	mvfR_Rev	GATTGCGCGGACCCTTGTTGAG		
pqsH	pqsH_Fw	AGGCGAACGAGGGTATTCCT	149	Present study
	pqsH_Rev	TCAGTGGGAATCGCCCTG		
lasB	lasB_Fw	CGCAGCGTGGAGAACGCCTA	183	Present study
	lasB_Rev	GTCGGAGAACGCTTCGTTCA		
phzM	phzM_Fw	CCGCGACATGGTGCTGTTCTA	170	Present study
	phzM_Rev	TTCATCGCCAGCAGGAAGCG		
rhlC	rhlC_Fw	TTCCTGCCGGCCATCCATCTCG	139	Present study
	rhlC_Rev	AAGTGGCCGAGGCGCTGGTAG		
rpsL	rpsL_Fw	GCAACTATCAACCAGCTGGTG	231	31
	rpsL_Rev	GCTGTGCTCTTGCAGGTTGTG		

Figure 5.25: List of the primers used in this study.

References: Chapter 5

1. Biljana Mojsoska, Ronald N. Zuckermann, and Håvard Jenssen. "Structure-Activity Relationship Study of Novel Peptoids That Mimic the Structure of Antimicrobial Peptides". Antimicrob Agents Chemother (2015); 59(7): 4112–4120.

2. Paola Saporito, Biljana Mojsoska, Anders Løbner Olesen, Håvard Jenssen. "Antibacterial mechanisms of GN-2 derived peptides and peptoids against Escherichia coli". BioPolymers (2019); Volume 110, Issue 6.

3. Biljana Mojsoska, Gustavo Carretero, Sylvester Larsen, Ramona Valentina Mateiu and Håvard Jenssen. "Peptoids successfully inhibit the growth of gram-negative E. coli causing substantial membrane damage". Scientific Reports volume 7, Article number: 42332 (2017).

4. A. Lone, A. Arnous, P. R. Hansen, B. Mojsoska, and H. Jenssen. "Synthesis of Peptoids Containing Multiple Nhtrp and Ntrp Residues: A Comparative Study of Resin, Cleavage Conditions and Submonomer Protection". Front. Chem. (2020), vol. 8, no. April, pp. 1–12.

5. Maochao Zheng, Miao Pan, Wancong Zhang, Huanchang Lin, Shenlang Wu, Chao Lu, Shijie Tang, Daojun Liu, Jianfeng Cai. "Poly(α-l-lysine)-based nanomaterials for versatile biomedical applications: Current advances and perspectives". Bioactive Materials (2021) Volume 6, Issue 7, Pages 1878-1909.

6. Sanne Gottschalk, Dan Ifrah, Sandra Lerche, Caroline T Gottlieb, Marianne T Cohn, Hiroshi Hiasa, Paul R Hansen, Lone Gram, Hanne Ingmer, Line E Thomsen. "The antimicrobial lysine-peptoid hybrid LP5 inhibits DNA replication and induces the SOS response in Staphylococcus aureus". BMC Microbiol. (2013), vol. 13, article number 192.

7. Mishra AK, Choi J, Moon E, Baek KH. "Tryptophan-Rich and Proline-Rich Antimicrobial Peptides". Molecules (2018). 23(4):815.

8. Hao Guo, John Andrew MacKay. "A pharmacokinetics primer for preclinical nanomedicine research". Nanoparticles for Biomedical Applications(2020). Chapter 8, pages 109-128.

9. Matuszewski, B. K., Constanzer, M. L., Chavez-Eng, C. M. "Strategies for the Assessment of Matrix Effect in Quantitative Bioanalytical Methods Based on HPLC-MS/TS". Anal. Chem. (2003). 75 (13), pages 3019-3030.

10. Harris, D. C. "Quantitative Chemical Analysis, 8th edition"; W.H. Freeman and Company (2010).

11. Pablo De Vicente. "Importance of Analysis to Prevent and Control the Presence of Mycotoxins in Cereals". Cereal Foods World (2020), Vol. 65, No. 1.

12. Bhanu Pratap Singh. "What is HPLC". Pharmaceutical Guidelines (2022).

13. Rocha SS, Adabo GL, Henriques GE, Nóbilo MA. "Vickers hardness of cast commercially pure titanium and Ti-6Al-4V alloy submitted to heat treatments". Braz Dent J. (2006); 17(2):126-9.

14. Fernandes, Daniel, Elias, Carlos, Valiev, Ruslan. "Properties and Performance of Ultrafine Grained Titanium for Biomedical Applications". Materials Research (2015).

15. S. Ferraris, S. Spriano, G. Pan, A. Venturello, C. L. Bianchi, R. Chiesa, M. G. Faga, G. Maina, E. Vernè. "Surface modification of Ti-6Al-4V alloy for biomineralization and specific biological response: Part I, inorganic modification", J. Mater. Sci. Mater. Med., (2011), vol. 22(3), pages 533–545.

16. Saldaña, Griselda & Reyes, Uvaldo & Salazar, Hadel & Oscar, Martínez & Moreno, Eduardo & Conde, Rosmery. "High Density Devices Applied to a Gamma-Camera Implementation" (2012).

17. Hixon, John, and Yana K. Reshetnyak. "Algorithm for the Analysis of Tryptophan Fluorescence Spectra and Their Correlation with Protein Structural Parameters" Algorithms (2009), volume 2 no. 3, pages 1155-1176.

18. James T. Vivian, Patrik R. Callis, Mechanisms of Tryptophan Fluorescence Shifts in Proteins, Biophysical Journal (2001), Volume 80, Issue 5, Pages 2093-2109.

19. Daniel I. Ranieri, Danielle M. Corgliano, Elliott J. Franco, Heike Hofstetter, Oliver Hofstetter. "Investigation of the stereoselectivity of an anti-amino acid antibody using molecular modeling and ligand docking". Chirality (2008), volume 20, Issue 3-4.

20. Dr Barry Whyte. "Tryptophan fluorescence can be used to study protein conformation. Find out how microplate readers can be used to detect tryptophan and investigate protein function." BMG LABTECH (2022).

21. https://www.medicalexpo.it/prod/zeiss-microscopy/product-104077-859917.html

22. Sourav Bhattacharjee, "DLS and zeta potential – What they are and what they are not?". Journal of Controlled Release (2016), Volume 235, Pages 337-351.

23. https://www.anton-paar.com/it-it/prodotti/dettagli/litesizer/

24. Farag MA, Sheashea M, Zhao C, Maamoun AA. UV Fingerprinting Approaches for Quality Control Analyses of Food and Functional Food Coupled to Chemometrics: A Comprehensive Analysis of Novel Trends and Applications. Foods. 2022 Sep 16;11(18):2867.

25. Thomas A. Germer, Joanne C. Zwinkels, Benjamin K Tsai, "Experimental methods in the physical sciences", Chapter 2 – Theoretical concepts in spectrophotometric measurements, 46, 11- 66, 2014.

26. https://www.news-medical.net/UV-2600UV-2700-UV-VIS-Spectrophotometer-from-Shimadzu

27. Kokubo, T. & Takadama, H. How useful is SBF in predicting in vivo bone bioactivity? Biomaterials 27, 2907–2915 (2006).

28. Thi MTT, Wibowo D, Rehm BHA. "Pseudomonas aeruginosa Biofilms". Int J Mol Sci. (2020); 21(22):8671.

29. B. Jovcic, Z. Lepsanovic, V. Suljagic, G. Rackov, J. Begovic, L. Topisirovic, M. Kojic, Emergence of NDM-1 metallo-β-lactamase in Pseudomonas aeruginosa clinical isolates from Serbia. Antimicrob Agents Chemother (2011) 55:3929-31. https://doi.org/10.1128/aac.00226-11

30. K.J. Livak, T.D. Schmittgen, Analysis of relative gene expression data using realtime quantitative PCR and the 2- $\delta\delta$ CT method, Methods 25 (2001) 402-408, https://doi.org/10.1006/meth.2001.1262

31. M. Malešević, F. Di Lorenzo, B. Filipić, N. Stanisavljević, K. Novović, L. Senerovic, et al., Pseudomonas aeruginosa quorum sensing inhibition by clinical isolate Delftia tsuruhatensis 11304: involvement of N-octadecanoylhomoserine lactones. Sci Rep (2019) 16465. http://doi.org/10.1038/s41598-019-52955-3

Chapter 6

Results and discussion

6.1 Characterization of the peptoid

In this project, five syntheses of the peptoid GN2-Npm9 were executed. The chromatograms have time as the independent variable on the x-axis and relative abundance on the y-axis. Subsequently, for each peak in the chromatogram, spectra were created to inspect the mass per charge molecules. These spectra were plotted with mass per charge values on the x-axis and relative abundance on the y-axis. Figure 6.1 shows the HPLC-MS results of peptoid GN2-Npm9 after the first synthesis.
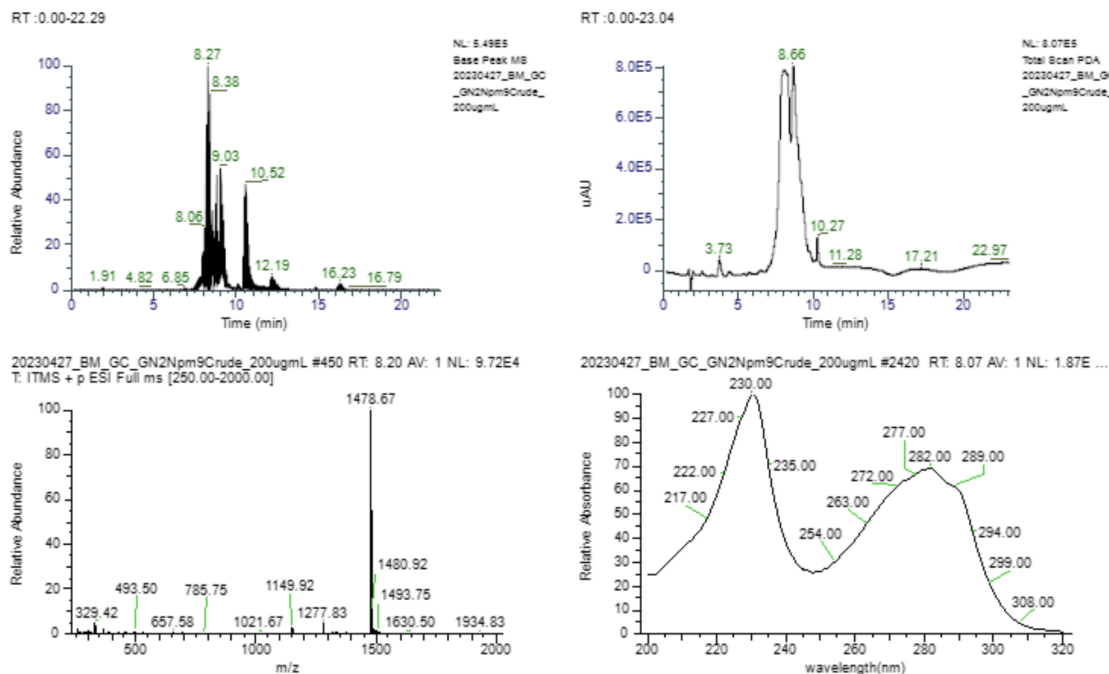
Figure 6.1: HPLC-MS results first synthesis.

In HPLC-MS detection of the peptoid, the presence of multiple distinct peaks indicates the presence of impurities in the solution. These impurities include submonomeric sequences that differ from the targeted peptoid, resulting in shorter and

significantly distinct peptoid variation coexisting within the same solution. Furthermore, the solution could also be contaminated by the reagents used during the synthesis process, such as DMF or DIC, that contribute to the impurity of the solution and the appearance of additional compounds in the HPLC-MS results. In addition, the intermitted interruption and resumption of each synthesis affected the overall yield. Considering the available results, it is challenging to precisely pinpoint the stage at which the impurities are introduced; a strategy to mitigate this issue involves the extraction of the sample after each displacement and its analysis after a cleavage process. Moreover, an incomplete TFA evaporation results in contamination during the initial lyophilization process and, consequently, to the absence of a singular and well-defined peak. TFA, being a small molecule, moves rapidly through the column during analysis. In order to avoid this issue, multiple lyophilization processes were performed, but the outcomes did not show substantial improvements. The presence of additional peaks in the mass spectrometry makes it more challenging to interpret. However, the precise evaluation of the presence of the peptoid in the solution remains determinable, thanks to our knowledge of the average molecular weight of GN2-Npm9, which is 1477 amu. This enables us to confirm the success of the synthesis by identifying the highest peak in the spectrum, which closely matches the expected molecular weight of the peptoid. Specifically, we observed a peak at 1478.87 amu, as shown in Figure 6.1, which corresponds closely to the expected value 1477 amu. Below, HPLC-MS results for the crude peptoid obtained after cleavage from second, fourth and fifth syntheses, are reported.
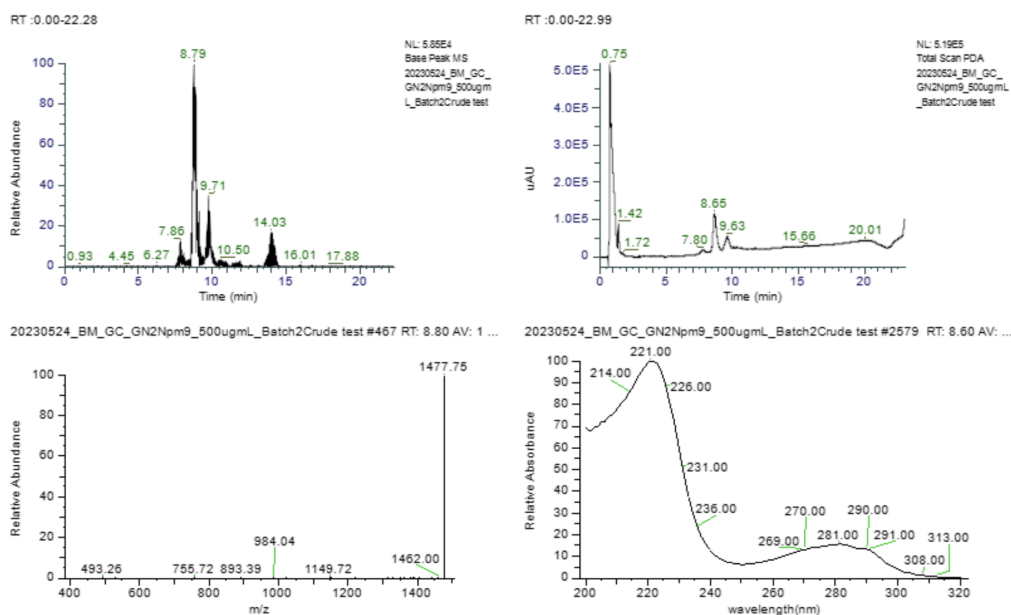

Figure 6.2: HPLC-MS results of the second synthesis. The success of the synthesis is validated by the noticeable presence of a high peak, which has a molecular weight value of 1477.75 amu, that closely aligns with the average molecular weight of the targeted peptoid. Furthermore, by comparing this analysis with the previously collected data, it is confirmed that the peptoid of interest eluted from the column at approximately 8 minutes, specifically at 8.79 minutes in this database.

Comparing each subsequent synthesis with the first one was crucial. This step was necessary because we already had confirmation of the success of the first synthesis, which was previously verified trough analysis after purification.
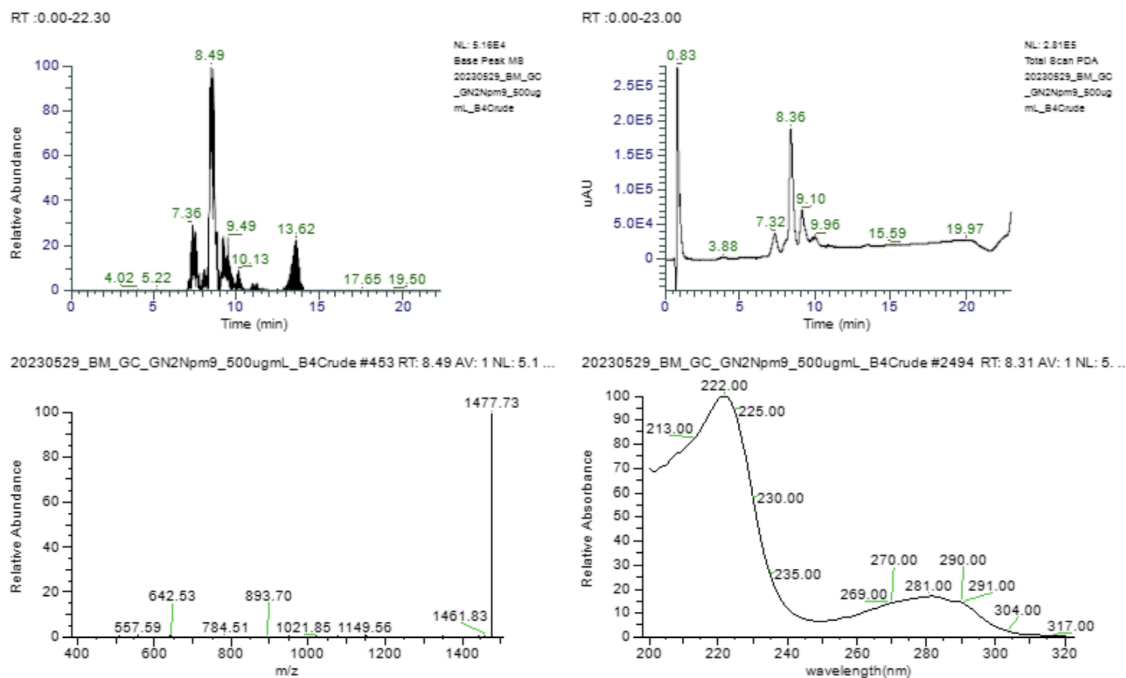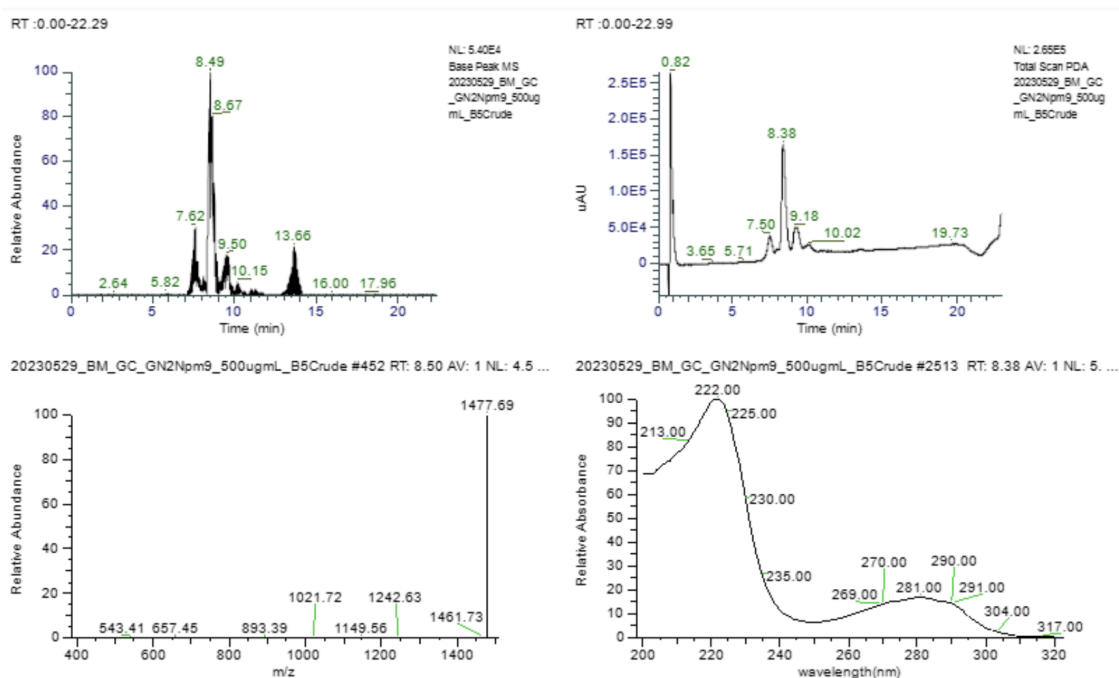

Figure 6.3: HPLC-MS results from the fourth synthesis. The success of the synthesis is confirmed by the presence of a predominant peak possessing a value of 1477.73 amu, closed to the average molecular weight of the targeted peptoid.

Figure 6.4: HPLC-MS results from the fifth synthesis. The success of the synthesis is confirmed by the presence of a predominant peak possessing a value of 1477.69 amu, closed to the average molecular weight of the peptoid of interest.

Figure 6.5 illustrates an unsuccessful synthesis. When comparing these graphs to the previous analysis, we observed three significant differences: there was no prominent peak with a molecular weight value close to 1477 amu, the compounds was not eluted after about 8 minutes (there is a high peak at 10.15 minutes), and there was a notable absence of signal intensity at a wavelength of 280 nm. This last information indicates that the presence of tryptophan-like residues in the peptoid generates a signal intensity at a wavelength of 280 nm, which was also visible in the other synthesis.
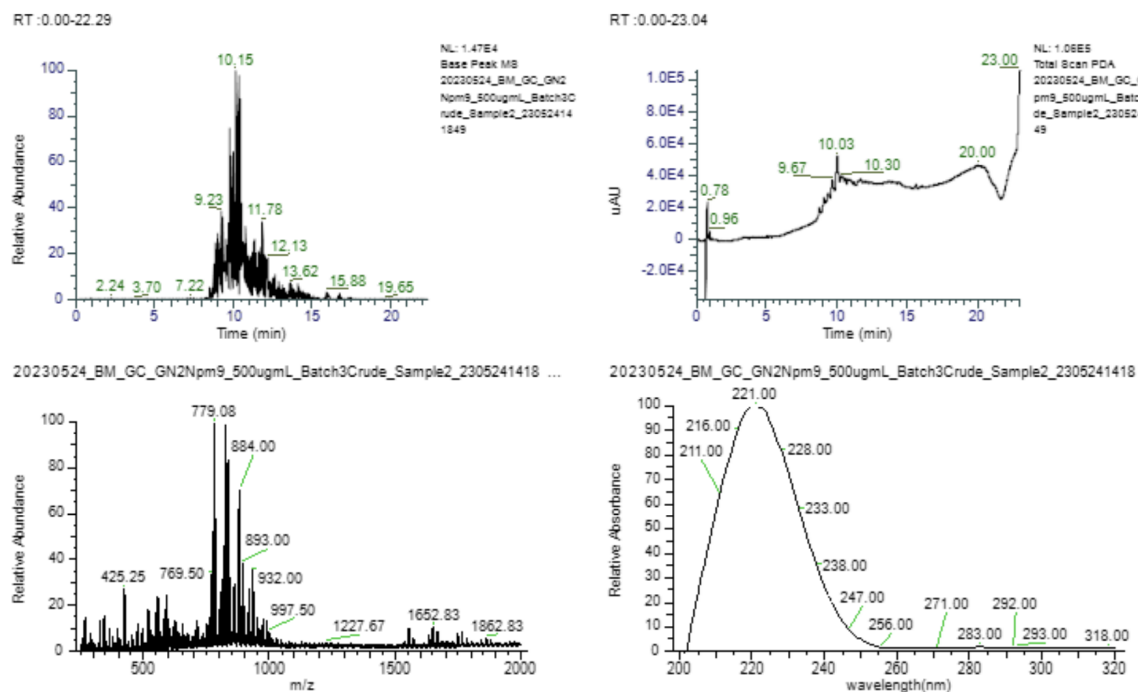
Figure 6.5: HPLC-MS results of the third synthesis.

6.2 Purification of the peptoid

The first phase was to determine the solvent composition to elute the peptoid. To achieve this, 1 ml of the solution was introduced into the analytical column, and it was eluted with a gradient of 10% acetonitrile to 70% acetonitrile (Figure 6.6). Given the lack of prior information about the peptoid, we implemented an extended gradient with a longer duration in the first method to ensure that the peptoid was effectively included in the analysis. Remaining material was directed to waste.
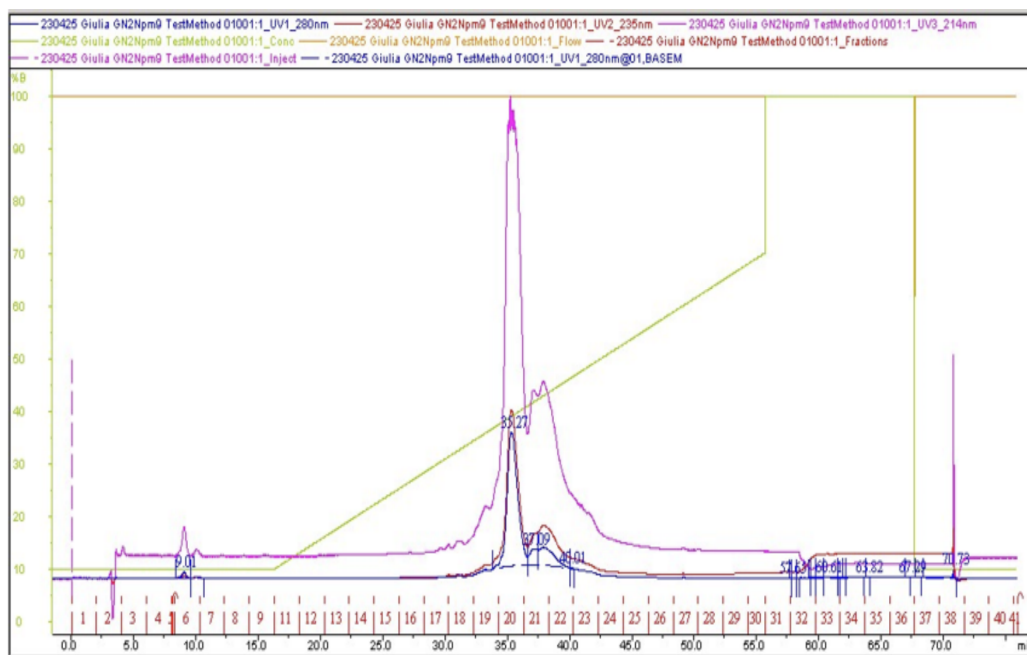
Figure 6.6: First method employed.

Upon examining the chromatograph obtained using the first method (Figure 6.6), we identified the region where the peptoid was located, corresponding to the fractions 20 and 21. In the subsequent method, we employed a gradient elution ranging from 20% to 50% acetonitrile. This adjustment aimed to enhance the gradient and, consequently, improve separation efficiency. Moreover, we directed the portions of the chromatograph were the peptoid was not eluted to waste, so that the fractions were collected in the portion of the gradient. This approach allowed for a more precise separation of solution component, resulting in a purer peptoid.
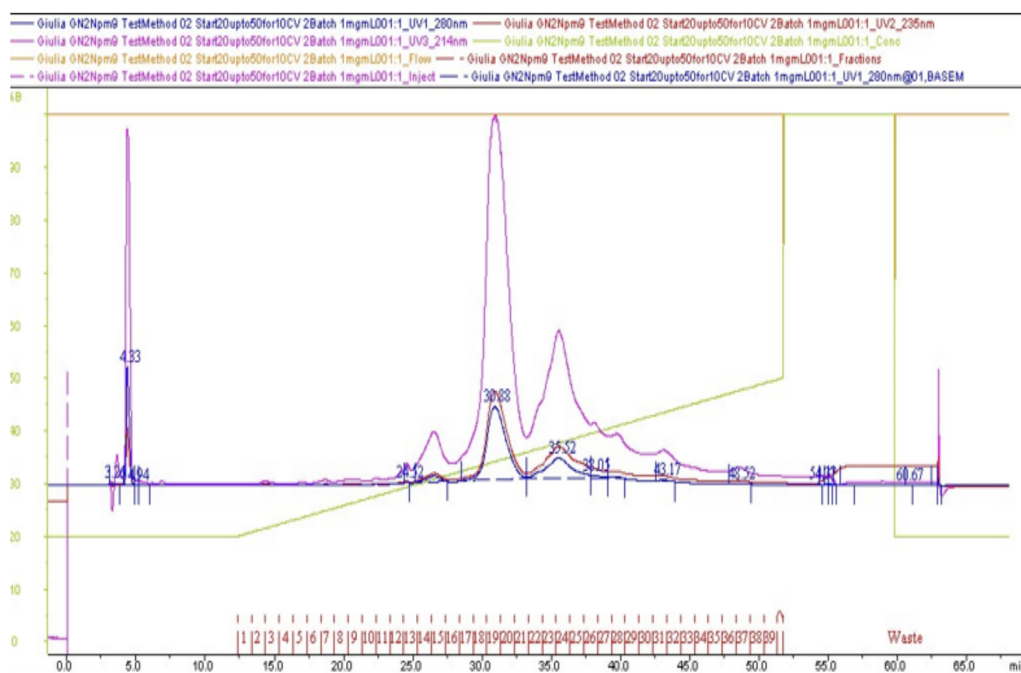
Figure 6.7: Second method employed.

By observing the chromatogram obtained with the second method (Figure 6.7), we noticed that the peak was divided in half between two fractions. However, our goal was to have the peptoid components in entire fractions. Moreover, we observed that the peptoid was completely eluted at around 40% acetonitrile. Therefore, the third method was implemented a gradient elution ranging from 25% to 35% acetonitrile in order to essentially include the peptoid in the gradient and make the peak wider, enhancing the separation.
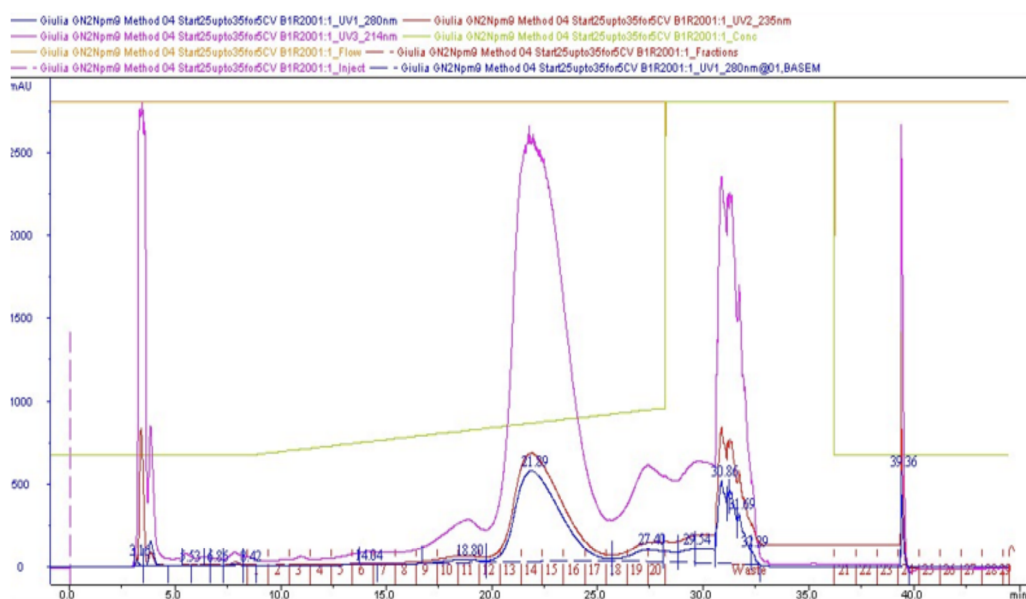
Figure 6.8: Third method. It was employed for the subsequent analysis.

After implementing the correct method (Figure 6.8), fractions containing the peptoid were collected and subjected to HPLC-MS analysis to assess their purity. The results are shown in Figure 6.9. In the chromatogram and in the spectrum, we can observe the presence of a single well-defined peak with a molecular weight value closer to GN2-Npm9 molecular weight than the data obtained from the crude product. Moreover, we noticed a considerably smaller number of shorter peaks, which indicated impurities.
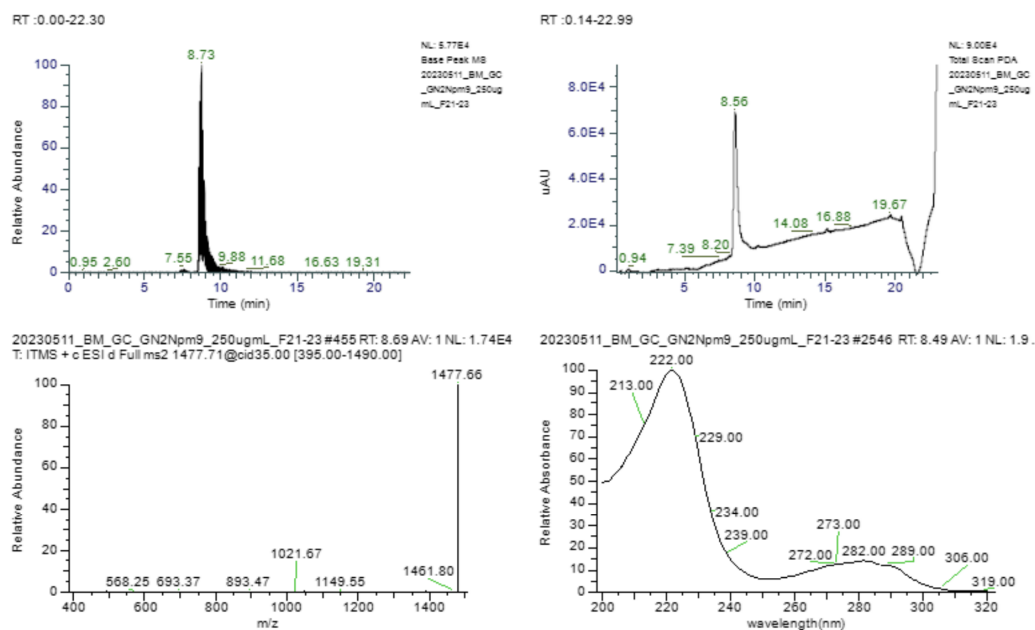
Figure 6.9: HPLC-MS results of purified peptoid obtained with the first synthesis.

6.3 Surface characterization

6.3.1 XPS

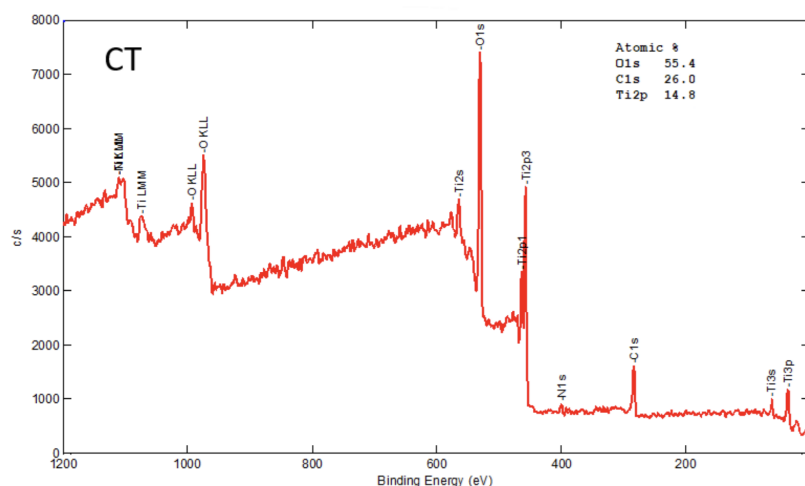|	O	C	Ti	N
CT	55.4	26.0	14.8	3.8
CT_GN2-Npm9	30.8	51.5	8.2	9.4

Figure 6.10: Atomic percentage of the elements detected on CT, and CT_GN2-Npm9.

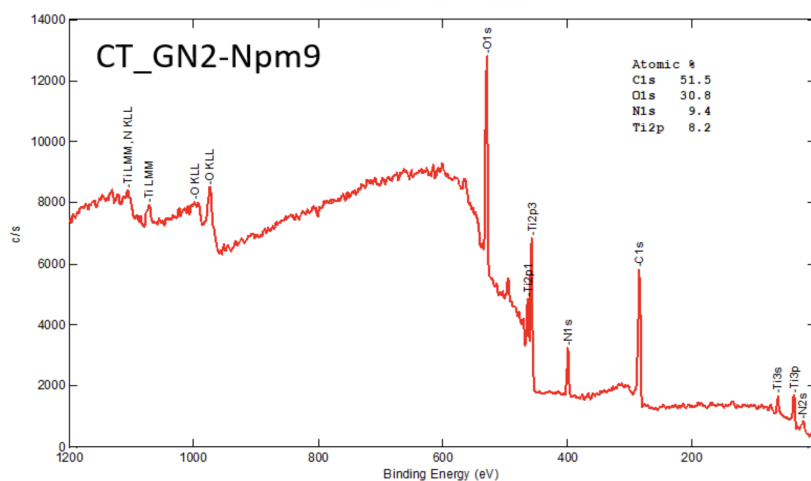Figure 6.11: Survey spectrum of CT specimen.

Figure 6.12: Survey spectrum of CT_GN2-Npm9 specimen.

XPS measurements were conducted to investigate the composition of the surface of the functionalized samples and the mechanism by which the peptoid is bound onto the titanium surface. CT_GN2-Npm9 spectra were compared with the CT control sample, both with an information depth of about 10 nm. In Figure 6.10 the surface composition of the specimens is reported, expressed as atomic percentage of the elements, and the survey spectra are shown in Figure 6.11 and Figure 6.12. A significant amount of oxygen was identified in the CT sample, which is attributed to the oxide layer formed on its surface. The significant decrease in the amount of titanium in CT_GN2-Npm9 confirmed the presence of a functionalized layer on the surface of the sample which does not allow the instrument to penetrate into the substrate. The presence of carbon on the CT sample is due to atmospheric contamination, as the chemical treatment performed did not involve the use of carbon compounds. Indeed, titanium and its alloys are characterized by an easy adsorption of contaminant carbon on their surface. The presence of the carbon doubles in the functionalized sample compared to the CT

sample, which is attributed to the organic peptoid on the surface. For the same reason, the percentage of the nitrogen significantly increased in the functionalized sample, while the percentage of nitrogen on CT surface, due to a contamination, is very low and as such negligible. The amount of oxygen in CT_GN2-Npm9 decreased because the oxide layer on titanium surface was partially covered by the functionalized layer.

High resolution spectra for the carbon, and oxygen were obtained for each sample, while high resolution spectra of nitrogen was only obtained for the functionalized sample, because the atomic percentage of nitrogen in CT sample was irrelevant. The spectra aimed to investigate the chemical state of the elements and their binding energy. Examining the oxygen spectra, the presence of distinctive peak associated with Ti-O at 530.4 eV was evident in CT specimens. This confirms the passive oxide formation after the chemical treatment, followed by an increase in the density of exposed hydroxyl groups on the surface.[1] It was also observed that the peak of OH acid (approximately 530.7 eV) was more significant compared to the peak of OH basic (approximately 531.6 eV).[1] This result confirms that CT samples displayed a distinct signal characterized by the acidic OH groups exposed on the surface. In addition, the peak of water at the energy level of approximately 533 eV is due to physisorbed water.[2] The spectrum of the CT_GN2-Npm9 sample was fitted with three components. The component at approximately 531.7 eV corresponds to the doubly bonded oxygen in the carboxyl group (O=C-OH)[5], while the component at 530.4 eV and 530.7 eV can be attributed, respectively, to Ti-O and OH acid. The signal attributed to the Ti-O bond decreased in agreement with the presence of a functionalized layer. The main contribution in the region of the OH group is attributed to OH acid groups of the titanium oxide layer (around 530.7 eV). The peak attributed to C-O bond was negligible in CT_GN2-Npm9 because of the absence of this bond in the skeleton of the peptoid. The binding scale energy was calibrated using the Ti-O bond at 530.4 eV as a reference.1 Examining the carbon spectra in detail (Fig. 6.12), it can be observed the presence of a main peak around 285 eV, attributed to C-C, and C-H bonds, which are on titanium surface because of incidental carbon contamination. It is caused by atmospheric carbonaceous contaminants that have adhered to the surface due to titanium affinity for these elements.[3] These chemical bonds were also found in the functionalized sample, attributed to the peptoid chain onto the surface. The contributions at 286 eV and 289 eV can be attributed, respectively, to C-O-C bond and carbonates.[4] The appearance of a carbonate-related peak in the CT specimen may be attributed to the presence of impurities. In the carbon spectrum of CT_GN2-Npm9 specimen the main peak observed at 285.0 eV was associated with the carbon atoms linked exclusively to other carbon atoms or hydrogen atoms, identifiable in the skeleton of the peptoid. In addition, the presence of aromatic rings in the structure of tryptophan-like residues is indicative of the presence of carbon atoms in sp2 hybridization state. These carbon atoms have a binding energy of 284.5 eV.5 The component observed at about 286 eV corresponds to sp2 hybridized carbon atoms bonded to nitrogen, denoted as C-N.5 Furthermore, the presence of double carbon-oxygen (C=O) bond at approximately 288 eV is inferred from the characteristic chemical bonds within the peptoid chain.[6]

The high-resolution nitrogen spectrum shows two distinguishable peaks (as indicated in Figure 6.13). It is of interest to specify that for amino acids and proteins, the

C-N bond is typically found in the range of 398.2-398.8 eV, the -NH2 group is located at 399.7-400.0 eV, and the NH3+ group (characteristic of electrostatic adsorption) is observed in the range of 401.3-400.8 eV.[7] Concerning the peptoid, the first peak, with a lower binding energy of approximately 400 eV, is attributed to the secondary amines (nitrogen within the C-NH-C group). Meanwhile, the second peak, appearing at 401.5 eV, corresponds to the tertiary amines (– NH2).[5,6] The nitrogen spectrum of the functionalized sample reveals that the most prominent groups are attributed to the bound -NH, present in the aromatic group of tryptophan-like residues. As a result, on the surface the main exposition of the peptoid is provided by the tryptophan-like residues. This aligns with the zeta potential results, where it is observed that the -NH2 groups of lysine are involved in binding with the exposed OH groups on the titanium surface. According to these results, it can be concluded that the functionalization process involves the electrostatic attraction between the -NH2 groups and the exposed acidic OH groups of the titanium oxide layer, exposing the groups of tryptophan-like residues.
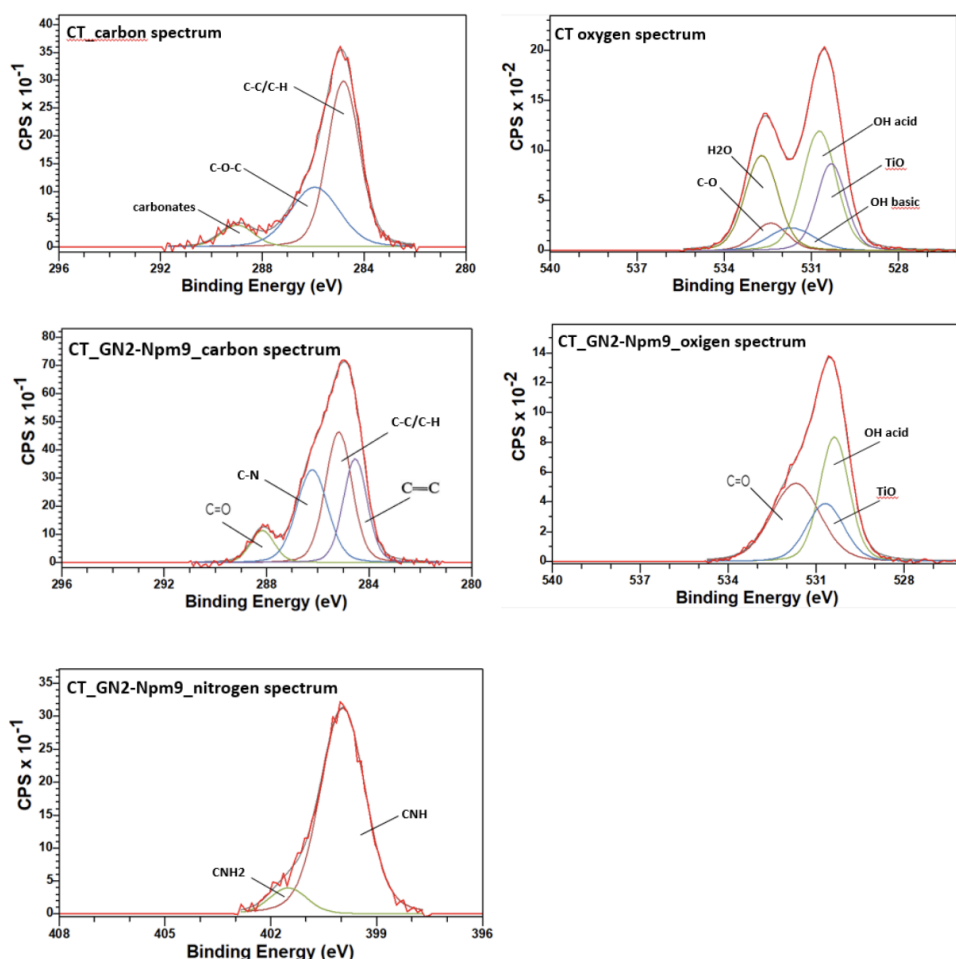

Figure 6.13: High-resolution XPS spectra of C and O1s regions of CT and CT_GN2-Npm9, and high-resolution XPS spectrum of N1s regions of CT_GN2-Npm9.

		CT						
	Oxygen	Spectrum			Carbon	Spectrum		
Energy (eV)	530.5-531	531.5-532	533-535	533	530	285	286	289.3
Functional bound	OH acid	OH basic	H2O	C-O	Ti-O	C-C/C-H	C-O-C	carbonates

		CT_GN2-Npm9						Nitrogen	Spectrum
	Oxygen	Spectrum			Carbon	Spectrum			
Energy (eV)	530.5-531	530	531.9		291.8	286.2	285	284.7	400.2	401.1
Functional bound	OH acid	Ti-O	C=O		C=O	C-N	C-C/C-H	C=C	NH	NH2

Figure 6.14: Theoretical XPS values for the functional groups of interest.

	Oxygen	Spectrum			Carbon	Spectrum		
Energy (eV)	530.7	531.6	533	532.5	530.4	285	286	289
Functional bound	OH acid	OH basic	H2O	C-O	Ti-O	C-C/C-H	C-O-C	carbonates

		CT_GN2-Npm9						Nitrogen	Spectrum
	Oxygen	Spectrum			Carbon	Spectrum			
Energy (eV)	530.7	530.4	531.7		288	286	285	284.5	400	401.5
Functional bound	OH acid	Ti-O	C=O		C=O	C-N	C-C/C-H	C=C	NH	NH2

Figure 6.15: XPS values obtained for the functional groups of interest.

6.3.2   Zeta potential

Zeta potential measurements have been conducted on peptoid in solutions at different pH values (Figure 6.16).
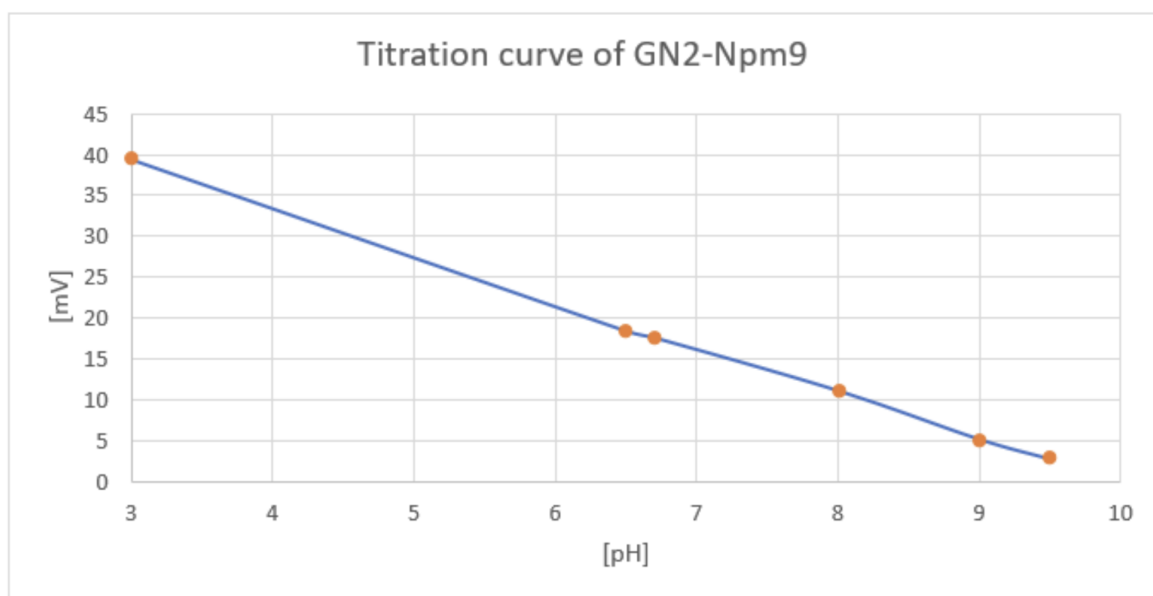

Figure 6.16: Titration curve of GN2-Npm9. At low pH levels, there is a high zeta potential. As the titration curve progresses, a slight decrease in the zeta potential is visible. A first plateau can be seen at pH value ranging from 6 to 7. Then, the second slight drop occurs. Overall, the curve shows a progressive lowering and not an abrupt decrease at the IEP as usual for the single aminoacids.

The zeta potential curve for a solution containing the peptoid GN2-Npm9 exhibits a high zeta potential at low pH levels, followed by a gradual decrease as the pH increases. A stable plateau is observed with onset pH 6, maintaining a zeta potential of approximately 18 mV. This plateau suggests the presence of homogeneous positively charged functional groups, primarily attributed to lysine-like residues. Subsequently, a second drop in the zeta potential is observed, but it remains in the positive range across the entire tested pH range, culminating in an isoelectric point (IEP) at approximately pH 9.5. This sustained positivity is attributed to the persistent positive charge carried by lysine residues, while other residues, which are apolar and hydrophobic, do not significantly impact the zeta potential. The observed curve can be explained by examining the analogous peptide chemical composition and structure. The positively charged residues in the peptide, lysine residues, are characterized by an IEP value of 9.7, pKa values of 2.2 for the alpha carboxylic group, 8.9 for the ammonium group, and 10.5 for the side chain.[8] The other component of the peptide, tryptophan-like residue, has an IEP value of 5.9, pKa values of 2.5 for the alpha carboxylic group and 9.4 for the ammonium group. In addition, tryptophan-like residue includes a hydrophobic and apolar side chain. Therefore, based on this information, the combination of lysine and tryptophan-like residues to form polypeptides leads to expected isoelectric point approximately at pH 10. It is expected to shift towards higher values when the peptide length is extended, without being influenced by the rearrangement of the side chain. This shift occurs because as more units are added, more carboxylic groups become involved in peptide bonding, making them less available for deprotonation. Meanwhile, the count of lysine's basic side chains increases, and they remain fully available for protonation. Considering the peptoid counterpart, the tryptophan-like residue is expected to exhibit a similar behavior, even if the titration curve can be altered in its values due to the shift from alpha carbon to the nitrogen, which can cause change in the pKa values. Indeed, the isoelectric point had been achieved at a pH value of 9.5. According to existing literature, the untreated MP_Ti6Al4V reaches an isoelectric point at approximately pH=4.7.[8] The surface modification achieved via chemical treatment is expected to result in a shift of the isoelectric point towards lower pH values (more acidic environment), approximately 3, due to the presence of acidic functional groups on the surface. In addition, a distinct plateau should be noticed in the potential curve of the treated specimen, within the basic pH range. The plateau is related to the presence of homogeneous functional groups on the surface, exhibiting the same acidic behavior. These groups are identified as hydroxyl groups (OH) as a result of the surface treatment. Indeed, at physiological pH (pH = 7.4), the surface of the treated sample exhibits a negative charge on non-functionalized CT sample.[9,10] This suggests that the adsorption process is primarily driven by electrostatic interactions. These findings indicate the titration curve of the peptoid of interest because it confirms that this peptoid can have an antibacterial action through its positive charge and it can be electrostatically adsorbed on the CT surface which has a negative surface charge at pH 7.4. It is also of interest that the zeta potential of the peptoid has a progressive lowering and not an abrupt decrease at the IEP as usual for the single aminoacids. This is an important result, because it indicates a distribution of cationic residues on the peptoid despite pH variations, which is essential for the electrostatic interaction
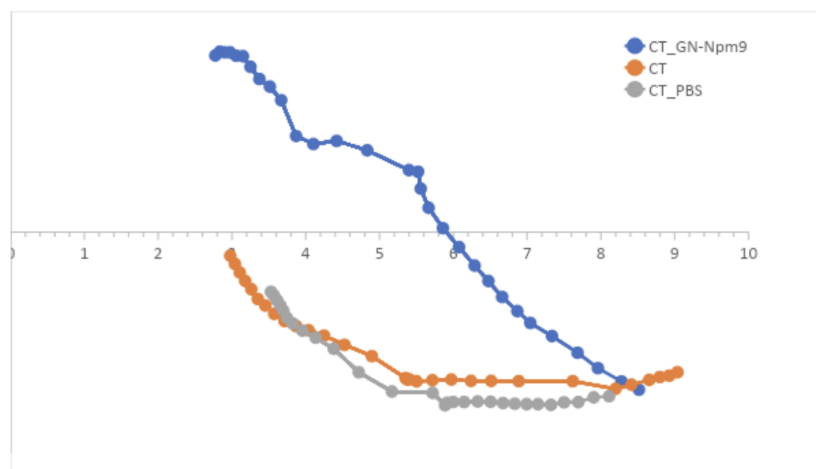
with OH groups.

Figure 6.17: Titration curve of CT, CT_GN2-Npm9, CT_PBS.11

The functionalized CT_GN2-Npm9 specimen reaches an IEP value of approximately 6, which is shifted towards more basic values compared to CT, indicating the success of the adsorption of the peptoid. However, it is of interest that the titration curve of the functionalized surface is not equal to that of the peptoid evidencing a partial covering of the CT surface. In addition, CT_GN2-Npm9 curve exhibits positive zeta potential at pH lower than 6, in contrast to CT titration curve, as previously discussed, due to the exposed positively charge amine groups of the peptoid. At pH 4-5.5 the plateau indicates the deprotonation of CT's OH groups. In this context, the balance between surface-exposed species with different electrical charges plays a crucial role. A higher inclination in the curve of CT_GN2-Npm9 compared with the solely peptoid in the solution and the substrate CT, moving towards the basic range, can be associated with a rapid increase in apolar and hydrophobic residues (tryptophan-like) interacting with the surrounding solution, and, meanwhile, with an increase of the electrostatic interaction between the hydrophilic residue of the peptoid, lysine, and the OH groups on CT surface. This explanation aligns with the shift of IEP from 9.5 in the titration curve of GN2-Npm9 to an IEP of 6 in the titration curve of CT_GN2-Npm9. This is thus linked to the decreased exposure of positively charged groups by the peptoid.

6.3.3 Confocal microscopy

In this analysis, the results anticipated the absence of fluorescence in CT_Ti6Al4V specimen, which was instead expected to be highly visible in the functionalized sample CT_GN2-Npm9_Ti6Al4V, as previously discussed in chapter 5. Moreover, from the analysis of the sample after 1 week of release testing, we anticipated one of two possible outcomes: either the absence of fluorescence, indicating the complete release of the peptoid in water, or a reduced level of fluorescence when compared to fluorescence analysis of CT_GN2-Npm9_Ti6Al4V, which would indicate a partial release of the molecule from titanium specimen. The images obtained by subjecting the specimens

to confocal microscopy are shown in Figure 6.18,6.19,6.20. In each image, the contrast was adjusted to -50 to better appreciate the differences in term of fluorescence.
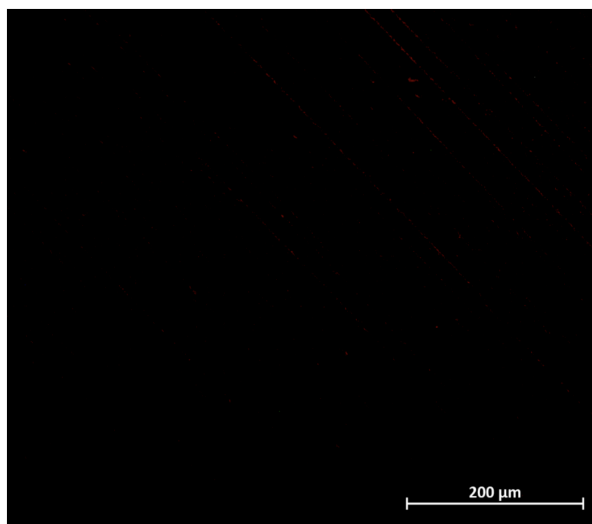

Figure 6.18: Fluorescence microscopy images of CT_Ti6Al_4V. No visible fluorescent signal; the image appears almost totally black.
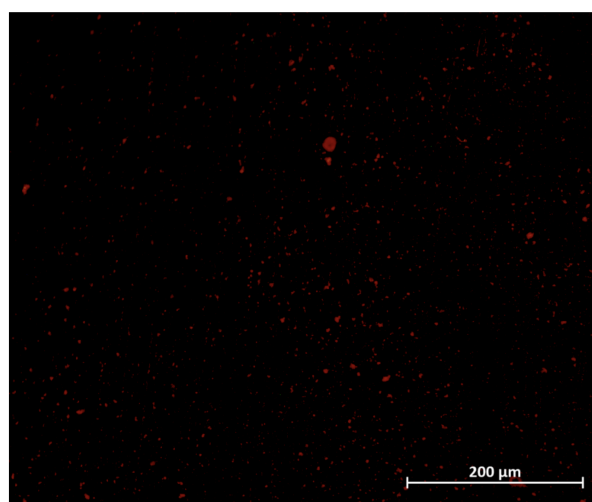

Figure 6.19: Fluorescence microscopy images of CT_GN2-Npm9_Ti6Al_4V. The surface is highly fluorescent due to the presence of tryptophan-like residues in the peptoid.
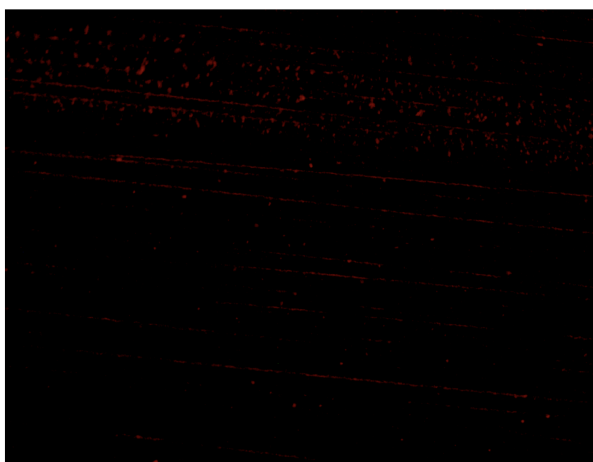
Figure 6.20: Fluorescence microscopy images of CT_GN2-Npm9_Ti6Al_4V after a release testing of 1 week. A significant decrease in fluorescence can be seen.

The fluorescence microscopy clearly showed the uniform presence of red fluorescence spots distributed on the titanium surface, providing evidence that the surface of the sample had been successfully functionalized with the bioactive peptoid. Conversely, the Ti sample lacking the peptoid exhibited no discernible presence of fluorescence probe. Indeed, it has been observed that CT_Ti6Al4V does not show fluorescence, except for some straight lines attributable to an imperfect polishing of the specimen. On the other hand, the presence of peptoid in the functionalized sample renders the surface highly fluorescent. It agrees with the zeta potential titration curve of functionalized specimen, which shows considerable differences when compared to the titration curve of control sample (CT_Ti6Al4V) and titration curve of a Ti6Al4V specimen immersed in PBS.[12] In Figure 6.19, the presence of some aggregates exhibiting heightened fluorescence indicates the ascertainable homogeneity of the coating. However, there is not a uniform distribution of these spots on CT surface. This observation aligns with the zeta potential titration curve of the functionalized surface, clearly indicating that the peptoid is homogeneously dispersed on the CT surface, but it does not cover it as a uniform film. Following 1 week of release, in Figure 6.20, the persistence of straight lines, previously addressed, remains evident. As anticipated, the presence of peptoid is significantly reduced, indicating that the peptoid has been largely released into the solution after the test, thus demonstrating its efficacy in being released within the damaged site. However, even after the release, the peptoid is not uniformly distributed on the CT surface, as discussed in Figure 6.19. This result is of interest, because it evidences that a release of the peptoid occurs from the functionalized surface, and this can be related to the antibacterial activity. On the other hand, the kinetic of the release is slow and it is not complete after 1 week. Considering the risk of late infections and the fact that most antibacterial agents are active only after few hours after implantation, this is of great interest. This suggests that the peptoid can effectively be attached to the treated surface of a titanium sample and be subsequently released, further supporting the scientific interest that has already been established in the investigation of antibacterial properties in titanium samples functionalized with peptides to prevent

implant-associated infections.[13,14]

6.4 UV-Vis release

Most experiments utilizing UV-Vis spectroscopy typically focus on amino acids. However, it has been demonstrated that UV-Vis spectroscopy can also be carried out to detect peptides and proteins containing aromatic amino acids.[15] Tryptophan, which possesses two aromatic rings (a pyrrole ring and a benzene ring), is one of the aromatic residues that can absorb ultraviolet (UV) light for excitation. It functions as a natural fluorophore in many proteins.[15,17] The absorbance and fluorescence signals of tryptophan tend to increase as the concentration of tryptophan-like residues in the solution rises, providing indications about their release in a solvent.[15] Figure 6.21 illustrates how aromatic amino acids and proteins containing aromatic amino acids are detected with distinctive UV absorption profiles. The peak centered around 280 nm results from the absorption of UV light by the aromatic ring component of their structure, specifically due to the excitation of π–π^* transitions in the indole part of the molecule.[14,17] Conversely, the lower-wavelength peak arises from the absorption of peptide and carboxylic acid groups within the compounds. Concerning molar absorbance, tryptophan exhibits higher absorbance at 280 nm compared to the other two aromatic amino acids capable of UV absorption, tyrosine, and phenylalanine. In the case of tryptophan, its absorption spectrum is characterized by a strong band at 220 nm and a weaker one at 280 nm.[19]
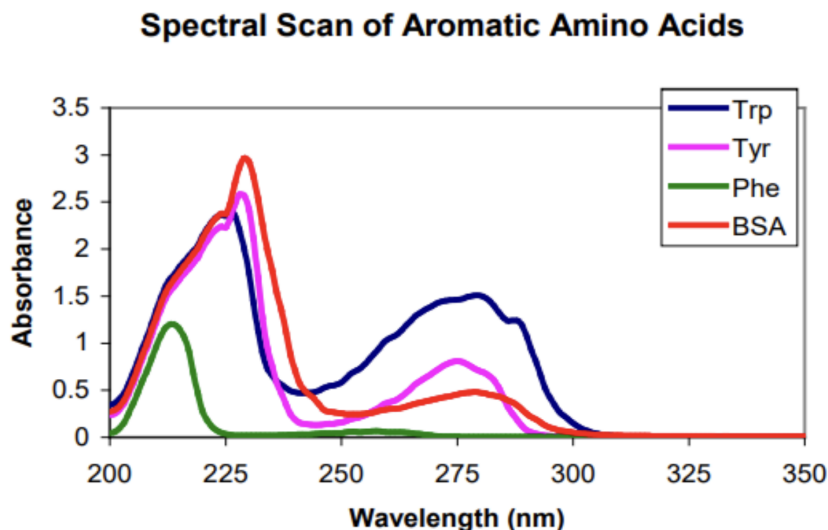

Figure 6.21: Absorbance Spectral of the aromatic amino acid tryptophan (Trp) in water solution, compared with tyrosine (Tyr), phenylalanine (Phe) and bovine serum albumin (BSA) utilizing a Synergy HT multi-detection microplate reader.[15]

A recent study has also demonstrated that peptoids containing tryptophan-like residues can also be detected using UV-Vis spectrometry. Specifically, this study has shown that the peptoid GN2-Npm9, the tryptophan-rich peptoid of interest in our

project, exhibits a single peak in the absorbance spectrum when immersed in water and exposed to UV light. This peak is attributed to the absorption of the tryptophan-like residue, typically detected at 280 nm, as previously discussed.19 The peak at 220 nm is lower when compared to peptide, likely due to the diverse structure of the peptoid compared to peptide.
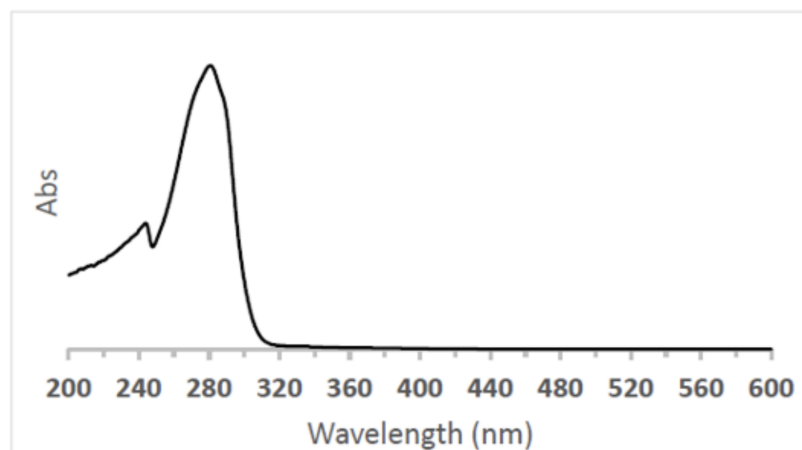

Figure 6.22: Absorbance Spectral of the peptoid GN2-Npm9 in water; concentration 1 mg/ml.

However, the absorption maxima (λmax) of UV/Vis spectra are influenced by the local environment surrounding the aromatic acid.14 These shifts in the wavelength at which a molecule absorbs or emits light can be toward longer wavelengths (redshift) or shorter wavelengths (blueshift), depending on the specific interactions between the molecule and the solvent. High polarizability of the solvent leads the absorption peak to shift towards lower-energy regions. This blueshift is generally related to intermolecular interactions and it occurs because the excited state becomes more stable as a result of the induced dipole interaction between the transition moment and the solvent molecule. Factors such as the charge in dipole moment during electronic transitions, solvent dipole moment, and the sizes of solvent and solute molecules play a crucial role in these interactions. In polar or hydrogen bonding solvents with permanent dipole moments, a blue shift occurs in λmax with increasing solvent polarity. The interaction of polar solvents, including those capable of hydrogen bonding, with various chromophores leads to changes in charge distribution within the molecule, resulting in increased delocalization.[21] Besides the shifts in wavelength in terms of absorbance, the solvent also influences the way tryptophan behaves in terms of fluorescence. When the solvent becomes less polar, the fluorescence spectrum moves towards shorter wavelengths and becomes more intense. This is why tryptophan residues located within the hydrophobic regions of folded proteins often show a spectral shift of 10 to 20 nm.[15]. In our project, we examined the UV spectra of three functionalized samples, whose release of peptoid was analyzed and compared at various time intervals (see paragraph 5.7). In Figure 6.23, 6.24 and 6.25 the results are shown.
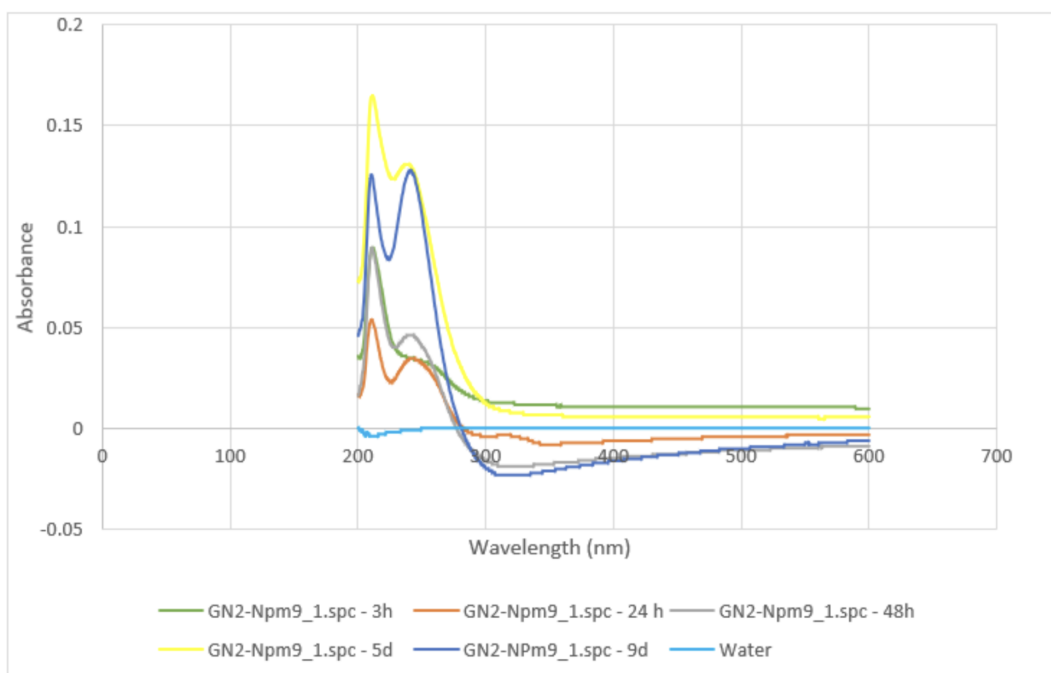
Figure 6.23: UV spectra of release solutions of the first sample analyzed. The release was investigated after 3hours (green), 24 hours (orange), 48 hours (grey), 5 days (yellow), and 9 days (blue).
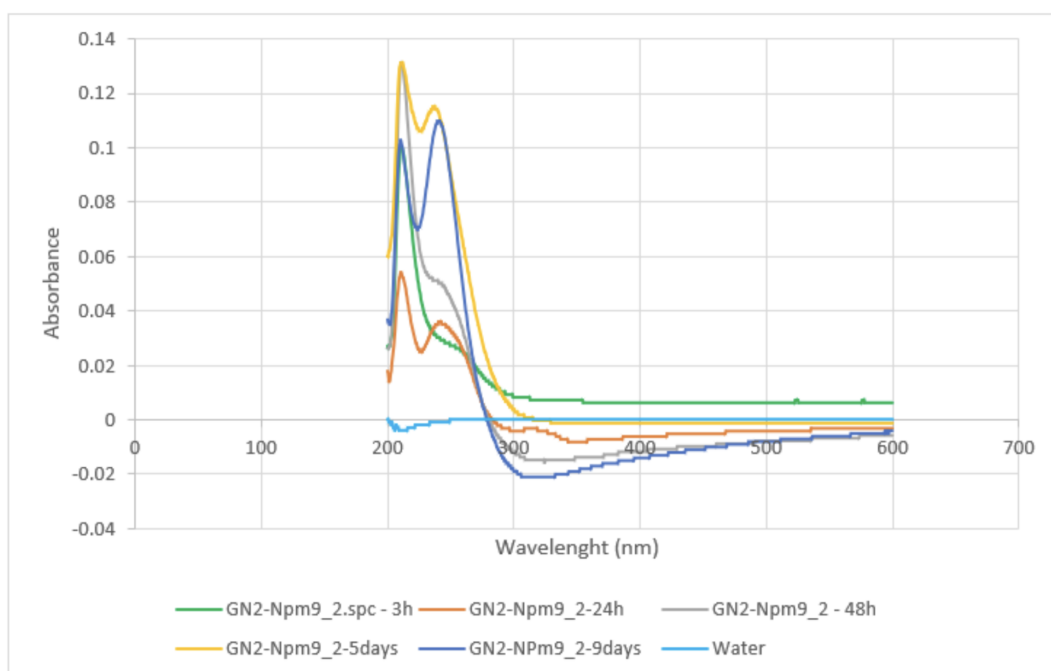

Figure 6.24: UV spectra of release solutions of the second sample analyzed. The release was investigated after 3hours (green), 24 hours (orange), 48 hours (grey), 5 days (yellow), and 9 days (blue).
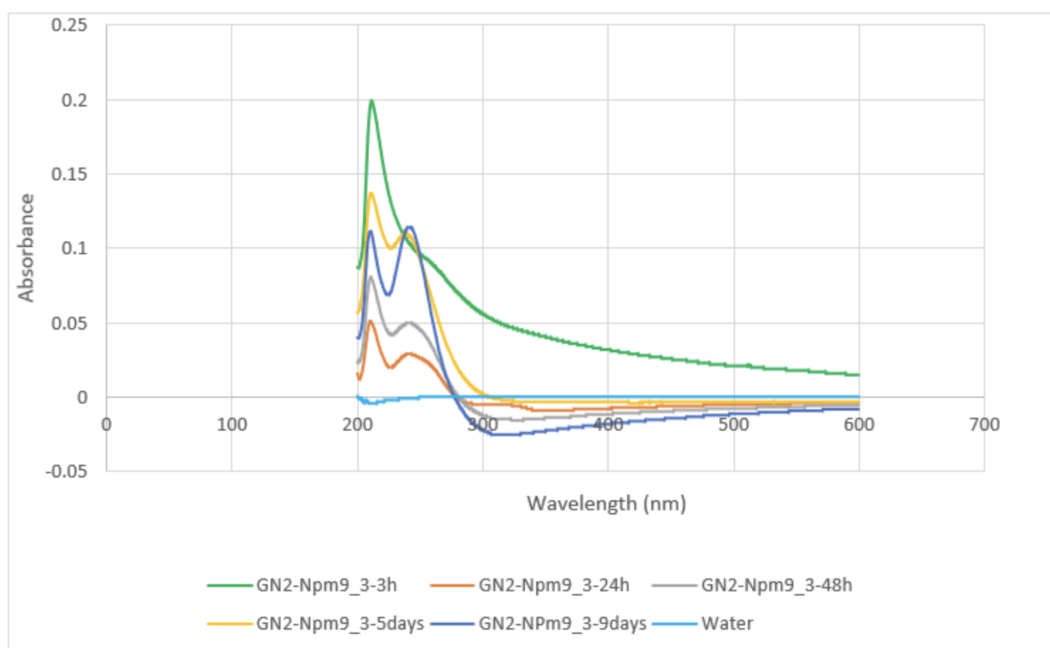
Figure 6.25: UV spectra of release solutions of the third sample analyzed. The release was investigated after 3hours (green), 24 hours (orange), 48 hours (grey), 5 days (yellow), and 9 days (blue).

As previously discussed, the use of water as solvent results in peaks shift toward lower wavelength due to its polarity. However, with the increase of the soaking time, the peaks are shifted toward the expected longer wavelengths. Especially, the second peak expected at 280 nm is also more defined when the soaking time increases and seems to be higher than the peak at 220 nm in relation with time. This aligns with the reported spectrum in Figure 6.21. A possible explanation of this behavior can be related to a previous study in which a linear correlation between the concentration of a tryptophan-like residue (L-tryptophan) and its absorbance at the expected wavelength value was demonstrated.[20] These results seem to confirm this relationship. At low concentrations, tryptophan can be well dissolved in water. In this case, the solution is still largely polar due to the abundance of water molecules, and the peaks are more distant from the wavelength at which tryptophan-like residue absorbs. As the concentration of tryptophan in the solution increases, the polarity of the solution may start to change. The polar part of tryptophan can interact with water molecules, maintaining some polarity in the solution. However, if the concentration of tryptophan becomes significantly high, tryptophan molecules tend to interact with each other through hydrophobic interactions involving their nonpolar parts. These interactions can reduce the overall polarity of the solution. If the concentration of tryptophan continues to increase, the polarity of the solution may decrease due to the aggregation of tryptophan molecules into non-polar regions. Under these conditions, tryptophan molecules may form hydrophobic aggregates, which can shift the peaks toward right. Therefore, the peaks are moved toward longer wavelength as the solution polarity decreases because of the increased concentration of tryptophan. In this context, after 3 hours, the second peak is not visible, due to the low concentration of tryptophan in the solution, indicat-

ing a negligible release of peptoid. After 24 hours, the second peak begin to be more detailed, but a significant change in the spectrum is visible after 9 days of soaking, when the second peak overcomes the first. It suggests that the release of peptoid is not instant. This aligns with the results observed in the fluorescence images detected on the functionalized sample after 1 week of release (Figure 6.20). In summary, we can conclude that for all the analyzed samples, there is a shift of the peaks to the left, as previously discussed, due to solvent-solute interactions, as tryptophan tends to interact with water through hydrogen bonds and dipole forces, which influence the electronic transitions of the peptoid.[22] Moreover, the peaks corresponding to the theoretical wavelength of 280 nm do not appear prominently and visibly until at least 48 hours, becoming more defined on day 9. This leads to the conclusion that after 3 hours, the concentration of tryptophan is very low relative to the quantity, making the peak invisible, as shown in Figures 6.[18,20] With increasing soaking time, the graph consistently rises, indicating a higher concentration of peptoid GN2-Npm9 released into the water.

6.5   Halo test

The halo assay aimed to evaluate the sensibility of the bacterium to the peptoid GN2-Npm9. Although the peptoid had still demonstrated an antibacterial activity against S. Epidermidis (chapter 6.3.1, 6.3.2, and 6.3.3), the test didn't show the expected results, as there were no differences compared to the control sample, due to the absence of a halo around the functionalized samples. After the incubation time of 24 hours, as depicted in the photograph (Figure 6.26), each sample did not exhibit a zone of inhibition. These results may be associated to different explanations: the nature of the bacterium, a non-pathogenic and non-biofilm forming bacterium, or an antibacterial action not involving a release of the peptoid in the surrounding, or the absence of a killing action on bacteria. Experimental errors occurred in the analysis and/or in the functionalization of the sample cannot be completely excluded, but we had no evidence of them during the experiments. The fluorescence images detected on the functionalized samples after 1 week of release (Figure 6.17) evidence that a partial release occurs, at least after 1 week. In addition, UV spectra of release solutions (Figure 6.18, 6.19, 6.20) do not show a significant release of peptoid after 24 hours. The antibacterial action of the peptoid needs a further investigation.

Figure 6.26: Agar plate with samples of control and samples functionalized with GN2-Npm9 peptoid, after incubation of 24 hours at 35°C. There were no differences among the considered specimens, and the absence of halo.

6.6 Biological evaluation

6.6.1 Antibacterial activity

The Figure 6.27 below shows the metabolic activity of the bacteria in close contact with the surface of the samples. Both CT and CT-pep significantly reduce the metabolic activity of the bacteria compared to the titanium-based control. Furthermore, the metabolic activity of bacteria grown in CT-pep is significantly lower than that of CT.
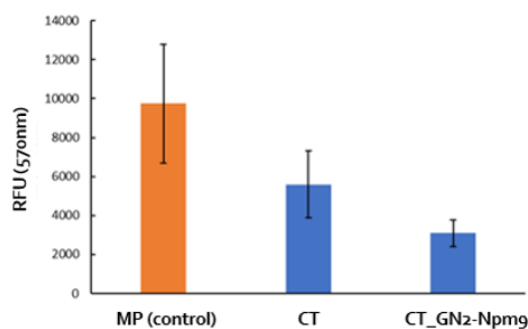
Figure 6.27: Evaluation of antibacterial activity. * $p < 0.05$ vs Ti(Ctl); $ $p < 0.05$ vs Ct

6.6.2 Peptoids surface prevent biofilm formation - UoB

To evaluate the effect of PBS that contains the bacteria detached from the biofilm surface on clinical isolate P. aeruginosa MMA83 biofilm formation, fluorescence microscopy was applied. Compared to the untreated control, the biofilm formation of P. aeruginosa MMA83 was significantly inhibited in the presence of PBS that contained the bacteria detached from the biofilm surface of TI6AL4V, POLY, and CT-GN-NpMg (Fig.6.26) After the treatment the MMA83 biofilm was hindered, and a significant decrease in confluence and density with more dispersed biofilm aggregates was observed. However, after the treatment with PBS that contained the bacteria detached from the biofilm surface of CT, the impact on biofilm formation of MMA83 was not observed, compared to the untreated control (MMA83). The obtained results show the strong effect of the supernatant of CT-GN-NpMg sample on MMA83 biofilm formation (Fig. 6.27). Compared to the control, the biofilm formation of P. aeruginosa MMA83 was significantly inhibited in the presence of the supernatant of CT-GN-NpMg sample, resulting in a very loose biofilm with a considerable number of individual cells.
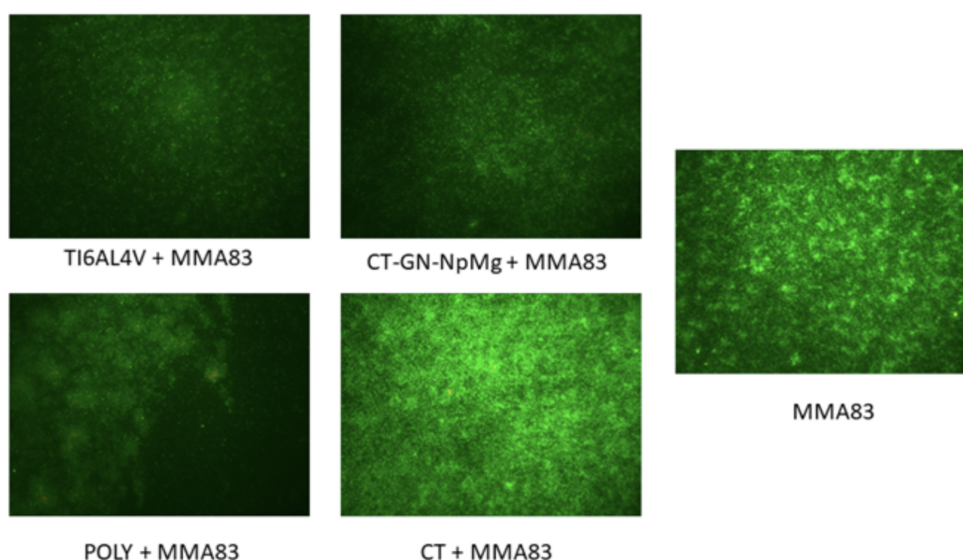

Figure 6.28: The effect of PBS that contains the bacteria detached from the biofilm surface on biofilm formation of multidrug-resistant clinical isolate P. aeruginosa MMA83. Fluorescence micrographs of the MMA83 biofilm (2000 × magnification) show the efficiency of TI6AL4V, POLY and CT-GN-NpMg to prevent biofilm formation. The effect of CT on biofilm formation of MMA83 was not recorded.
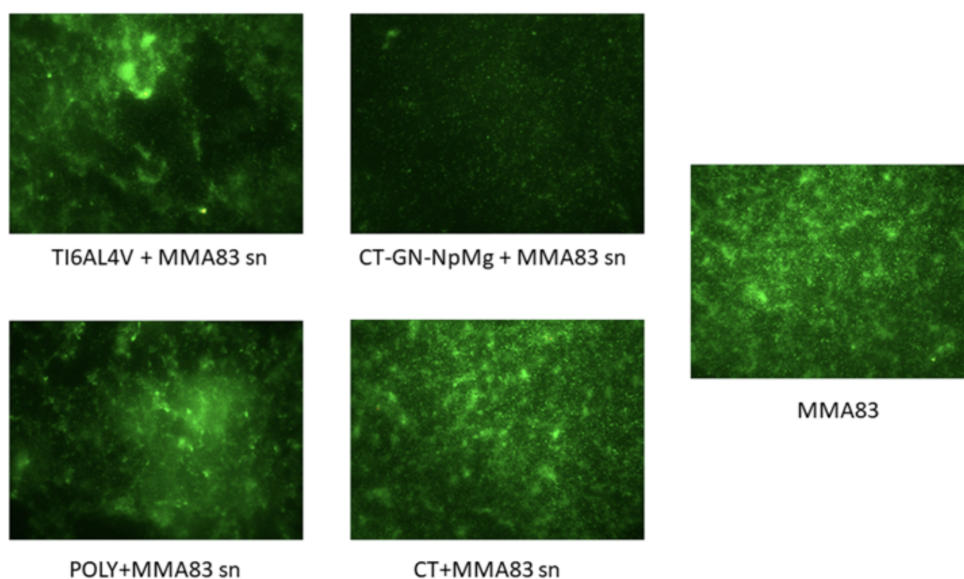
Figure 6.29: The effect of supernatant of different Ti-based surfaces (TI6AL4V, CT-GN-NpMg, CT) and POLY on biofilm formation of multidrug-resistant clinical isolate P. aeruginosa MMA83. Fluorescence micrographs of the MMA83 biofilm (2000 × magnification) show the high efficacy of CT-GN-NpMg in preventing biofilm formation.

The oral cavity is a dynamic environment that contains a broad spectrum of bacterial species that form oral microbiota. It is showed that only a few bacterial species are connected with oral infections such as dental caries and periodontitis.[19] Their eradication from dental plaques seems to be more challenging due to their higher resistance to antibiotics and ability to form complex and very resistant biofilms.[20] Pseudomonas aeruginosa is described as one of the bacterial species with increasing incidence of causing oral infections such as dental caries and periodontitis.[21] The initial burst release of peptoids coupled with CT could explain the most stricking anti-quorum sensing and antibiofilm effect of supernatant after 24h of incubation with CT-GN-NpMg sample.[22] These results are in line with previously reported data about the ability of peptoids to effectively inhibit P. aeruginosa biofilm formation.[24]

6.6.3 RT-qPCR

The RT-qPCR results showed that supernatant obtained from the chemically treated (rough) material which is functionalized with the peptoid (CT-GN-NpMg) has the most striking effect on the relative mRNA level of genes involved in QS of MMA83. The expression of rhlI, rhlR, pqsA, and mvfR is reduced by 35, 25, 45, and 55%, respectively, while it almost completely prevents the expression of the pqsH gene of MMA83. It also showed that pqsH gene expression was significantly reduced in all samples (Fig.6.28) Also, supernatant obtained from the chemically treated (rough) material which is functionalized with the peptoid (CT-GN-NpMg) reduces the relative mRNA of the lasB gene, which is involved in elastase synthesis, by 40%. The reduction of the relative mRNA level of lasB gene was observed after treatment with the supernatant obtained

from the CT and POLY, for 40 and 30% respectively. The reduction was not detected after treatment with the supernatant obtained from the sample with TI6AL4V (Fig.6.29).
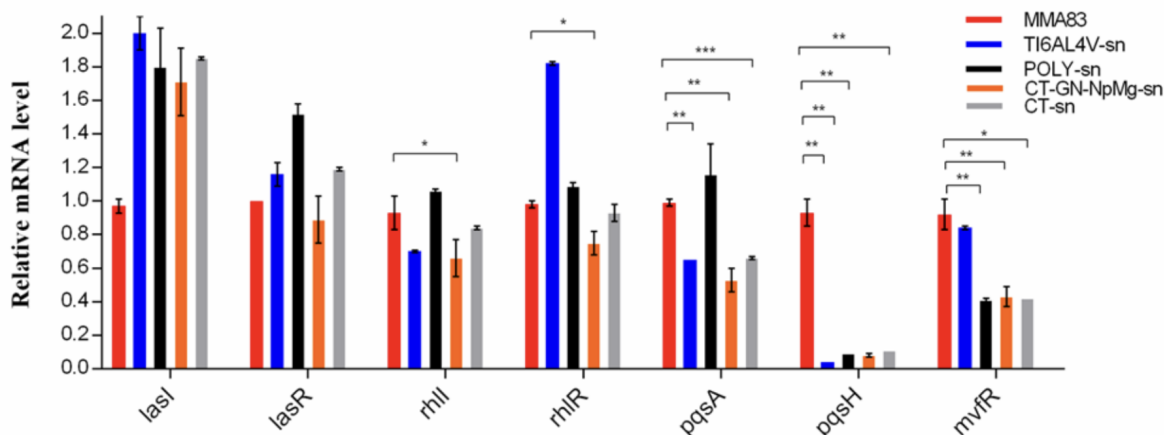

Figure 6.30: The effect of supernatant of different Ti-based surfaces (TI6AL4V, CT-GN-NpMg, CT) and POLY on relative mRNA level of genes involved in the QS system of P. aeruginosa MMA83. The results were obtained using RT-qPCR. Unpaired Student's t-test was used to evaluate if there was a significant difference between the control and treated group (*p<0.05, **p< 0.01, ***p<0.001).
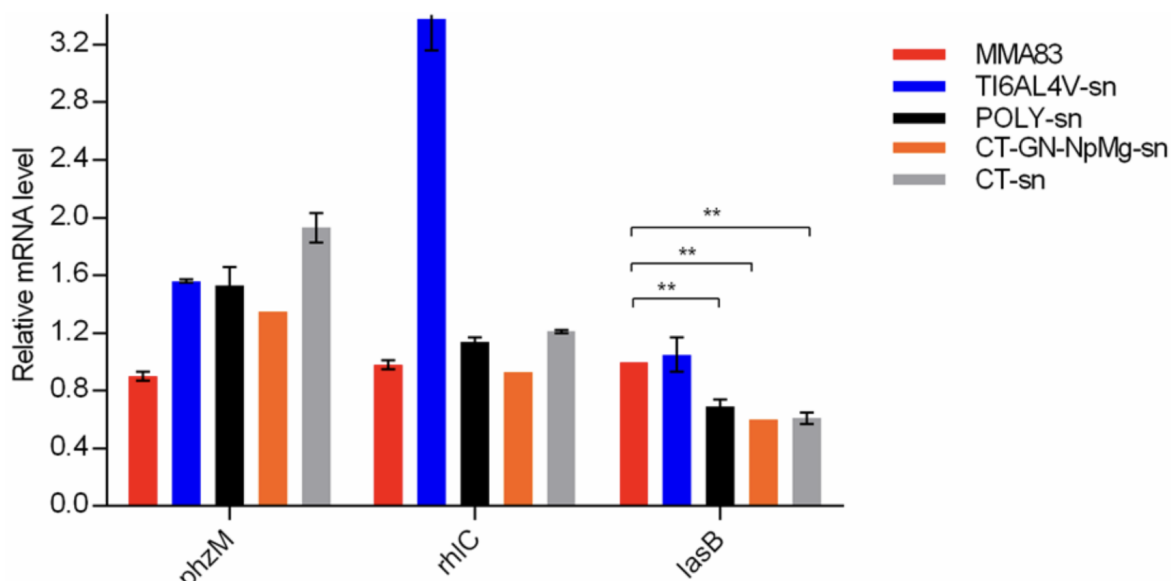

Figure 6.31: The effect of supernatant of different Ti-based surfaces (TI6AL4V, CT-GN-NpMg, CT) and POLY on relative mRNA level of virulence factor genes of P. aeruginosa MMA83. The results were obtained using RT-qPCR. Unpaired Student's t-test was used to evaluate if there was a significant difference between the control and treated group, (**p< 0.01).

Considering the poor penetration of antibiotics into biofilms and the easy spread of antimicrobial resistance genes between bacteria within the biofilm[28], preventing biofilm

formation and disrupting preformed biofilms may increase the susceptibility of P. aeruginosa to antibiotics or phages. These results indicate that peptoids could be promising agents to prevent bacterial colonization of medical implants and impair the quorum sensing signaling network of pathogenic bacteria. Considering that QS plays a vital role in biofilm formation by P. Aeruginosa[29] we further evaluated the expression of the QS genes belonging to three QS networks las, rhl, and pqs. Results show that the supernatant derived from the CT-GN-NpMg sample exhibited the capacity to reduce the expression of rhlI (C4- HSL synthase gene); rhlR (the response regulator gene); pqsA (the first gene in the PQS synthesis gene cluster), and mvfR (the transcriptional regulator) of P. aeruginosa MMA83. Notably, the observed reduction in lasB elastase gene expression in the CT-GN-NpMg supernatant-treated MMA83 cannot be solely attributed to a reduction in QS, because RT-qPCR results did not demonstrate down-regulation of the las system gene expression, which is a principal regulator of lasB gene expression.[30] However, it is crucial to recognise that the regulation of lasB gene expression is not regulated by the las system alone, but that the rhl system is also involved in its regulation.[31] Furthermore, we have to keep in mind that the QS signaling network of P. aeruginosa operates within a complex, multilayered hierarchy that includes interconnected signaling mechanisms that control gene expression in intricate ways, the full regulation of which is still unknown.[32] In addition, it is important to note that the interaction of dental plaque bacteria incubated with the samples could have a different interaction with P. aeruginosa MMA83 that affects quorum sensing and virulence factor expression in MMA83. However, the exact mechanisms underlying this interaction are not yet known and require further investigation. Nonetheless, it is evident that the functionalization of chemically treated (rough) titanium alloy with peptoids, owing to their antiquorum sensing and antibiofilm properties, stands out as the most auspicious strategy for advancing the design of innovative medical devices when compared to alternative materials.

References: Chapter 6

1. M. Cazzola et al., "Grafting of the peppermint essential oil to a chemically treated Ti6Al4V alloy to counteract the bacterial adhesion," Surf. Coatings Technol. (2019), vol. 378.

2. Matthew Smith, Louis Scudiero, Juan Espinal, Jean-Sabin McEwen, Manuel Garcia-Perez. "Improving the deconvolution and interpretation of XPS spectra from chars by ab initio calculations". Carbon (2016), Volume 110, Pages 155-171.

3. X. Zhang, S. Ferraris, E. Prenesti, and E. Verné, "Surface functionalization of bioactive glasses with natural molecules of biological significance, Part I: Gallic acid as model molecule," Applied Surface Science (2013), vol. 287, pp. 329–340.

4. B. V. Crist, "Demo Version (87 pages) PDF Handbooks of Monochromatic XPS Spectra Volume 1 - The Elements and Native Oxides (for Ag-Au)," Elements (2019), vol. 1.

5. A Artemenko, A Shchukarev, P Štenclová, T Wågberg, J Segervald, X Jia and A Kromka. "Reference XPS spectra of amino acids". IOP Conf. Ser.: Mater. Sci. Eng.

6. Wang, G., Zhang, J., Lin, S. et al. "Environmentally friendly nanocomposites based on cellulose nanocrystals and polydopamine for rapid removal of organic dyes in aqueous solution". Cellulose 27, 2085–2097 (2020).

7. Exploring proteins in Roughland: on the adsorption of proteins on biomaterials for osseointegration" (2022) - Politecnico di Torino - DISAT

8. C. Zvacek and F. Hagen, "An assessment of catalytic residue 3D- ensembles for the prediction of enzyme function FernUniversität in Hagen Prof . Dr . Jörg Keller An assessment of catalytic residue 3D-ensembles for the prediction of enzyme function Master ' s thesis Submitted by:," no. September 2014, 2016.

9. Roessler, S., Zimmermann, R., Scharnweber, D., Werner, C. & Worch, H. Characterization of oxide layers on Ti6Al4V and titanium by streaming potential and streaming current measurements. Colloids Surfaces B Biointerfaces 26, 387–395 (2002).

10. Ferraris, S. et al. Antibacterial and bioactive nanostructured titanium surfaces for bone integration. Appl. Surf. Sci. 311, 279–291 (2014).

11. S. Spriano, S. Ferraris, M. Cazzola, and V. Peretti, "Investigation Of Surface Functionalization And Coatings For Biomedical Applications By Zeta 81 Potential And Adsorption Measurements On Solid Surfaces," Materials and Contact Characterisation VIII (2017), vol. 116, pp. 379-390.

12. Francesca Gamna, Andrea Cochis, Biljana Mojsoska, Ajay Kumar, Lia Rimondini, Silvia Spriano. "Nano-topography and functionalization with the synthetic peptoid GN2-Npm9 as a strategy for antibacterial and biocompatible titanium implants". In press.

13. BaoHong Zhao, WeiMing Tian, HaiLan Feng, In-Seop Lee, FuZhai Cui. "Effects of RGD peptide grafting to titanium dental implants on the adhesion of human gingival fibroblasts and epithelial cells". Current Applied Physics (2005), Volume 5, Issue 5, Pages 407-410.

14. Kazemzadeh-Narbat M, Lai BF, Ding C, Kizhakkedathu JN, Hancock RE, Wang R. Multilayered coating on titanium for controlled release of antimicrobial peptides for the prevention of implant-associated infections. Biomaterials. 2013 Aug;34(24):5969-77.

15. Quantitation of Peptides and Amino Acids with a Synergy™HT using UV Fluorescence

16. Barik S. "The Uniqueness of Tryptophan in Biology: Properties, Metabolism, Interactions and Localization in Proteins". Int J Mol Sci. (2020);21(22):8776.

17. Khrustalev Vladislav Victorovich, Khrustaleva Tatyana Aleksandrovna, Poboinev Victor Vitoldovich, Stojarov Aleksander Nicolaevich, Kordyukova Larisa Valentinovna, Akunevich Anastasia Aleksandrovna. "Spectra of tryptophan fluorescence are the result of co-existence of certain most abundant stabilized excited state and certain most abundant destabilized excited state". Spectrochimica Acta Part A: Molecular and Biomolecular Spectroscopy (2021), Volume 257, 119784, ISSN 1386-1425.

18. Anshul Baral, Francesca Cavalieri, Santanu Chattopadhyay, and Muthupandian Ashokkumar. "Synthesis of Gold Nanosheets with Controlled Morphology by Combining a Natural Amino Acid with High-Frequency Ultrasound". ACS Sustainable Chemistry & Engineering (2021); 9 (41), 13953-13962.

19. Li R, Dhankhar D, Chen J, Cesario TC, Rentzepis PM. "A tryptophan synchronous and normal fluorescence study on bacteria inactivation mechanism". Proc Natl Acad Sci U S A. (2019);116(38):18822-18826.

20. Gamna, Francesca. "Multifunctional bioinspired surfaces for different host responses". Politecnico di Torino (2023). Doctoral Thesis.

21. Study of Solvent Effect on UV-Visible Spectra of a Newly Synthesized Zn(II), Co(II) and Cd(II) Complexes with L-Tryptophan Fatimah A. Abdulsayid* &

HAMAD M. ADDRESS HASAN. International Journal of Innovative Science, Engineering & Technology, Vol. 7 Issue 5, May 2020.

22. Lara-Popoca J, Thoke HS, Stock RP, Rudino-Pinera E, Bagatolli LA. Inductive effects in amino acids and peptides: Ionization constants and tryptophan fluorescence. Biochem Biophys Rep. (2020); 24:100802.

23. Zaatout, Nawel. "Presence of non-oral bacteria in the oral cavity." Archives of microbiology 203.6 (2021): 2747-2760.

24. Souto R, Colombo APV (2008a) Prevalence of Enterococcus faecalis in subgingival biofilm and saliva of subjects with chronic periodontal infection. Arch Oral Biol 53(2):155–160.

25. Wade WG (2013) The oral microbiome in health and disease. Pharmacol Res 69(1):137–143.

26. Kazemzadeh-Narbat, Mehdi, et al. "Multilayered coating on titanium for controlled release of antimicrobial peptides for the prevention of implant-associated infections." Biomaterials 34.24 (2013): 5969-5977.

27. Kapoor, Rinki, et al. "Antimicrobial peptoids are effective against Pseudomonas aeruginosa biofilms." Antimicrobial agents and chemotherapy 55.6 (2011): 3054-3057.

28. C. Uruén, G. Chopo-Escuin, J. Tommassen, R.C. Mainar-Jaime, J. Arenas, Biofilms as promoters of bacterial antibiotic resistance and tolerance. Antibiotics (2020) 1-3.

29. F.F. Tuon, L.R. Dantas, P.H. Suss, V.S. Tasca Ribeiro, Pathogenesis of the Pseudomonas aeruginosa biofilm: A review. Pathogens (2022) 300.

30. Casilag, Fiordiligie, et al. "The LasB elastase of Pseudomonas aeruginosa acts in concert with alkaline protease AprA to prevent flagellin-mediated immune recognition." Infection and immunity 84.1 (2016): 162-171.

31. Choi, Ha-Young, Duc Dat Le, and Won-Gon Kim. "Curvularin Isolated From Phoma macrostoma Is an Antagonist of RhlR Quorum Sensing in Pseudomonas aeruginosa." Frontiers in Microbiology 13 (2022): 913882.

32. Lee, Jasmine, and Lianhui Zhang. "The hierarchy quorum sensing network in Pseudomonas aeruginosa." Protein & cell 6.1 (2015): 26-41.

Chapter 7

Conclusion

In conclusion, this thesis has presented a comprehensive investigation into the synthesis, purification, characterization, and antibacterial properties of the peptoid GN2-Npm9, as well as its application as antimicrobial agent on chemically modified surface of Ti6Al4V alloy, widely used in orthopedic and dental implants. The research encompassed several key aspects, each contributing valuable insights into the behavior and potential applications of GN2-Npm9 to prevent bacterial adhesion and biofilm formation, also with the purpose of promoting osseointegration through chemical treatments of titanium substrates. To accomplish these goals, our attention was directed towards a controlled surface oxidation procedure aimed at rendering the surface both chemically and topographically suitable to enhance the attachment of the positively charged peptoid onto the surface, for their antibacterial properties, and to promote osseointegration. The synthesis of the peptoid GN2-Npm9 was undertaken through solid-phase synthesis at Roskilde University (Copenhagen). Firstly, the resulting chromatogram and mass spectrum revealed multiple peaks, indicating the presence of impurities. These impurities posed a significant challenge, as they could be attributed to sub-monomeric sequences, reagent contamination, or incomplete synthesis. Therefore, purification of GN2-Npm9 was explored to obtain a more defined product. The chromatogram and the spectrum showed that purification indeed resulted in a single, well-defined peak with a molecular weight closer to the expected value, which had demonstrated the success of the synthesis. The surface treatments and the functionalization of titanium surface with the molecule were conducted at the laboratories of Politecnico of Turin, including zeta potential analysis, XPS, halo assay, UV-Vis release, fluorescence microscopy and biological evaluation. The zeta potential curve of the peptoid GN2-Npm9 solution displayed a distinct pattern, showing a high positive zeta potential at low pH levels, followed by a gradual decrease as pH increased and indicating the presence of positively charged functional groups, with an isoelectric point at 9.5. This sustained positivity was attributed to the persistent positive charge carried by lysine residues, while other apolar and hydrophobic residues had minimal impact on the zeta potential. This information supported the potential antibacterial action of the peptoid due to its positive charge. On the prepared samples, surface characterizations by XPS analyses were carried out, concluding that the functionalization process involved the electrostatic attraction between the positively charged -NH2 groups and the exposed

negatively charged acidic OH groups of the titanium oxide layer. On the surface of the functionalized sample the exhibition of the tryptophan-like residues groups was displayed. Fluorescence microscopy also revealed the successful functionalization of the titanium surface with a bioactive peptoid, as evidenced by the presence of uniform red fluorescence spots. In contrast, the peptoid was absent on the untreated titanium sample, except for some imperfections probably due to polishing. After 1 week, straight lines persisted, indicating the peptoid's release into the solution, demonstrating its efficacy in targeted release within damaged areas. This release suggested potential antibacterial activity. The slow-release kinetics, coupled with the sustained presence of the peptoid, hold promise for preventing late infections in functionalized titanium implants, supporting ongoing research into antibacterial properties. The UV-Vis release also indicated a gradual release of peptoid into the water. The halo assay was performed in a period of 24 hours, and it indicated there were no observable differences compared to the control sample, and no halo formed around the treated samples. Possible explanations included the non-pathogenic nature of the bacterium and the slow release of the peptoid in solution. Indeed, although fluorescence images after a week suggested some peptoid release, UV spectra after 24 hours didn't show significant release. Biological evaluation demonstrated that both CT and CT-pep significantly reduced the metabolic activity of the bacteria compared to the titanium-based control. Furthermore, the metabolic activity of bacteria grown in CT-pep is significantly lower than that of CT. Currently, commercially available titanium implants with antibacterial features are lacking. The promising solution lies in the development of surfaces that can not only effectively exhibit antimicrobial activity but also maintain this action over an extended period. Furthermore, these surfaces should seamlessly integrate with the host bone without causing any cytotoxicity concerns. Oral bacteria are linked to dental infections, and Pseudomonas aeruginosa is increasingly causing them. Peptoids in CT-GN-NpMg samples inhibit P. aeruginosa biofilms and quorum sensing, potentially increasing antibiotic effectiveness. While some gene expression changes are observed, complex interactions with dental plaque bacteria require further study. Overall, peptoid-functionalized titanium alloy shows promise for medical device design compared to other materials.

Acknowledgments